Monitoring mitochondrial translation with spatial resolution and high throughput strategies

Dissertation

for the award of the degree
Doctor rerum naturalium
(Dr. rer. nat.)
by the Georg-August-Universität Göttingen

within the doctoral program *IMPRS for Molecular Biology*
of the Georg-August University School of Science (GAUSS)

submitted by

Roya Yousefi

born in
Ghazvin, Iran

Göttingen, 2022

Members of the Thesis Advisory Committee

Prof. Dr. Peter Rehling (First referee)	Department of Cellular Biochemistry, University Medical Center, Göttingen
Prof. Dr. Silvio O. Rizzoli (Second referee)	Department of Neuro- and Sensory Physiology, University Medical Center, Göttingen
Prof. Dr. Stefan Jakobs	Department of NanoBiophotonics, Max Planck Institute for Biophysical Chemistry, 37077 Göttingen, Germany.

Members of the examination board

Dr. Sarah Adio	Department of Molecular Structural Biology, Institute for Microbiology and Genetics, Göttingen
Dr. Sonja Lorenz	Research group Ubiquitin Signaling Specificity, Max Planck Institute for Biophysical Chemistry, Göttingen
Dr. Alexander Stein	Research Group Membrane Protein Biochemistry, Max Planck Institute for Biophysical Chemistry, Göttingen

Date of oral examination: June 16th, 2022

Table of Contents

Declaration ..... **iii**

Summary ..... **v**

Chapter 1: Introduction **3**

1.1. Mitochondria - a brief overview of the cell's powerhouse 3

1.2. Mitochondrial genome 5

1.3. Mitochondrial biogenesis 5

1.3.1. Mitochondrial biogenesis in neurons 7

1.4. Gene expression in mitochondria 9

1.4.1. Mitochondrial transcription 9

1.4.2. Mitochondrial translation 10

1.5. Regulation of mitochondrial gene expression 12

1.5.1. Phosphorylation in regulation of mitochondrial gene expression 13

1.6. Diseases related to mitochondrial gene expression 15

1.7. Methods for studying gene expression in mitochondria 15

1.7.1. Analyzing mtDNA 16

1.7.2. Analyzing mitochondrial gene expression at transcription level 16

1.7.3. Analyzing mitochondrial gene expression at translation level 17

1.8. Aim of this project 20

Chapter 2: First Manuscript **23**

Chapter 3: Second Manuscript **41**

3.1. Introduction 44

3.2. Results 46

3.2.1. Depletion of cellular kinases affects mitochondrial translation. 46

3.2.2. Ablation of kinases affects mitochondrial function and ATP levels. 48

3.2.3. Downregulation of selected kinases show changes in energetic state and mitoribosome integrity. 51

3.2.4. Effect of downregulation of selected kinases on individual proteins 53

3.3. Discussion 54

3.4. Material and Methods 57

3.4.1. Cell line and cell culture 57

3.4.2. Transfection of HeLa cells with Human Kinase siRNA library 58

3.4.3. HPG-labeling of mitochondrial translation in 96-well plate 58
3.4.4. Click-chemistry and immunostaining of fixed cells 59
3.4.5. Image acquisition and analysis 59
3.4.6. Radioactive-labeling of mitochondrial translation products 60
3.4.7. Steady-state analysis of protein level with western blotting 60
3.4.8. RNA extraction, cDNA synthesis and qRT-PCR 60
3.4.9. Real-time respirometry 61
3.4.10. Cellular ATP detection assay 61

3.5. Acknowledgement 62

3.6. References 62

3.7. Supplementary information 69
3.7.1. Supplementary figures 69
3.7.2. Supplementary tables 72

Chapter 4: Discussion 91

4.1. Mitochondrial-FUNCAT as a versatile tool in studying mitochondrial gene expression with spatial resolution 93

4.2. Mitochondrial-FUNCAT for studying the heterogeneity of mitochondria 94
4.2.1. Heterogeneity of mitochondria in neurons 94

4.3. Mitochondrial-FUNCAT as a tool for diagnosis of mitochondrial pathologies 97

4.4. A high throughput mitochondrial-FUNCAT approach 99

4.5. Introducing kinases with potential roles in regulation of mitochondrial gene expression 100

4.6. Future perspectives 101

Chapter 5: Appendices 103

Bibliography 105

List of Figures 131

List of Abbreviations 133

Acknowledgment 141

Resume 145

Declaration

I hereby declare that I have written this thesis independently, and with no other sources and aids than quoted.

Göttingen, April 30th, 2022

Summary

Nearly all mitochondrial proteins are encoded in the nuclear genome, synthesized in the cytosol, and imported into mitochondria. However, mitochondria are semi-autonomous and possess their own genome, the mitochondrial DNA (mtDNA). In humans, mtDNA encodes 13 proteins, all of which are essential components of the oxidative phosphorylation system (OXPHOS). Despite the limited number of genes on the mitochondrial genome, gene expression and maintenance are of great importance, and dysfunction in these processes is associated with diseases. All mitochondrial proteins responsible for mitochondrial genome maintenance and expression, including mitochondrial ribosomes, are nuclear-encoded and synthesized in the cytosol. Therefore, close coordination between the nuclei, cytosol, and mitochondria is critical for proper synthesis of mitochondrial-encoded proteins and biogenesis of OXPHOS complexes. In addition, each mitochondrion contains multiple copies of mtDNA, resulting in heterogeneity among mitochondria in a single cell. How mitochondrial heterogeneity affects protein synthesis and how mitochondrial gene expression is regulated in response to cellular requirements is not fully understood.

In this project, we explored two questions. First, given the strong coordination between mitochondrial gene expression and numerous nuclear-encoded proteins, we asked whether mitochondria express their genome differently in regions spatially distant from the nucleus, such as in the synaptic regions of neurons. To answer this question, we extended the use of a fluorescence-based technique to label nascent protein synthesis in mitochondria. In this method, an alkyne-containing amino acid was incorporated into the sequence of proteins encoded by mitochondria and then reacted with an azide-containing fluorophore. This provided visualization of nascent mitochondrial-encoded proteins using a fluorescence microscope (mitochondrial-FUNCAT). The spatial resolution of this technique allowed us to detect heterogeneous protein synthesis in mitochondria of different cell types and disease models. Moreover, we applied this technique in primary hippocampal cultures and detected new protein synthesis along axons and dendrites as well as in the pre- and postsynapse of hippocampal neurons. Thus, we provided further evidence for local biogenesis of mitochondria at the synapse. These results are presented in Chapter 2 as a published article.

Given the high specificity and ability of mitochondrial-FUNCAT to detect small changes in mitochondrial protein synthesis, in the second part of the project we investigated whether it could be used to screen novel factors and pathways in the regulation of mitochondrial gene expression. To this end, we optimized mitochondrial FUNCAT in a high-throughput setup with

a low error. Labeling mitochondrial protein synthesis in a 96-well format opened a new possibility to screen different factors and to find potential regulators of mitochondrial gene expression.

Next, we combined high throughput mitochondrial-FUNCAT and transfection with an siRNA library of human kinases to explore the potential cellular players of mitochondrial gene expression. We introduced 65 kinases whose downregulation altered the level of mitochondrial protein synthesis. Among them, several kinases were associated to mitochondria in different databases with less-described functions. Preliminary investigation of these candidates opened new possibilities for understanding the gene expression regulation in mitochondria and the associated pathologies. These results are presented in Chapter 3 as a manuscript prepared for submission.

Chapter 1: Introduction

1.1. Mitochondria - a brief overview of the cell's powerhouse

Eukaryotic cells have their cellular space separated into different membrane-enclosed compartments, each providing a distinct microenvironment and compartment-specific functions (Diekmann et al., 2013). Mitochondria were the first organelles isolated and characterized in the early 20th century (Chance et al., 1956). They have a unique structure with two surrounding membranes, outer and inner mitochondrial membrane (OMM and IMM) (Saccone et al., 2000). The membrane-enclosed space inside the IMM forms the mitochondrial matrix and the space between the two membranes is termed intermembrane space (IMS) (Figure 1). The two membranes are very different in terms of their lipid and protein composition and characteristics (Giacomello et al., 2020). The OMM is permeable to small molecules (2-6 kD) through protein pores while the IMM permeability is strictly controlled (Vogel et al., 2006). The IMM forms invaginations called mitochondrial cristae that increases its surface area and forms microdomains with specific protein content (Vogel et al., 2006). Most functions of mitochondria are carried out by the proteins located in the IMM and mitochondrial matrix.

Mitochondria fulfill many important metabolic functions in the cell (McBride et al., 2006; Vakifahmetoglu-Norberg et al., 2017) (Figure 1). They are for example home to the enzymes responsible for several metabolic pathways including the citric acid cycle (Kreb’s cycle), fatty acid oxidation (ß oxidation), and urea cycle. Furthermore, the biosynthesis of the heme group, cardiolipin (a special lipid component of IMM), and ubiquinol (coenzyme Q, CoQ) occurs entirely or partially in mitochondria. Additionally, mitochondria synthesize Fe-S clusters which are essential electron transport cofactors in many biological activities. Mitochondria have Ca^{2+} transporters and play a role in Ca^{2+} buffering. Cytoplasmic Ca^{2+} concentration triggers many important signaling cascades and it is tightly regulated. The role of mitochondria in Ca^{2+} homeostasis alongside the endoplasmic reticulum (ER) has become more prominent, especially by discovering that Ca^{2+} concentration is locally elevated at the microdomains of mitochondria-ER contact sites upon Ca^{2+} release from the ER (K.-S. Lee et al., 2018). This allows the efficient uptake of Ca^{2+} by mitochondrial low-affinity transporters.

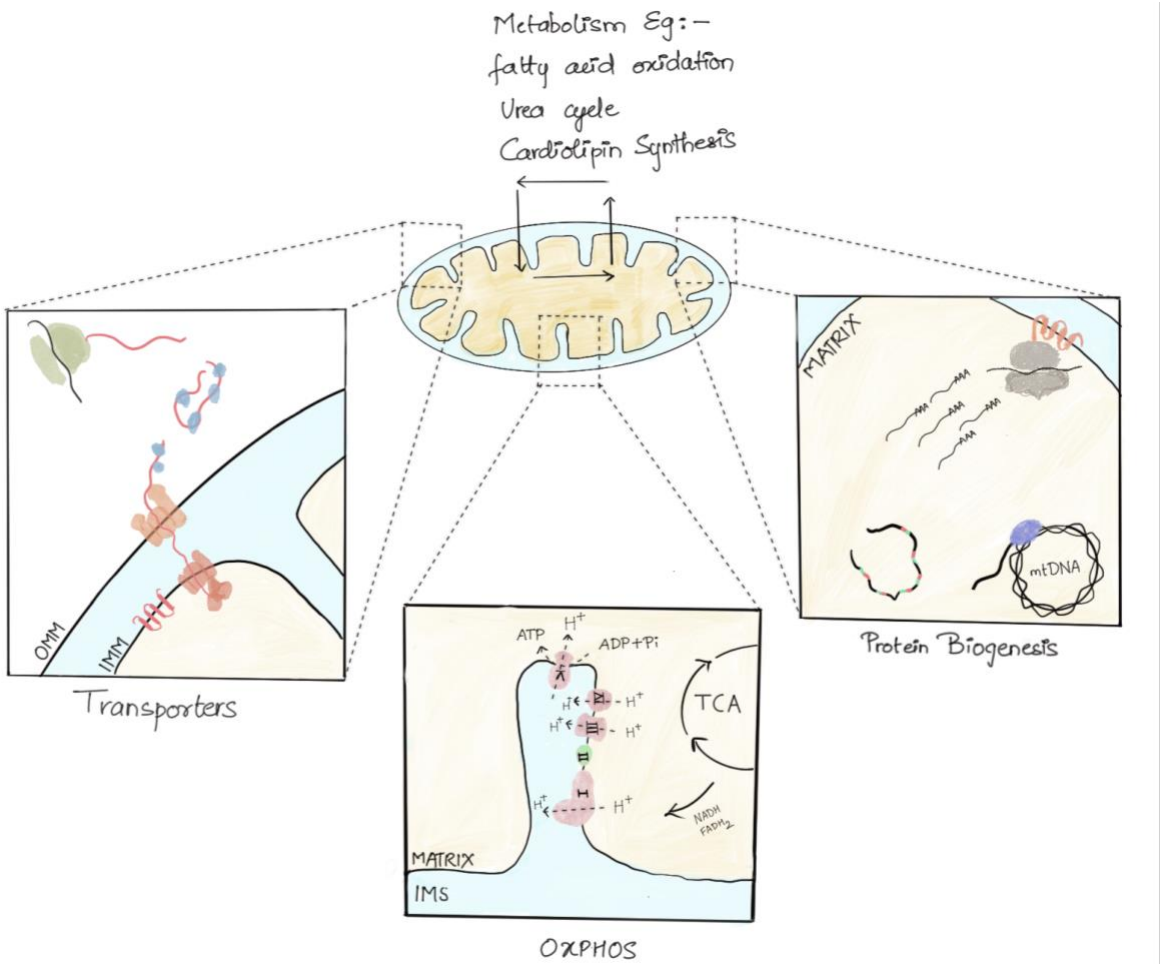

Figure 1. Mitochondria structure, function, and protein biogenesis. Mitochondria are surrounded by two membranes (OMM, outer mitochondrial membrane and IMM, inner mitochondrial membrane), which form distinct suborganellar spaces (IMS, intermembrane space and mitochondrial matrix). Most mitochondrial proteins are synthesized in the cytosol and imported into the mitochondria using transporters on the OMM and IMM. One major function of mitochondria is oxidative phosphorylation (OXPHOS) which is carried out by five protein complexes of the IMM (complex I-V). Electron is transferred from the donors such as NADH and $FADH_2$ along the OXPHOS complexes I to IV and a proton gradient is formed. Complex V uses the proton gradient to produce ATP. Mitochondrial DNA (mtDNA) encodes several components of the OXPHOS complexes which are transcribed as polycistronic RNAs, are translated on mitochondrial ribosomes, and assembled into the IMM. TCA, tricarboxylic acid cycle. Illustrated by Anusha Valpadashi.

The foremost role of mitochondria is still considered energy production and they are often referred to as powerhouses of the cell. They produce a large portion of the cellular ATP via oxidative phosphorylation (OXPHOS) in which electrons are transported from the reduced substrates such as NADH and $FADH_2$ to molecular oxygen as the final electron acceptor. Four protein complexes (complex I, II, III, and IV) of the OXPHOS system, located in the IMM, facilitate the transport of the electrons. Consequently, a proton (H^+) gradient is created across the membrane. Finally, complex V of the OXPHOS system, the ATP synthase, exploits the electrochemical gradient across the IMM to produce ATP by transferring inorganic phosphate

group to ADP. The obtained ATP can be transported from the mitochondrial matrix to the cytosol.

Mitochondria are semi-autonomous, meaning that they are dependent on the cytosol for their biogenesis and function. Nevertheless, mitochondria possess their own genome and gene expression system.

1.2. Mitochondrial genome

The origin of mitochondria is commonly explained by the endosymbiotic theory. According to this theory, mitochondria trace back to free-living alpha-proteobacteria that were engulfed by ancestors of eukaryotic cells and were gradually developed into present-day organelles. It is proposed that during endosymbiosis, the majority of the endosymbiont's genes were transferred to the host genome. However, mitochondria have retained a DNA genome that exists in multiple copies inside each organelle (Taanman, 1999).

Mitochondrial DNA (mtDNA) is highly conserved among animals and is usually wrapped around a set of proteins into a structure called nucleoid (Bogenhagen, 2012). In human, mtDNA is a circular double-stranded DNA of around 16.5 kbp. It is a compact genome and lacks intergenic sequences, introns, and 5'-untranslated regions (UTR) on the encoded-mRNAs (Taanman, 1999). The mtDNA contains 37 genes including 2 rRNAs, 22 tRNAs, and 13 protein-coding genes. Most of them are located on one strand of the DNA which is called the heavy strand (H-strand), due to a higher content of Guanine (G) + Adenine (A) bases. Only 8 tRNAs and one protein are encoded on the light strand (L-strand). All 13 proteins encoded by mtDNA are core subunits of the OXPHOS complexes. Together with nuclear-encoded subunits, they form the functional OXPHOS system. Genome replication, transcription and translation take place inside mitochondria. However, mitochondria are not independent of the nuclear genome. Approximately, 99 percent of the mitochondrial genome including the gene maintenance and genome expression machineries are encoded on the nuclear DNA (nDNA), synthesized in the cytosol, and transported into mitochondria (Dennerlein et al., 2017; Grevel et al., 2019; K. G. Hansen et al., 2019; Wiedemann et al., 2017) (Figure 1).

1.3. Mitochondrial biogenesis

Mitochondria play important roles in sustaining the metabolic homeostasis of the cells. Therefore, they must be maintained in sufficient levels in terms of mitochondrial mass and

function. This is achieved via a fine balance between mitochondrial biogenesis and degradation of the defective ones (mitophagy) (Popov, 2020). Mitochondrial biogenesis is the process of increasing mitochondrial mass and number through the growth and fission of the existing mitochondria. Mitochondria usually form an interconnected network within a cell. The network can dynamically change via fission and fusion which partially regulate mitochondrial metabolism and preserve their quality (Sebastián et al., 2018). For the biogenesis of mitochondria, all components have to be synthesized and supplied to the new organelle, including the outer and inner mitochondrial membranes, mitochondrial proteins (both nuclear- and mitochondrial-encoded ones), and sufficient copy number of mtDNA (Popov, 2020).

The main regulator of mitochondrial biogenesis is the peroxisome proliferator-activated receptor-γ coactivator-1α (PGC-1α). Upon activation, PGC-1α increases the expression of several transcription factors that results in the synthesis and import of mitochondrial proteins including subunits of the OXPHOS complexes (Jornayvaz et al., 2010; Virbasius et al., 1994). One of the main factors that is upregulated upon activation of PGC-1α is mitochondrial transcription factor A (TFAM). TFAM is an important regulator of mtDNA replication and transcription (Parisi et al., 1993). It is encoded on the nuclear DNA, synthesized in the cytosol, and imported into the mitochondria. TFAM regulates mtDNA copy number, stability, and expression (Falkenberg, 2018). In addition to TFAM, upregulation of several other components of the mitochondrial gene expression system occurs in the process of mitochondrial biogenesis (Puigserver et al., 1998; Wu et al., 1999).

Multiple cellular factors stimulate mitochondrial biogenesis through activation of PGC-1α and TFAM. Low energy level of the cells depicted by high AMP/ATP or NAD^+/NADH ratio activates the mitochondrial biogenesis pathway either by increasing PGC-1α transcription or its post translational modification. Moreover, high intracellular Ca^{2+} induces expression of PGC-1α and TFAM through different signaling cascades (Ojuka et al., 2003; Wright et al., 2007). The pathways mediated by elevated AMP or Ca^{2+} levels can result in phosphorylation of cAMP-response element binding protein (CREB) that binds to the PGC-1α promoter and activates its transcription (Handschin et al., 2003; Herzig et al., 2001). CREB is also known to localize to mitochondria, bind to mtDNA and change the expression of mitochondrial-encoded proteins (Cammarota et al., 2002; J. Lee et al., 2005; Marinov et al., 2014).

Altogether, there seems to be a pivotal association between mitochondrial genome and gene expression and the biogenesis of functional mitochondria.

1.3.1. Mitochondrial biogenesis in neurons

Neurons have a complex morphology that is specialized to transmit information in the nervous system. They form long processes of the dendrites and axons extending from the cell body where the nucleus is located (soma). The information is transmitted along the neurons in the form of action potentials and passes to the next cell through special cellular junctions termed synapses. In chemical synapses, action potential causes the release of neurotransmitter from the synaptic vesicles into the synaptic cleft in order to act on the next neuron or the effector cell (Jahn et al., 2012). Mitochondria are an essential part of the majority of both pre- and postsynapses. Neuronal development and synaptic transmission are highly energy demanding processes that rely on the ATP produced by mitochondria (Hall et al., 2012; Pathak et al., 2015). In addition, Ca^{2+} signaling plays a crucial role in the excitability and neurotransmitter release at the synapse (KATZ et al., 1967; Sudhof, 2012). Ca^{2+} transporters located in the mitochondrial membrane together with the channels and transporters of the endoplasmic reticulum and the plasma membrane cooperate to modulate Ca^{2+} level at the synapse (Gleichmann et al., 2011; K.-S. Lee et al., 2018).

Impaired mitochondrial biogenesis is associated with many neurodegenerative disorders such as Huntington's, Parkinson's and Alzheimer's diseases (L. Cui et al., 2006; Shin et al., 2011; Uittenbogaard et al., 2014). A close coordination between the expression of nuclear-encoded proteins and mitochondrial gene expression is required for the biogenesis of mitochondria. How is mitochondrial biogenesis organized in neurons with long neural processes in which mitochondria locate in far distances from the soma? Although the answer is not fully known, two possible routes can maintain mitochondrial homeostasis away from the soma (Cardanho-Ramos et al., 2021): Transport of mitochondria in both directions between the soma and the terminal synapses (Sheng, 2014; Sheng et al., 2012) and local biogenesis of mitochondria at the synapse (Figure 2).

It is assumed that mitochondrial biogenesis occurs mainly in the soma and mitochondria are transported to the synapse to fulfill their function. Defected organelles can also be removed from the synapse with retrograde transport to the soma. Although it is technically challenging

to measure the speed of mitochondrial transport in neurons, many studies have estimated it to be in the range of 0.1-2 µm/s (Bros et al., 2015; MacAskill et al., 2010).

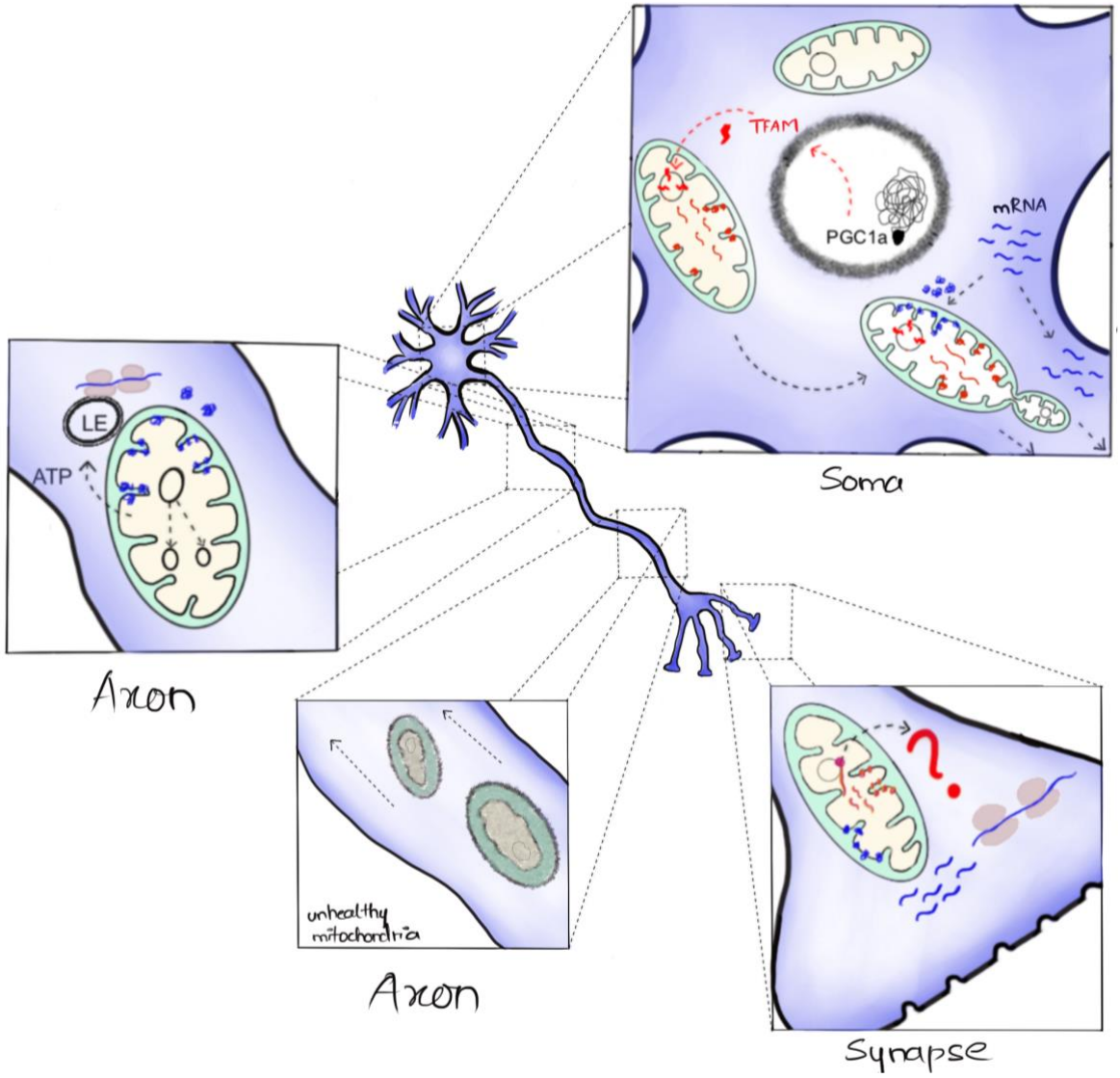

Figure 2. Mitochondrial biogenesis in neurons. The main regulator of the mitochondrial biogenesis, PGC-1α, activates several transcription factors in the nucleus, which leads to the activation of the mitochondrial transcription factor A (TFAM), increases the synthesis of mitochondrial RNA and proteins. mtDNA is replicated in both soma and along the axon. Fresh mitochondria and mitochondrial mRNAs are transported along the axon. While unhealthy mitochondria are transported back toward the soma. Local synthesis of mitochondrial proteins occurs both in the axon and at the synapse. Late endosomes (LE) act as a platform for protein synthesis in the axon. Newly-synthesized proteins are imported into the mitochondria and are assembled into functional complexes. Whether mitochondrial-encoded proteins are synthesized locally at the synapse was not shown before the start of this project. Illustrated by Anusha Valpadashi.

This speed might not be efficient for supplying the new mitochondria especially to the long motor neurons. Besides, only a small portion of mitochondria are mobile at a time and this process decreases with age (Lewis et al., 2016; Misgeld et al., 2007). On the other hand, synapses have been shown to contain many mRNA transcripts and protein synthesis

machineries (Hafner et al., 2019). Local synthesis of proteins that are important for synaptic function, has been detected at the synapse (Rosenberg et al., 2014; Truckenbrodt et al., 2018) and mitochondria fuel this local translation (Rangaraju et al., 2019). Therefore, the biogenesis of mitochondrial proteins can occur at the synapse. This hypothesis has been further strengthened by several observations. mtDNA replication has been observed in the axon (Amiri et al., 2008; van Laar et al., 2018). Moreover, mRNA transcripts encoding mitochondrial proteins have been shown to move along the axon on endosomes (Cioni et al., 2019) and being ultimately translated at the synapse (A. Aschrafi et al., 2008; Natera-Naranjo et al., 2012). In transcriptome analysis of the axons of sympathetic neurons, more than 100 nuclear-encoded mitochondrial mRNAs were enriched (Armaz Aschrafi et al., 2016; Cioni et al., 2018). Quantitative mass spectrometry of the local protein synthesis in stimulated synaptoneurosomes revealed numerous mitochondrial proteins (Kuzniewska et al., 2020). These proteins were shown to be imported into the mitochondria and assembled into the functional complexes. Likewise, mRNAs coding for mitochondrial proteins have been detected in association with the poly-ribosomes at the synapse (Kuzniewska et al., 2020). Together, these studies support the idea that mitochondrial biogenesis may take place, at least partially, away from the soma. Whether local biogenesis of mitochondria at the synapse includes the expression of the genes on the mtDNA is not known.

1.4. Gene expression in mitochondria

As mentioned, mtDNA codes for only 37 genes. Nevertheless, 20-25% of the mitochondrial proteome is imported into the mitochondria to maintain the mtDNA and regulate the expression of its 37 genes (Morgenstern et al., 2017; Richter-Dennerlein et al., 2015; Sickmann et al., 2003). Therefore, it is essential to understand the mechanisms underlying gene expression and regulation in mitochondria.

1.4.1. Mitochondrial transcription

In mtDNA, most genes are located consecutively, including two genes, which even have overlapping regions (Anderson et al., 1981). Therefore, it is not surprising that the genes are transcribed as polycistronic RNAs. One transcription promoter region on the L-strand (LSP) and two on the H-strand (HSP1 and HSP2) are the binding sites for the transcription factors (TFAM and TFB2M). TFAM recruits mitochondrial RNA polymerase (POLRMT) and TFB2M

mediates the rewinding of the mtDNA and opening of the promoter (Falkenberg et al., 2002). The mitochondrial transcription elongation factor (TEFM) increases the processivity of the POLRMT through facilitating the interaction with the DNA-RNA template (D'Souza et al., 2018; Minczuk et al., 2011).

The products of the mitochondrial transcription are two polycistronic transcripts synthesized from both strands of the mtDNA. In the transcript of the H-strand, most tRNAs are positioned between the protein-coding and rRNA genes (Anderson et al., 1981; Montoya et al., 1981). The polycistronic transcripts are processed by ribonuclease P (RNase P) and ribonuclease Z (RNaseZ, also named ELAC2) cleaving the tRNAs on the 5' and 3' ends, respectively, and releasing the individual transcripts (Bhatta et al., 2021). This model is known as "tRNA punctuation model of RNA processing" (Ojala et al., 1981). However, not all of the mRNA transcripts are flanked by tRNAs at both sides. A family of Fas-activated Serine/Threonine kinases (FASTK) is proposed to be involved in the processing of these mRNA transcripts (Boehm et al., 2017; Jourdain et al., 2017; Ohkubo et al., 2021). Overall, The processing of the long mitochondrial transcripts, releases monocistronic mRNAs. Exceptions are the mRNAs of MTATP8/MTATP6 and MTND4/MTND4-L that have overlapping open reading frames.

All mRNAs except for MTND6 (coded on the L-strand) are polyadenylated by mitochondrial poly(A) polymerase (mtPAP). The stop codon on 7 of these mRNAs is formed after the polyadenylation. Interestingly, polyadenylation changes the stability in a transcript-specific manner (D'Souza et al., 2018).

1.4.2. Mitochondrial translation

Mitochondrial-encoded proteins are synthesized by the mitochondrial ribosome (mitoribosome) which is significantly smaller than the cytosolic and the bacterial counterparts (D'Souza et al., 2018). Furthermore, the RNA content is significantly less (30 percent comparing to 70 percent in bacteria) while the protein content is higher in mitoribosomes, such that some RNA binding domains are absent and the space is filled with proteins (Amunts et al., 2015; Greber et al., 2014, 2015; Kaushal et al., 2014).

Recognition of the start codon is not fully understood in mitochondrial mRNAs as they lack a Shine-Dalgarno sequence or Kozak sequence. The binding of the f-Met-tRNA^{Met} and the mitochondrial small subunit (mt-SSU) happens preferentially to the first AUG codon on the

transcript (Christian et al., 2010). How an internal start codon is recognized in the bicistronic mRNAs of MTATP8/MTATP6 and MTND4/MTND4-L is not well described.

Translation in mitochondria occurs in four stages: initiation, elongation, termination, and recycling (reviewed in (Kummer et al., 2021; Mai et al., 2017)). The number of mitochondrial translation factors is significantly less compared to the cytosolic or bacterial counterparts. It is still not clear how translation is facilitated with the reduced number of factors involved. It has been suggested that some of the conserved roles are taken over by other existing factors. An example is the mitochondrial translation initiation factor 2 (mtIF2) with a conserved 37-amino acid insertion that replaces the function of bacterial initiation factor 1 (IF1) (Gaur et al., 2008).

Elongation is the most conserved step in mitochondrial translation. The first step is the new tRNA-aminoacyl positioning and the peptide bond formation, followed by translocation placing the new codon at the A-site. The membrane insertion of the nascent peptide chains is proposed to occur co-translationally in mitochondria. The protein OXA1L and the mitochondrial specific phospholipid (cardiolipin) play roles in the process (Itoh et al., 2021; R. G. Lee et al., 2020; Stiburek et al., 2007; Thompson et al., 2018).

Termination occurs when a stop codon is positioned at the A-site. The binding of the release factors and the hydrolysis of the ester bond releases the nascent peptide from the last tRNA. Mitochondria have two unconventional stop codons (AGA and AGG). Whether these stop codons are recognized by different release factors or -1 frameshifting causes the common stop codon to be exposed is still controversial (Mai et al., 2017).

Unlike yeast, in which mRNAs have unique translation activators binding to the 5’ UTR, in human, there is only one translation activator discovered so far (Dennerlein et al., 2017; Herrmann et al., 2013). Translational activator of mitochondrially encoded cytochrome C oxidase 1 (TACO1) is involved in the translation of MTCO1 and its mutant is linked to complex IV deficiency and Leigh syndrome (Weraarpachai et al., 2009). How exactly TACO1 mediates the translation of the MTCO1 mRNA is not well understood. Moreover, the synthesis of proteins inside mitochondria is strongly linked to the assembly of the OXPHOS complexes. Several assembly factors have been identified which their absence can affect the synthesis of MTCO1 (Szklarczyk et al., 2012; Weraarpachai et al., 2012). Whether more translation activators exist responsible for the translation of other mitochondrial-encoded proteins requires further investigation.

1.5. Regulation of mitochondrial gene expression

Gene expression in mitochondria is assumed to be regulated according to cellular demands (Dennerlein et al., 2017). In reverse, mitochondrial malfunction induces stress response pathways. In these stress situations, mitochondria communicate with the cytosol and the nucleus in order to reduce the protein load into the mitochondria, increase the synthesis of mitochondrial chaperones and proteases, and decrease the translation of mitochondrial-encoded proteins (Aldridge et al., 2007; Martinus et al., 1996; Münch et al., 2016; Quirós et al., 2016; Rainbolt et al., 2013). Certain stimuli such as fever or physical exercise increase mitochondrial translation and trigger the biogenesis of mitochondria (Popov, 2020). Moreover, mitochondrial translation is adapted to the availability of the nuclear-encoded subunits (Richter-Dennerlein et al., 2015). For example, during the synthesis of mitochondrial-encoded cytochrome c oxidase I (MTCO1), mitoribosome is stalled. It is only released and completes the synthesis if the nuclear-encoded COX4 subunit is present (Richter-Dennerlein et al., 2016). This model of translational plasticity allows the coordination of subunits from two genetic origins in forming functional OXPHOS complexes. Our knowledge about the mechanisms involved in the modulation of gene expression in mitochondria are expanding. Every stage of the gene expression process can be regulated including mtDNA stability and copy number, transcription, RNA modification and turnover, ribosome assembly, and translation (Kummer et al., 2021). The proteins responsible for modulating mitochondrial gene expression are encoded entirely in the nucleus, synthesized in the cytosol and are imported into mitochondria.

Some of the regulatory proteins play their roles by binding to mRNA and modulating RNA processing and stability (Jedynak-Slyvka et al., 2021). For example, leucine-rich PPR-motif-containing protein (LRPPRC) in complex with steroid receptor RNA activator (SRA) stem-loop interacting RNA-binding protein (SLIRP) act as a general chaperone for mRNAs (Sondheimer et al., 2010). The LRPPRC-SLIRP complex stabilizes the mRNA transcripts and promotes their polyadenylation (Ruzzenente et al., 2012). Moreover, it fosters the translation of the mRNAs, supposedly by delivering them to the mitoribosomes (Sasarman et al., 2010).

Another family of mitochondrial RNA binding proteins is the FASTK family, originally found to function in the nuclei and the cytosol (Tian et al., 1995). Members of this family play roles in mitochondrial mRNA maturation, stability, and translation. Their function is specific towards

subsets of mRNAs and in some cases, they even show opposing effects. For example, while FASTKD4 stabilizes the majority of mRNAs, FASTKD1 and FASTKD3 destabilize the mRNA encoding MTND3, and FASTKD3 increases the translation of MTCO1, specifically (Jourdain et al., 2017).

Another RNA-binding protein is mitochondrial transcription rescue factor 1 (MTRES1). Its putative roles in both mitochondrial transcription and translation have been recently described in different studies (Gopalakrishna et al., 2019; Kotrys et al., 2019). The exact mechanism of action is not known. However, it has been shown to associate with POLRMT. Moreover, knockout of MTRES1 is suggested to decrease the mitochondrial mRNA association to the mitoribosome diminishing translation (Gopalakrishna et al., 2019).

Post-transcriptional modifications (PTM) have been detected in all types of mitochondrial RNAs (Bohnsack et al., 2017). Methylation and pseudouridylation are the most prominent modifications in all types of mt-RNAs. Modification of the rRNA changes its folding and assembly into the mitoribosomes. mt-tRNA modifications modulate the recognition of unconventional codons and the stability (Haag et al., 2016; Suzuki et al., 2020; Van Haute et al., 2017). In addition to the poly-adenylation that affects the stability of the mt-mRNAs, pseudouridylation is found in several nucleotides of mt-mRNAs. The exact role of these modifications in the expression of the mt-mRNAs are not well understood, however, the pattern seems to reflect environmental signals (Carlile et al., 2014).

Major RNA processing and maturation occur in distinct structures called mitochondrial RNA granules (MRGs) (Antonicka et al., 2015). MRGs are close to the mitochondrial nucleoids and many RNA modifying enzymes, mitoribosome assembly factors and subunits have been detected there. Therefore, they are considered as regulation hubs for the gene expression in mitochondria (Pearce et al., 2017).

1.5.1. Phosphorylation in regulation of mitochondrial gene expression

Phosphorylation plays a critical role in the regulation of many mitochondrial processes. Phosphoproteomic data has shown that around 40 percent of the mitochondrial proteome is phosphorylated (Giorgianni et al., 2014; Kruse et al., 2017) and an increasing number of kinases are being described to either localize to mitochondria or to have mitochondrial targets (Kotrasová et al., 2021; Lucero et al., 2019). Phosphorylation of proteins in the OMM modulates mitochondrial fission/fusion and mitophagy (Cribbs et al., 2007; Kashatus et al.,

2015; Toyama et al., 2016). Besides, phosphorylation of several components of the translocase machineries in the OMM regulate import into mitochondria (O. Schmidt et al., 2011; Walter et al., 2021). Important metabolic pathways inside mitochondria are controlled via phosphorylation, as well (Kotrasová et al., 2021; Lushchak et al., 2014). An example is the protein complex of pyruvate dehydrogenase (PDC) which links glycolysis in the cytosol to the citric acid cycle and fatty acid synthesis in mitochondria. The activity of PDC is regulated by multiple reversible phosphorylations (Haan et al., 2016; Linn et al., 1969; Rardin et al., 2009). The OXPHOS system in mitochondria is also subject to phosphorylation as many of the subunits from different complexes have been shown to be phosphorylated. These modifications alter the mitochondrial respiration activity and ATP production in response to different stimuli (Kotrasová et al., 2021).

In the process of genome maintenance and gene expression, several critical proteins have been found phosphorylated in different organisms (Cho et al., 2001). TFAM has been shown to have several potential phosphorylation sites in the positions that are in contact with mtDNA (Rubio-Cosials et al., 2011). Phosphorylation of TFAM impairs its binding ability to the mtDNA and decreases mitochondrial transcription (Lu et al., 2013). The activity of other transcription and translation factors such as mitochondrial termination factor 1 (mTERF1) and mitochondrial elongation factor Tu (mEF-Tu) is also modulated by phosphorylation. Mitochondrial CREB, when phosphorylated through cAMP-mediated signal transduction pathways, promotes the synthesis of mitochondrial-encoded proteins (Acin-Perez et al., 2009; de Rasmo et al., 2009, 2010; J. Lee et al., 2005; Ryu et al., 2005).

Another potential aspect of regulation is the phosphorylation of the mitoribosome subunits (Koc et al., 2012). Many phosphorylated ribosomal proteins have been identified upon *in vitro* phosphorylation and also in steady state analysis with anti-phosphorylation immunoblotting (J. L. Miller et al., 2009). Many of the detected subunits have phosphorylated homologs in bacteria and most of them are located at the critical functional domains of the mitoribosome. *In vitro* phosphorylation of the mitoribosome was shown to decrease its ability in protein synthesis (J. L. Miller et al., 2009). With the new advancements of mass spectrometry in detecting phosphorylated proteins, the knowledge on phosphoproteome of mitochondria is rapidly expanding. Many questions are remained to be answered such as where the proteins are phosphorylated, what are their functional roles, and which are the effective kinases.

Altogether, phosphorylation serves as an important regulatory strategy that can adapt mitochondrial gene expression and metabolism to the cellular context.

1.6. Diseases related to mitochondrial gene expression

Mitochondrial diseases are a group of genetically and clinically diverse disorders that lead to malfunctions of the mitochondrial OXPHOS system (Gorman et al., 2016; Mai et al., 2017). Mitochondrial diseases usually show a broad range of organ-specific clinical representations, with severe phenotypes in heart, liver, skeletal muscle, and brain (Area-Gomez et al., 2019; Dimauro, 2019). The incidence rate of mitochondrial diseases is estimated 1 in 5000 individuals (Gorman et al., 2015). A recent analysis of the human mitochondrial proteome revealed that defects in about one third of mitochondrial proteins are associated with diseases (Morgenstern et al., 2021). Many of these proteins are responsible for gene expression in mitochondria.

The defects leading to impaired mitochondrial gene expression can originate from mutations in the nuclear genes encoding mitochondrial proteins or in the mtDNA. It is estimated that 1 in 200 healthy persons carries a pathogenic mtDNA mutations that can potentially cause mitochondrial diseases in the offspring of the female parents (Elliott et al., 2008).

Upon mutation in the mtDNA, the clinical manifestations of the disease depend on the level of heteroplasmy. Heteroplasmy is the ratio of mutated to wildtype copies of mtDNA. The threshold ratio for showing the disease phenotype can differ depending on the gene. Disease-causing mutations have been observed in most mitochondrial protein-coding genes, besides rRNAs and tRNAs (Russell et al., 2014). These mutations usually lead to malfunction of either one or several OXPHOS complexes and the consequent defects in mitochondrial ATP production (Gorman et al., 2016).

1.7. Methods for studying gene expression in mitochondria

Gene expression and the regulatory mechanisms have been studied extensively in the nuclear genome using broadly available techniques. Technologies have been developed for manipulating genes, RNAs, or proteins of interest to study the subsequent effects in cells or *in vivo*. Many of the techniques are applicable to mitochondria. However, manipulating the mitochondrial genome and gene expression is not as advanced as of the nuclear genome. Improving the tools for analyzing the mitochondrial genome and gene expression is required

for designing experiments that help to understand the mechanisms of mitochondrial gene expression and regulation at different levels (Apostolopoulos et al., 2022).

1.7.1. Analyzing mtDNA

The human mitochondrial genome was the first complete genome sequence that was documented and published in 1981 (Anderson et al., 1981). There is a huge polymorphism in the sequence of mtDNA among different ethnic groups (Lott et al., 2013). For diagnosis purposes, methods have been developed to detect common mtDNA point mutations and large deletions using targeted PCR assays and southern blotting (He, 2002; Moraes et al., 2003). Whole genome sequencing is the gold standard to detect any modifications in the nucleotide composition of the mtDNA (Chen et al., 2021; Wang et al., 2011). However, traditional Sanger sequencing has a limitation in detecting low-level heteroplasmic mutations and distinguishing nuclear homologs of mitochondrial DNA (H. Cui et al., 2013). A more recent technology is called massively parallel sequencing and it analyzes the whole mtDNA as a single amplicon that is enriched with a long-range PCR approach (Zhang et al., 2012).

In addition to the sequence of mtDNA, its absolute copy number is another critical factor in studying the mitochondrial genome as it is associated to aging processes and many disorders such as mtDNA depletion syndromes, neurodegenerative diseases, and cancers (Filograna et al., 2021). Various techniques are available to label and quantify mtDNA copy number that are based on Southern blotting, real-time polymerase chain reaction (RT-PCR), fluorescent labeling, and microscopy (Nicklas et al., 2004; Prole et al., 2020; Wheeler et al., 2019). While Southern blotting with labeled probes is semi-quantitative and requires more DNA sample, RT-PCR provides high sensitivity and can be adjusted in order to obtain the absolute copy number of mtDNA. Fluorescence-based methods allow to study mtDNA in single-cell resolution (Brüser et al., 2021). Diverse probes with different properties are available and can be used depending on the purpose of the study in live and fixed conditions such as DNA binding dyes, fluorescent nucleotide analogues, fluorescently-tagged DNA binding proteins and DNA antibodies (Boutorine et al., 2013).

1.7.2. Analyzing mitochondrial gene expression at transcription level

The number of mitochondrially encoded RNA species is limited, therefore, the conventional complementary hybridization techniques such as Northern blot are feasible to analyze the

steady state level of the individual RNAs (Heddi et al., 1993). Moreover, the copy number of each RNA can be quantified using specific primer sets and RT-PCR (Mercer et al., 2011). While Northern blotting is semi-quantitative and time-consuming, RT-PCR offers a more sensitive high-scale quantification.

Additionally, high-throughput transcriptome methods, such as microarray libraries and RNA-sequencing (RNA-seq), also cover mitochondrial RNAs (Crimi et al., 2005; Mercer et al., 2011). A more recent approach for quantifying specific RNA transcripts is nanoString nCounter Technology that is based on microarrays and hybridization of predesigned probes to the target transcripts. Each probe is conjugated to a set of fluorophores and the unique order of fluorophores functions as a color barcode on each probe. After hybridization, the probes are fixed and aligned on an electric field and scan-imaged with a simple microscope. Analyzing the barcode images provides a quantification for respective transcripts. Unlike RNA seq, an amplification step is not required and the analysis is simpler in nanoString nCounter Technology. The method has been extended for RNA transcripts quantification in a single-cell resolution manner.

1.7.3. Analyzing mitochondrial gene expression at translation level

The steady state and the synthesis rate of mRNA transcripts provide a valuable overview on the gene expression in mitochondria. However, many known and unknown factors break the positive correlation between the level of transcripts and the respective synthesized proteins (Pearce et al., 2017). Post-transcriptional modifications, secondary structure of the transcript, the charge and the folding of the nascent peptide are some of the factors that can influence the rate of ribosome activity and, subsequently, protein synthesis. Therefore, direct approaches are required for monitoring gene expression at the ribosome and translation level (Figure 3).

One useful method is ribosome profiling, in which the fragments of transcripts that are bound to the ribosomes are analyzed at any given time (Ingolia et al., 2009, 2012). Ribosome binding to the fragments protects them from RNase treatment. The protected transcript fragments are applied to deep sequencing revealing the ribosome footprints. The more a transcript is being synthesized, the more abundant is the fragment in the ribosome footprint. Moreover, ribosome stalling at any step can change the binding profile. This method has been used to

study the dynamic of the translation and the mechanism of ribosomes in mitochondria (Gao et al., 2018; Rooijers et al., 2013).

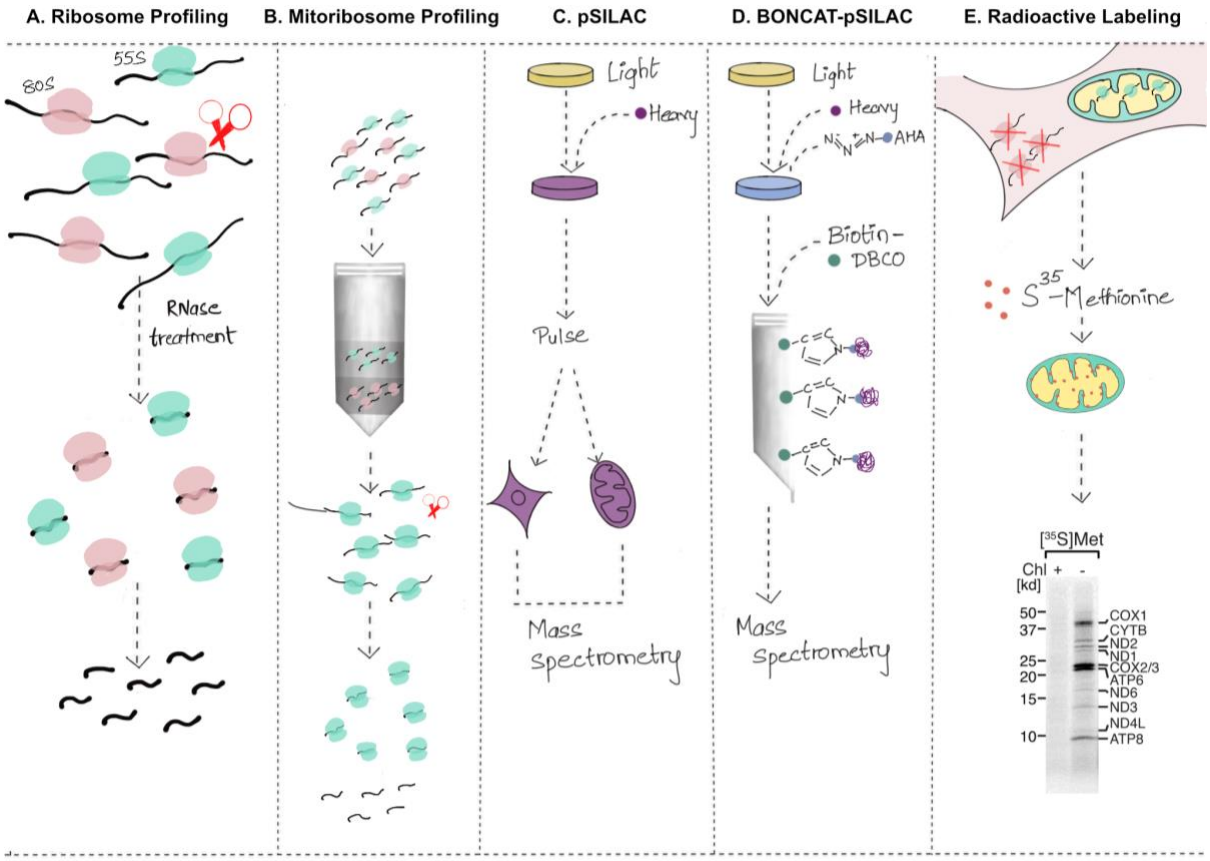

Figure 3. Methods to analyze gene expression at translation level in mitochondria. (A) Ribosome Profiling: mRNA fragments bound to the cytosolic and mitochondrial ribosomes are analyzed by deep sequencing. **(B) Mitoribosome Profiling:** purification of the mitoribosomes by ultracentrifugation enriches the mitochondrial-encoded mRNAs. **(C) pSILAC:** Newly synthesized proteins can be labeled in a pulse with a heavy isotope contained amino acid and detected with mass spectrometry. **(D) BONCAT-pSILAC:** To enrich the low abundant proteins such as mitochondrial-encoded ones in pSILAC approach, a parallel labeling with a click chemistry compatible amino acid homolog (eg. L-Azidohomoalanine, AHA) can be used as an affinity tag, reacted to biotin-DBCO through strain promoted cycloaddition and captured on streptavidin columns. **(E) Radioactive labeling:** Newly synthesized mitochondrial-encoded proteins are labeled using [^{35}S]-methionine in the presence of an inhibitor for cytosolic ribosomes. The labeled proteins are revealed by autoradiography. Radioautograph adapted from Yousefi et al., 2021. Illustrated by Anusha Valpadashi.

A different strategy for measuring the level of protein synthesis is to label nascent peptides that are actively elongated at the ribosomes (Apostolopoulos et al., 2022). This is achieved by either incorporating amino acid analogs in the elongating nascent peptide in an approach that is called metabolic labeling or placing a tag such as puromycin on the nascent peptide (Beynon et al., 2005; E. K. Schmidt et al., 2009). Puromycin is a translation inhibitor that covalently binds to the nascent peptide and releases it from the ribosome. Specific antibodies against puromycin can detect the labeled nascent peptides. Alternatively, chemical modifications of

puromycin are available that allow different detection strategies, such as biotinylated puromycin that can be detected with streptavidin (Aviner, 2020). Despite its wide application in labeling cytosolic translation products, mitochondrial-encoded peptides have not been exclusively labeled and monitored with puromycin. However, metabolic labeling with radioisotope amino acids has been extensively applied to label mitochondrial translation products since the 90's (Chomyn, 1996). In this approach, mainly [^{35}S]-methionine is added to cultured cells or isolated mitochondria while cytosolic translation is inhibited. The mitoribosomes incorporate the labeled methionine into the newly synthesized proteins which are then separated on SDS page gels and visualized by autoradiography. This labeling method is fast and reliable and with a good separation, all the proteins can be detected and their synthesis level can be compared in different conditions.

A metabolic labeling approach can be combined with global mass spectrometry (MS) proteomics in order to increase the yield and the sensitivity of the detection. One example is the pulsed Stable Isotope Labeling of Amino acid in Cell culture (pSILAC) in which the newly synthesized protein pool is labeled with heavy-isotope-contained arginine or lysine in a given time and detected with MS alongside with the old non-labeled protein pool (Fierro-Monti et al., 2013). Similar approaches have been used to study the turnover of mitochondrial proteins in yeast and human (Bogenhagen et al., 2020; Saladi et al., 2020). However, due to the low abundance and high hydrophobicity, the full coverage of all mitochondrial-encoded proteins is difficult to achieve. Enriching labeled proteins by purifying mitochondria might help to overcome the problem (Imami et al., 2021). Another potential enrichment technique is combining the pSILAC approach with Bio-Orthogonal Non-canonical Amino acid Tagging (BONCAT, (Bagert et al., 2014; Dieterich et al., 2006; Howden et al., 2013)). The main principle of BONCAT is the specific reaction between an alkyne and an azide moiety via Cu(I)-catalysed azide-alkyne cycloaddition (CuAAC). Amino acid analogs containing either an azide or an alkyne group are incorporated into the elongating polypeptides at the ribosome and are afterward reacted to the complementary alkyne or azide-conjugated probes. Fluorescent variation of BONCAT has been used to detect newly synthesized proteins in the cytosol (Dieterich et al., 2010). Fluorescent Non-canonical Amino acid Tagging (FUNCAT) uses azide- or alkyne-fluorophores to detect the proteins under the microscope. This method was specifically developed to detect local protein synthesis in the neurons and synapse (Dieterich et al., 2010; Hafner et al., 2019; Kos et al., 2016).

Altogether, progress has been made in the methodologies to detect newly synthesized proteins. Specifically, non-canonical amino acids and CuAAC reactions have provided versatile tools for studying instant protein translation. Nevertheless, most of the methods were established for cytosolic translation or have limited applications for detecting the newly-synthesized mitochondrial-encoded proteins. Additionally, most of the developed techniques lack a spatial resolution to distinguish mitochondrial transcription and translation within a cell. The latter is specifically essential when there are different pools of mitochondria in highly specialized cells, such as neurons and cardiomyocytes.

1.8. Aim of this project

Mitochondria sustain the metabolic homeostasis of the cells and provide most of the energy required for cellular functions. Mitochondrial biogenesis is dependent on the nuclear genome and cytosolic protein synthesis and is modulated by the activation of several nuclear-encoded proteins (Popov, 2020). Mitochondrial gene expression is tightly associated with the process of mitochondrial biogenesis. In distal regions of neurons, replication of mtDNA and synthesis of multiple mitochondrial proteins suggest that mitochondrial biogenesis can happen locally (Cardanho-Ramos et al., 2021). Whether mitochondrial-encoded proteins are also synthesized locally and how gene expression and mitochondrial biogenesis are coordinated in the distal regions of neurons is not well understood.

Techniques are available to analyze mitochondrial gene expression both at the mRNA and protein levels. However, current methods do not provide a spatial resolution in order to study the heterogeneity of mitochondrial translation among different cells. Moreover, within a single cell, different populations of mitochondria might express their genome distinctly. A single cell resolution has been missing in studying mitochondrial gene expression. This becomes particularly important in studying mitochondrial biogenesis in specialized cells such as neurons.

Taking this into account, in the first part of this project, we aimed to develop a method to label and visualize newly translated mitochondrial proteins in single cells. Besides the spatial resolution, specificity and the sensitivity were of great importance. We were particularly interested to apply this method in neurons, as highly polar and specialized cells in which mitochondria are distributed far away from the nucleus. Moreover, mitochondrial biogenesis and turnover could be addressed in the context of mitochondrial translation in the synaptic

regions of the neurons. To this end, we focused on fluorescence-based labeling and microscopy to have the desired cellular resolution in studying mitochondrial translation. In the next chapter, I report the result of this project which was published as an original article in EMBO Reports.

For the second part of this project, using the developed labeling strategy, we focused on finding new factors which play roles in the regulation of gene expression in mitochondria with the aim of introducing new pathways and proteins involved in this process. In order to achieve this purpose, establishing a high throughput framework for screening the effect of different factors in mitochondrial protein synthesis was necessary. Considering the importance of reversible phosphorylation in modulating mitochondrial function and an emerging number of kinases associated to mitochondria, we aimed to explore the role of cellular kinases in mitochondrial gene expression. The result of this project is communicated in chapter 3 as a manuscript prepared for submission.

Chapter 2: First Manuscript

“Monitoring mitochondrial translation in living cells”

Monitoring mitochondrial translation in living cells

Published in EMBO Reports (2021)22:e51635

Roya Yousefi, Eugenio F. Fornasiero, Lukas Cyganek, Julio Montoya, Stefan Jakobs, Silvio O. Rizzoli*, Peter Rehling* & David Pacheu-Grau

1 Department of Cellular Biochemistry, University Medical Center Göttingen, D-37073 Göttingen, Germany.

2 Department of Neurophysiology, University Medical Center Göttingen, D-37073 Göttingen, Germany.

3 Clinic for Cardiology and Pneumology, University Medical Center Göttingen D-37075 Göttingen, Germany.

4 German Center for Cardiovascular Research (DZHK), partner site Göttingen, D-37075, Germany.

5 Departamento de Bioquímica, Biología Molecular y Celular, Universidad de Zaragoza, Zaragoza, Spain.

6 Centro de Investigaciones Biomédicas en Red de Enfermedades Raras (CIBERER), Madrid, Spain.

7 Instituto de Investigación Sanitaria de Aragón (IIS Aragón), Universidad de Zaragoza, Zaragoza, Spain.

8 Department of NanoBiophotonics, Max Planck Institute for Biophysical Chemistry, 37077 Göttingen, Germany.

9 Clinic of Neurology, University Medical Center Göttingen, D-37075 Göttingen, Germany.

10 Cluster of Excellence "Multiscale Bioimaging: from Molecular Machines to Networks of Excitable Cells" (MBExC), University of Goettingen, Germany.

11 Max-Planck Institute for Biophysical Chemistry, D-37077, Göttingen, Germany.

Personal contribution: I performed the experiments, interpreted the data, prepared the figures, and contributed in writing the manuscript.

First Manuscript

Report

OPEN ACCESS

EMBO reports

Monitoring mitochondrial translation in living cells

Roya Yousefi[1], Eugenio F Fornasiero[2], Lukas Cyganek[3,4], Julio Montoya[5,6,7], Stefan Jakobs[8,9,10], Silvio O Rizzoli[2,10,*], Peter Rehling[1,10,11,**] & David Pacheu-Grau[1]

Abstract

Mitochondria possess a small genome that codes for core subunits of the oxidative phosphorylation system and whose expression is essential for energy production. Information on the regulation and spatial organization of mitochondrial gene expression in the cellular context has been difficult to obtain. Here we devise an imaging approach to analyze mitochondrial translation within the context of single cells, by following the incorporation of clickable non-canonical amino acids. We apply this method to multiple cell types, including specialized cells such as cardiomyocytes and neurons, and monitor with spatial resolution mitochondrial translation in axons and dendrites. We also show that translation imaging allows to monitor mitochondrial protein expression in patient fibroblasts. Approaching mitochondrial translation with click chemistry opens new avenues to understand how mitochondrial biogenesis is integrated into the cellular context and can be used to assess mitochondrial gene expression in mitochondrial diseases.

Keywords gene expression; hippocampal neuron; mitochondria; synapse; translation

Subject Categories Methods & Resources; Translation & Protein Quality

DOI 10.15252/embr.202051635 | Received 31 August 2020 | Revised 5 January 2021 | Accepted 13 January 2021 | Published online 15 February 2021

EMBO Reports (2021) 22: e51635

Introduction

Mitochondria support the metabolic and bioenergetic demands of cells. The mitochondrial oxidative phosphorylation system (OXPHOS) transforms energy from reducing equivalents into ATP. During evolution, mitochondria retained a genome (mtDNA), which encodes a small set of proteins (thirteen proteins in human), all of which are core components of the OXPHOS system. All other mitochondrial proteins are nuclear-encoded, synthesized on cytosolic ribosomes, and transported into mitochondria (Wiedemann & Pfanner, 2017; Dennerlein *et al*, 2017; Grevel *et al*, 2019; Hansen & Herrmann, 2019). Accordingly, the OXPHOS system is formed from subunits of dual genetic origin. The challenge of this compound system is that cells need to adapt the availability of the nuclear- and mitochondrial-encoded proteins to each other, in order to generate membrane protein complexes of defined stoichiometry. Mitochondrial gene expression requires DNA replication, transcription, and translation of the mtDNA. Approximately 25% of the mitochondrial proteome participates in these processes (Sickmann *et al*, 2003; Richter-Dennerlein *et al*, 2015; Morgenstern *et al*, 2017). Given the importance of gene expression in mitochondria, it is not surprising that dysfunction in any of these processes causes severe human disorders, the so-called mitochondrial disorders, which frequently affect the central nervous system, skeletal muscle and heart (Ghezzi & Zeviani, 2018; Suomalainen & Battersby, 2018; Area-Gomez *et al*, 2019; DiMauro, 2019). However, tissue-specific pathologies of mitochondrial diseases are still not well understood, especially because the local regulation of these mitochondria processes remains unclear.

In addition, in highly differentiated cells such as cardiomyocytes and neurons, different mitochondrial subpopulations appear to be dedicated to fulfill certain functions within a single cell. These discrete pools can differ in their morphology, proteome, stress response, and can undergo different regulatory pathways (Palmer *et al*, 1977; Pivovarova *et al*, 2004; Hollander *et al*, 2014; Graham *et al*, 2017). Whether gene expression is heterogeneous within different mitochondria cannot be answered with conventional biochemical approaches as they lack the spatial resolution needed.

To address mitochondrial translation with spatial resolution, we established an imaging technique that allows monitoring mitochondrial translation in the cellular context. Using this method, newly synthesized mitochondrial peptides could be specifically labeled even at short labeling times. Our analyses reveal that not all

1 Department of Cellular Biochemistry, University Medical Center Göttingen, Göttingen, Germany
2 Department of Neuro- and Sensory Physiology, University Medical Center Göttingen, Göttingen, Germany
3 Clinic for Cardiology and Pneumology, University Medical Center Göttingen, Göttingen, Germany
4 German Center for Cardiovascular Research (DZHK), Göttingen, Germany
5 Departamento de Bioquímica, Biología Molecular y Celular, Universidad de Zaragoza, Zaragoza, Spain
6 Centro de Investigaciones Biomédicas en Red de Enfermedades Raras (CIBERER), Madrid, Spain
7 Instituto de Investigación Sanitaria de Aragón (IIS Aragón), Universidad de Zaragoza, Zaragoza, Spain
8 Department of NanoBiophotonics, Max Planck Institute for Biophysical Chemistry, Göttingen, Germany
9 Clinic of Neurology, University Medical Center Göttingen, Göttingen, Germany
10 Cluster of Excellence "Multiscale Bioimaging: from Molecular Machines to Networks of Excitable Cells" (MBExC), University of Goettingen, Göttingen, Germany
11 Max-Planck Institute for Biophysical Chemistry, Göttingen, Germany
*Corresponding author. Tel: +49 551 395911; Fax: +49 551 3966031; E-mail: srizzol@gwdg.de
**Corresponding author. Tel: +49 551 395947; Fax: +49 551 395979; E-mail: peter.rehling@medizin.uni-goettingen.de

© 2021 The Authors. Published under the terms of the CC BY NC ND 4.0 license

mitochondria translate to the same extent in different cell types. Using neuronal cultures, we were able to monitor mitochondrial translation in axonal and dendritic mitochondria as well as in pre- and post-synaptic regions. Moreover, we show that the approach could be utilized to detect even small changes in mitochondrial translation and therefore to assess mitochondrial translation in cellular disease models in a quantitative manner. Here, we show a widely applicable labeling approach for imaging-based analysis of mitochondrial protein synthesis with spatial resolution.

Results and Discussion

Visualizing mitochondrial translation in the cellular context

The standard procedure to analyze mitochondrial translation is radiolabeling of newly synthesized polypeptides in intact cells or in purified mitochondria (Sasarman & Shoubridge, 2012; Pacheu-Grau *et al*, 2013; Richter-Dennerlein *et al*, 2016; Nottia *et al*, 2020). However, this approach does not allow an assessment of translation in the context of the cellular anatomy, since it lacks spatial resolution. To monitor mitochondrial protein synthesis in the context of an individual cell and to obtain quantitative information on the translation process, we devised an imaging approach, based on the fluorescent non-canonical amino acid tagging (FUNCAT) procedure (Dieterich *et al*, 2010). For this, cytosolic translation was selectively inhibited by treatment with the antibiotic Harringtonine (Fig 1A) or other translation inhibitors (Fig EV1A and B), and cells were subsequently incubated with the alkyne-containing non-canonical amino acid L-homopropargylglycine (HPG). Under these conditions, HPG is specifically incorporated into mitochondrial translation products instead of methionine and can be visualized by a subsequent copper-catalyzed cycloaddition reaction (click) to azide-containing fluorescent dyes (Fig 1A). Using this approach, we monitored mitochondrial protein synthesis in HeLa cells and obtained HPG-specific fluorescent signals that colocalized well with mitochondria. As expected for mitochondrial translation products, the fluorescent signals were sensitive to the mitochondrial translation inhibitor Chloramphenicol (Fig 1B). Similarly, when we monitored mitochondrial protein synthesis in cells lacking mtDNA (Rho0 cells), HPG-specific fluorescent signals were lost (Fig 1C), demonstrating that HPG is specifically incorporated into mitochondrial translation products under these experimental conditions.

To test whether the translation products conform to the expected nature of the OXPHOS subunits, we compared our results with the classical method of pulse labeling with [^{35}S] methionine, followed by SDS–PAGE and autoradiography (Fig 1D). HGP-labeled proteins were detected with AF488-azide, and provided a similar pattern to [^{35}S] methionine labeling, which was, as expected, sensitive to Chloramphenicol (Fig 1D).

To confirm the identity of selected proteins, we first used a mutant cell line with a defect in mitochondrial translation of COX1 (m.6930G > A). In these cells, the full-length COX1 protein is not translated (Bruno *et al*, 1999; Richter-Dennerlein *et al*, 2016). This was correctly recapitulated by the HPG-based analysis (Fig 1E, left panel). In the absence of the thiol reductase COA6, COX2 stability has been found to be strongly decreased, and thereby indirectly, the abundance of COX1 and COX3 is affected (Stroud *et al*, 2015; Pacheu-Grau *et al*, 2015, 2020; Soma *et al*, 2019). HPG-dependent labeling of mitochondrial translation products in COA6 knockout cells (COA6^{KO}) resulted in the expected pattern of the loss of COX2, COX1, and COX3 (Fig 1E, right panel).

In summary, these experiments validated the imaging strategy to visualize mitochondrial translation in cells, which could be applied to determine mitochondrial gene expression in distinct cellular regions.

Differential levels of gene expression within mitochondria of a single cell

Mitochondria are optimized to fulfill the specific metabolic demands of different cell types. While it is becoming evident that the mitochondrial proteome is able to adapt to cell and tissue demands (Mootha *et al*, 2003; Williams *et al*, 2018; Bartolomeo *et al*, 2020), it is still unclear how mitochondrial gene expression is spatially coordinated to respond to differential demands within separate areas of single cells.

To compare mitochondrial translation within a single cell, we reasoned that the labeling time could be critical, as longer pulses might impede detection of small differences between individual mitochondria. In addition, in highly differentiated cells such as neurons, that display mitochondrial trafficking within a cell, shorter labeling time would be required to address local mitochondrial protein synthesis. Therefore, we assessed the minimum labeling time to obtain robust signal of mitochondrial translation. In HeLa cells, we observed a clear mitochondrial translation signal at 2 min

Figure 1. Visualizing mitochondrial translation in the cellular context.

A Schematic presentation of the approach. Cytosolic translation is inhibited with Harringtonine (Harr), while mitochondrial ribosomes are allowed to incorporate the alkyne-containing methionine homolog (HPG, orange) into newly synthesized proteins. In fixed cells, HPG moieties are clicked to an azide-conjugated fluorophore (star, magenta), through copper-catalyzed Huisgen cycloaddition (click), and can be visualized microscopically.

B WT HeLa cells were incubated with HPG for 30 min in the presence or absence of Harr and/or Chloramphenicol (Chl). After fixation, AF647-azide (magenta) was used for click reaction (see A), and cells were immunostained for TOM20 as mitochondrial marker (green). Representative epifluorescent microscopy images are shown. Magenta images shown in the presence of only Chl and in the absence of both inhibitors (none) are presented at lower brightness level than the other panels, duo to their very strong intensities. An inset of Harr panel is zoomed in the panel below for better visualization. Met, methionine. Scale bars, 50 and 10 μm for the zoom panel.

C Mitochondrial translation products in osteosarcoma 143B control and Rho0 cell lines as described in A. Scale bars, 25 μm.

D Comparison of mitochondrial translation labeling in control HEK cells using radioactive [^{35}S]Met or HPG followed by click reaction with AF488-azide, in purified mitochondria. Samples were analyzed by SDS–PAGE and either digital autoradiography or fluorescent gel imaging.

E Similar experiments, performed by click reaction in 143B COX1 mutant cells (m.6930G > A), derived from a patient, or in COA6^{KO} HEK293T cells, in comparison to the respective controls.

 © 2021 The Authors

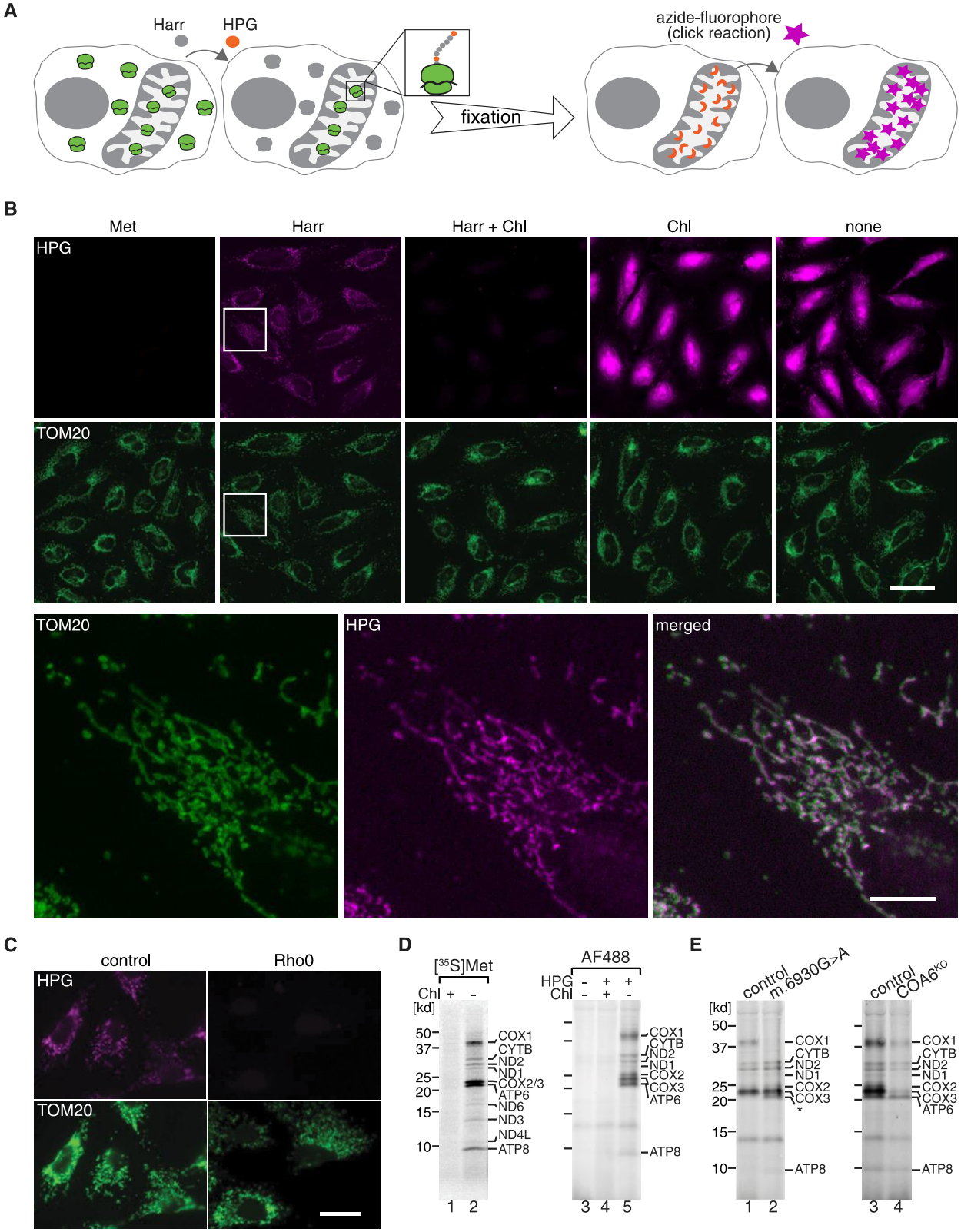
A
Harr
HPG
fixation
azide-fluorophore
(click reaction)
B
Met
Harr
Harr + Chl
Chl
none
HPG
TOM20
TOM20
HPG
merged
C
control
Rho0
HPG
TOM20
D
[35S]Met
Chl + -
[kd]
50
37
25
20
15
10
COX1
CYTB
ND2
ND1
COX2/3
ATP6
ND6
ND3
ND4L
ATP8
1 2
AF488
HPG - + +
Chl - + -
COX1
CYTB
ND2
ND1
COX2
COX3
ATP6
ATP8
3 4 5
E
control
m.6930G>A
[kd]
50
37
25
20
15
10
COX1
CYTB
ND2
ND1
COX2
COX3
*
ATP8
1 2
control
COA6KO
COX1
CYTB
ND2
ND1
COX2
COX3
ATP6
ATP8
3 4

Figure 1.

of labeling time which further increased upon extended labeling time up to 30 min (Fig 2A).

To determine the sensitivity of the technique in detecting changes in mitochondrial translation, we defined a labeling time during which the HPG incorporation remained linear (10–20 min). Next, we analyzed HPG signals in cells in 2-min time intervals. Using 25 random cells, we observed a linear increase of the detected label over time. By increasing the number of analyzed cells to 150, we detected ten percent differences between each consecutive point (Fig 2B). Accordingly, the sensitivity of the method is sufficient to detect differences of ten percent when adequate numbers of cells are assessed.

Next, we addressed if mitochondrial translation products could be identified in different cell types: human fibroblasts, human iPSCs-derived cardiomyocytes, and rat hippocampal neurons. In all three cases, mitochondrial translation products were readily detectable with only small variations among each cell type (Figs 2C and EV2A). Interestingly, the correlation analysis of newly synthesized translation products with the mitochondrial marker TOM20 identified regions of high and low mitochondrial translation, reflecting compartment specific mitochondrial translation in the cellular context of the different cell types (Figs 2C and EV2B and C). This observation was most striking in neurons, where profound differences could be noted between the spatial pattern of the mitochondria and the translation products (Fig 2C, bottom panel).

Accordingly, this labeling method allowed us to visualize actively translating mitochondria in different cell types even after short pulse times. Moreover, the spatial resolution of the technique revealed heterogeneous patterns of gene expression between mitochondria of a single cell in all the cell types.

Imaging mitochondrial translation with high resolution microscopy

Mitochondrial diseases present with many clinical manifestations affecting different tissues and organs. Defects in mitochondrial gene expression caused either by mutations in mtDNA or in nuclear-encoded factors may lead to pathologic conditions (Smits *et al*, 2010; Antonicka *et al*, 2010; Boczonadi & Horvath, 2014; Haute *et al*, 2015). Therefore, implementing new techniques to rapidly monitor mitochondrial protein synthesis in living cells derived from different tissues will be helpful for the evaluation and diagnosis of mitochondrial diseases. To address the potential of our approach as a diagnostic tool for mitochondrial disorders, we labeled mitochondrial translation products in primary fibroblast cultures from a healthy control and a patient with a mutation in the mitochondrial translation elongation factor Ts (TSFM) (Fig 3A). Interestingly, quantification of the incorporated HPG revealed an almost 60 percent decrease of mitochondrial translation in the patient cells, which correlated with the mitochondrial protein synthesis defect measured using [^{35}S] methionine radiolabeling (Fig 3A) and that had been reported previously (Emperador *et al*, 2017). In a similar fashion, mitochondrial translation products were labeled with both HPG and [^{35}S] methionine in control and COA6^{KO} cells (Fig 3B). The knockout cells showed a modest but significant decrease of mitochondrial translation, with both approaches. Accordingly, the labeling method represents a potential tool for screening defects in protein synthesis within mitochondria in a pathologic context.

To further assess the suitability of our approach to address biological questions related to the spatial organization of mitochondrial protein synthesis, we asked whether the synthesis of new proteins inside mitochondria could be localized at the suborganelle level. For that purpose, hippocampal neurons were labeled for their mitochondrial protein synthesis and further clicked with a high resolution STED compatible azide fluorophore (ATTO 590-azide) and immunostained for TOM20 to detect mitochondria (Fig 3C). The representative deconvolved STED image resolves the localization of the newly synthesized mitochondrial peptides within the chain of connected mitochondria. This confirms the potential application of the technique to study spatial localization of the mitochondrial synthesis products in a highly resolved manner.

Mitochondrial translation can be tracked compartmentally in neurons

Mitochondria provide more than 90% of the ATP that is required for neuronal activity and are thus essential for synaptic transmission (Harris *et al*, 2012). Moreover, the presence of mitochondria at synaptic boutons has been suggested to regulate the size of the synapse and the number of vesicles (Smith *et al*, 2016), and these mitochondria also appear to present a distinct proteome, specialized for energy supply (Völgyi *et al*, 2015). This finding indicates that mitochondria may undergo function-specific proteostasis in order to adapt to distinct subcellular processes. Different studies have addressed local protein synthesis at synaptic terminals and its relevance for proteome remodeling and plasticity in neurons (Richter & Klann, 2009; Hafner *et al*, 2019; Cioni *et al*, 2019). Previous studies revealed translation of mRNAs for nuclear-encoded mitochondrial proteins in pre-synaptic nerve terminals (Gioio *et al*, 2001; Kaplan *et al*, 2009). Moreover, mitochondrial proteins represent an important portion of locally synthesized proteins in synaptoneurosomes. Interestingly, many of

Figure 2. Different levels of gene expression in mitochondria of a single cell.

A Mitochondrial translation products were labeled in WT HeLa cells for indicated time lengths (heat map) and cells immunostained for TOM20 (gray). Representative confocal images are shown for each time point. The same 5-min image was used in both rows with different brightness as a reference for intensity comparison of the other time points in the row. Scale bars, 10 μm. Mitochondrial protein synthesis was quantified over time. Thirty cells from $N = 3$ independent experiments were analyzed for each time point (average of the HPG intensity in the mitochondrial area was calculated and the baseline was set to zero by subtracting the value of time point 0 from all the values. Error bars, ± SEM). A hyperbolic graph was fitted to the data. $R^2 = 0.97$.

B As in A, mitochondrial translation products were labeled for increasing time (10 and 20 min) in HeLa cells. The number of analyzed cells was increased in the plots from 25 to 300 per time point. 150 or 300 random cells from $N = 3$ independent experiments were analyzed. Kruskal–Wallis followed by Fisher's test. ****$P < 0.0001$. Error bars, ± SEM.

C Mitochondrial translation products were labeled for 30 min and clicked with AF647 (magenta) and cells immunostained for TOM20 (green) in fibroblasts, iPSCs-derived cardiomyocytes, and hippocampal neurons. Representative epifluorescent microscopy images are shown. The correlation of HPG and TOM20 channels is represented in fire lookup table, after calculating the Pearson correlation values over each pixel of the images. Scale bars, 25 μm.

 © 2021 The Authors

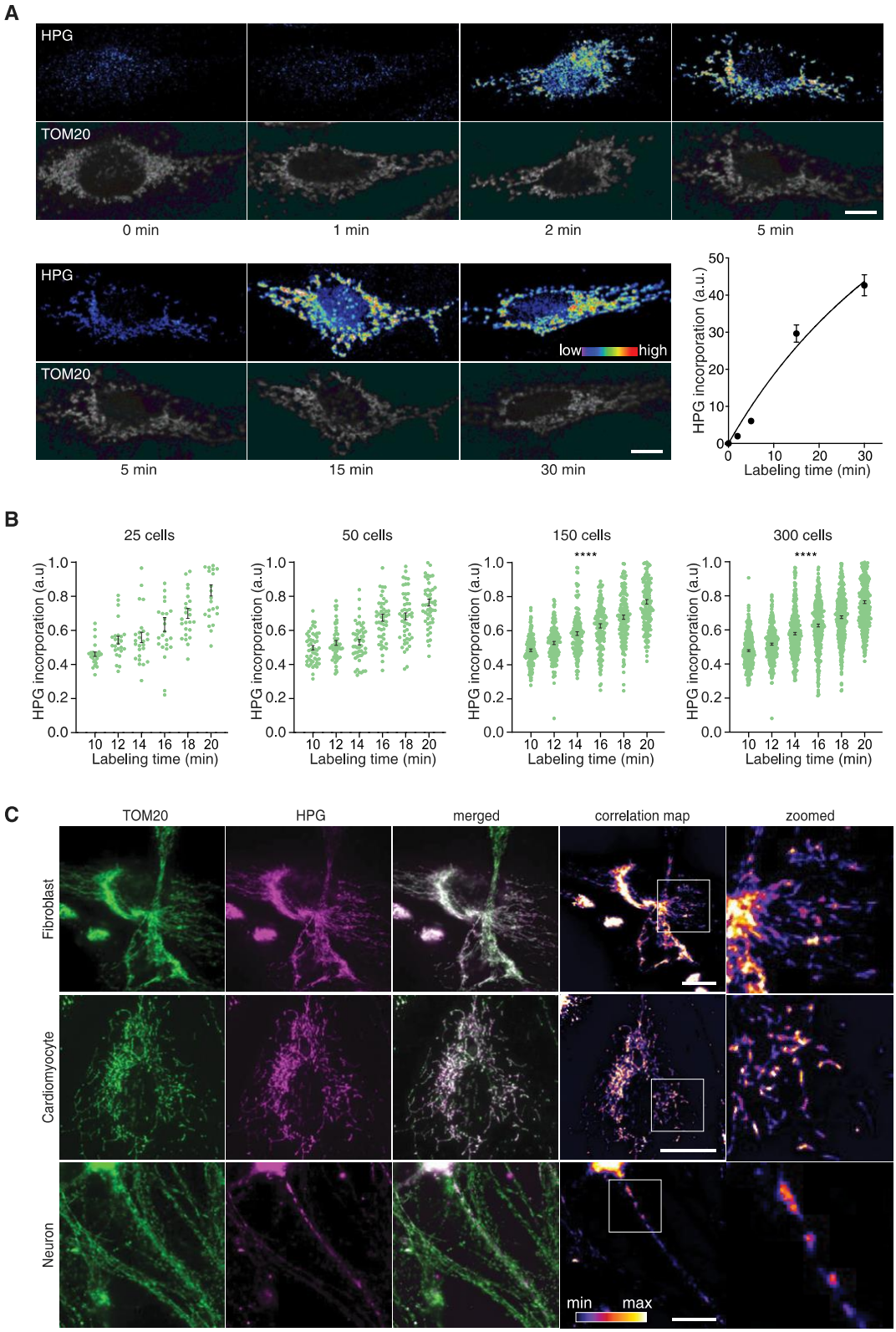
A
HPG
TOM20
0 min
1 min
2 min
5 min
HPG
TOM20
low
high
5 min
15 min
30 min
HPG incorporation (a.u.)
Labeling time (min)
B
25 cells
50 cells
150 cells
300 cells
****
****
HPG incorporation (a.u)
Labeling time (min)
C
TOM20
HPG
merged
correlation map
zoomed
Fibroblast
Cardiomyocyte
Neuron
min
max

Figure 2.

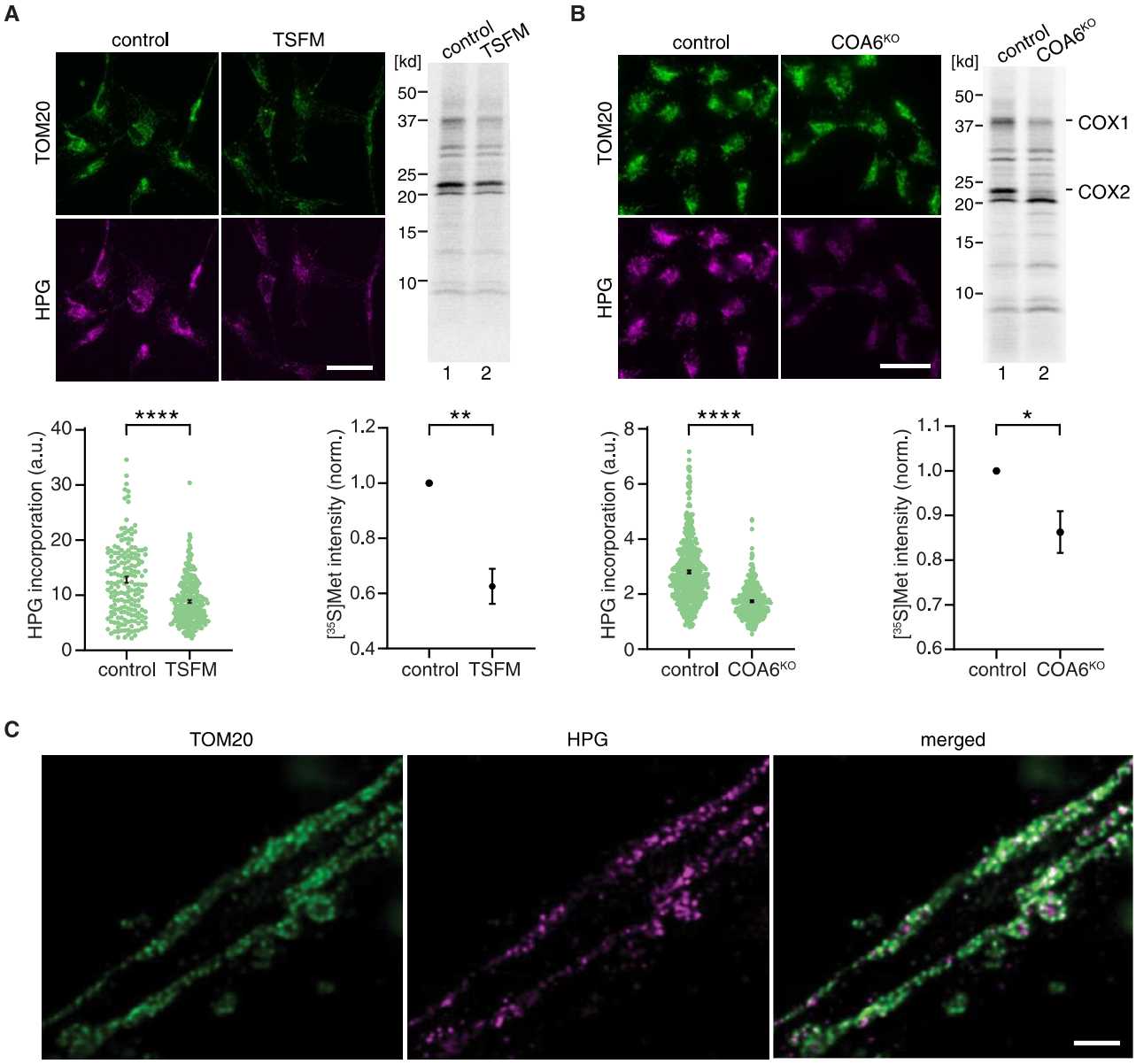

Figure 3. Utilizing HPG labeling in a disease context and mapping mitochondrial translation with super resolution microscopy.

A Mitochondrial translation products were labeled using HPG and [^{35}S]Met in control and TSFM patient fibroblasts. Representative epifluorescent microscopy and the autoradiography images are shown. Scale bars, 50 μm. Changes in mitochondrial protein synthesis were quantified for both approaches. For microscopy image analysis, > 300 cells from $N = 3$ independent experiments were analyzed for each cell type. Mann–Whitney U-test, ****$P < 0.0001$. For radiolabeling analyses, $N = 3$ independent samples were quantified for each cell type. Student t-test, **$P < 0.01$. Error bars, ± SEM.

B As in A using control and COA6^{KO} HEK cells. Scale bars, 25 μm. For microscopy image analysis, ****$P < 0.0001$, and for radiolabeling experiments, *$P < 0.05$ were calculated. Error bars, ± SEM.

C Mitochondrial protein synthesis was monitored in hippocampal neurons, using HPG clicked to ATTO 590-azide (magenta) and cells immunostained for TOM20 (green). A representative deconvolved STED microscopy image is shown. Scale bars, 1 μm.

these proteins are components of the OXPHOS system, which need to be locally imported and integrated into functional enzyme complexes (Kuzniewska *et al*, 2020). These findings indicate that biogenesis of mitochondrial proteins occurs locally and distant from the soma. However, it has not been addressed whether mitochondrial-encoded proteins are locally expressed in different neuronal compartments, distant from the soma. To answer this question, we labeled mitochondrial translation products in hippocampal neurons and immunostained the samples for ANK-G, a protein located in the axon initial segment. The plasma membrane of the neurons was stained using a lipophilic dye DiO. When used in low concentration, DiO sparsely labels cells in the sample by unselectively incorporating into the

 © 2021 The Authors

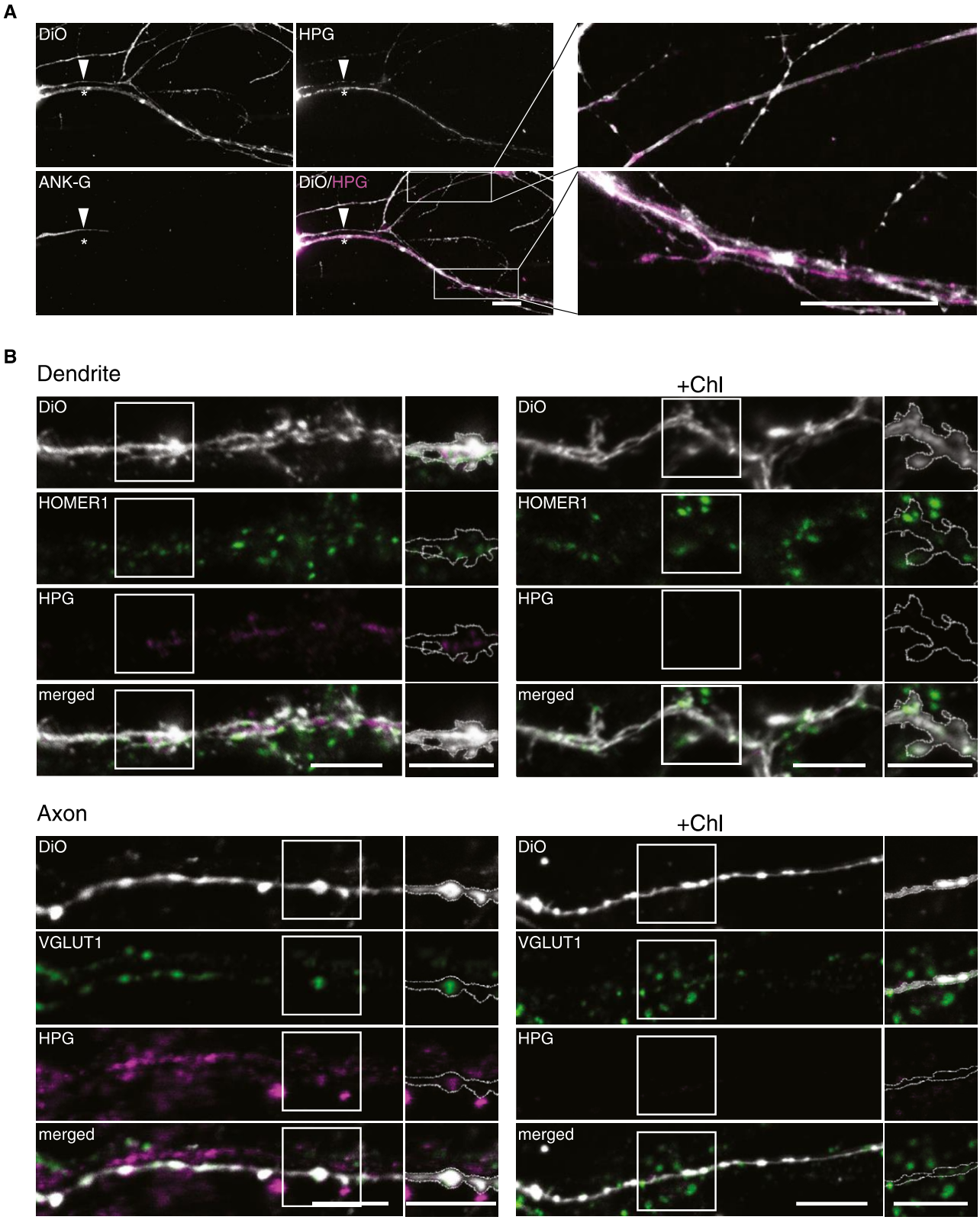
A
DiO
HPG
ANK-G
DiO/HPG
B
Dendrite
+Chl
DiO
HOMER1
HPG
merged
Axon
VGLUT1

Figure 4.

Figure 4. Mitochondrial translation in neurons.

A Mitochondrial translation products were labeled with HPG in hippocampal neurons, immunostained for ANK-G (initial axon segment), and plasma membrane was stained with DiO. Representative epifluorescent images and zoomed insets of neural branches are shown. In both axon (ANK-G positive, arrow) and dendrite (star), HPG incorporation revealing mitochondrial protein synthesis was detected. Scale bars, 20 μm.

B Representative confocal images of a dendrite (top) and an axon (bottom) in which mitochondrial translation products were labeled with HPG (magenta). HOMER1 and VGLUT1 were used as post- and pre-synapse markers, respectively (green) and DiO-stained randomly neurites (gray). In each neurite, an exemplary region was selected and the DiO was outlined to mark the outer edge of the region. As a control, cells were treated with Chloramphenicol (Chl) to inhibit mitochondrial translation. Scale bars, 5 μm.

membrane and spreading across the plasma membrane of single cells. This allows for staining of neurons (or neurites) in a random manner. This approach enabled us to differentiate between axons and dendrites, as neurites containing ANK-G, or devoid of it and to visualize single neurites in the culture. Mitochondrial translation products were found in both axons and dendrites (Fig 4A, the arrow and the star mark the axon and the dendrite, respectively).

We then analyzed pre- and post-synaptic regions for mitochondrial translation using HPG labeling. As a marker for pre-synaptic sites, we labeled synaptic vesicles with an antibody against vesicular glutamate transporter 1 (VGLUT1). In a separate set of experiments, HOMER1 antibody was used to visualize post-synaptic regions. The membrane of neurites was stained with DiO. We then imaged DiO-stained dendrites and axons by confocal microscopy. Mitochondrial translation was readily detected along both axons and dendrites. Using Chloramphenicol, we validated the specificity of the detected mitochondrial translation signal. For a closer look at the synaptic regions, we outlined the DiO staining to define outer edge of the branch. To this end, we detected the HPG signal present at both pre- and post-synaptic regions (Figs 4B and EV3). Accordingly, mitochondrial translation appears to occur at pre- and post-synaptic regions of neurites.

In summary, our work provides a first view of mitochondrial translation in neurons, demonstrating that this process can be detected in axons and dendrites and in functionally distinct compartments of the pre- and post-synapse.

Conclusion

Here, we have implemented a new imaging approach that specifically allows to label mitochondrial translation products for fluorescent microscopic imaging. The strategy can be applied in a timely resolved manner with different labeling time and in a variety of different cell types. In addition, the labeling technique can be combined with super resolution microscopy to address questions regarding the spatial organization of mitochondrial protein synthesis. To this end, labeling of mitochondrial translation with HPG and subsequently click chemistry represents a powerful approach that could be applied in diagnostics of mitochondrial diseases and that opens new opportunities to study mitochondrial biogenesis in specialized cells such as neurons with spatial resolution.

Material and Methods

Cell lines and cell culture

All non-primary cell lines and primary human fibroblasts were cultured in Dulbecco's modified Eagle's medium (DMEM, Thermo Fischer) and were supplemented with 10% (V/V) heat-inactivated fetal bovine serum (Biochrom, Berlin, Germany), 2 mM L-glutamine, 1 mM sodium pyruvate, and 50 μg/ml uridine. They were incubated at 37°C with 5% CO_2 and passaged on a regular basis. HeLa was purchased from the DSMZ collection at the Leibnitz institute. HEK293T Flp-In™ T-REX™ was purchased from Invitrogen. WT fibroblasts, $COA6^{KO}$ HEK293T, WT, and Rho0-143B cell lines were previously reported (King & Attardi, 1989; Gómez-Durán *et al*, 2010; Pacheu-Grau *et al*, 2018, 2020). The G6930A 143B cell line was a gift from G. Manfredi and J. Montoya (Bruno *et al*, 1999; Richter-Dennerlein *et al*, 2016). TFSM mutant patient fibroblasts were previously reported (Emperador *et al*, 2017). For imaging purposes, the cells were seeded on PLL-coated glass coverslips (0.1 mg/ml) 1 day before the start of the experiments.

The use of human iPSC lines was approved by the Ethics Committee of University Medical Center Göttingen (approval number: 10/9/15) and was carried out in accordance with the approved guidelines. Written informed consent was obtained from all participants prior to the participation in the study.

Human iPSC lines from a healthy donor (isWT11.8/UMGi130-A) were used in this study. Human iPSCs were maintained on Matrigel-coated plates (growth factor reduced, BD Biosciences), passaged every 4–6 days with Versene solution (Thermo Fisher Scientific), and cultured in StemMACS iPS-Brew XF medium (Miltenyi Biotec) supplemented with 2 μM Thiazovivin (Merck Millipore), for 24 h after passaging with daily medium change. Directed differentiation of human iPSCs into iPSC-cardiomyocytes was performed via WNT signaling modulation and subsequent metabolic selection, as previously described (Cyganek *et al*, 2018). Differentiated iPSC-cardiomyocytes were cultured for 2 months and were subjected to molecular and functional analyses. Cell cultures were incubated in a humidified incubator with 5% CO_2 at 37°C.

Neuronal hippocampal cultures were obtained from dissociated hippocampi of new-born rats, as previously published (Banker & Cowan, 1977; Kaech & Banker, 2006; Truckenbrodt *et al*, 2018). For imaging purposes, the cells were plated at a concentration of ~30,000/cm^2 on coverslips coated with 1mg/ml PLL, after being treated as previously described (Truckenbrodt *et al*, 2018). Following dissection and plating, the cells were left to adhere for 1–4 h at 37°C in a cell incubator, with 5% CO_2. After adhesion, the medium was replaced to Neurobasal-A medium (Gibco, Life Technologies, Carlsbad, CA, USA), containing 1:50 B27 supplement (Gibco) and 1:100 GlutaMAX (Gibco). Neurons were kept in culture at 5% CO_2 and 37°C, for 14–21 days before use.

In vivo labeling of newly synthesized mitochondrial-encoded peptides with HPG

To label newly synthesized mitochondrial-encoded peptides, a click chemistry-based approach was adapted (Estell *et al*, 2017).

 © 2021 The Authors

Briefly, cells were transferred to methionine-free medium. In neurons, the labeling was done in warm Hank's Balanced Salt Solution (HBSS, Thermo Fisher). Cytosolic translation was stopped using Harringtonine (200μM, Carbosynth) for 20 min. Emetine (100 μg/ml, Merck) and Cycloheximide (Chx, 50 μg/ml, Roth) were used in a similar fashion. For control experiments blocking mitochondrial translation, 150 μg/ml Chloramphenicol was added 50 min before the start of the labeling. 500 μM of L-Homopropargylglycine (HPG, Thermo Fisher) was then added for 30 min (unless mentioned otherwise). Cells were then transferred to buffer A containing 10 mM HEPES, 10 mM NaCl, 5 mM KCl, 300 mM sucrose, and 0.015% digitonin, for 2 min on ice, followed by 15 s in buffer A without digitonin. Coverslips were fixed using 4% PFA in PBS (137 mM NaCl, 2.7 mM KCl, 10 mM Na_2HPO_4, 2 mM KH_2PO_4) at pH 7.5 for 30 min at room temperature and were then further processed for click chemistry and immunostaining.

Click chemistry and immunostaining of fixed cells

After formaldehyde fixation, coverslips were washed for 5 min with PBS quenched for 15 min with 100 mM NH_4Cl in PBS. Blocking and permeabilization were performed in staining solution (PBS + 5% BSA + 5% tryptone peptone + 0.1% Triton X-100), using 3 solution exchanges, each for 5 min. After a brief wash with 3% BSA in PBS, coverslips were clicked for 20 min using a commercial kit (Click-iT Cell Reaction Buffer Kit; Thermo Fisher), with 3 μM AlexaFluor 647-azide (Thermo Fisher) or 5 μM ATTO 590-azide (ATTO-TEC). After another quick wash with 3% BSA in PBS, primary and secondary antibodies were diluted in the staining solution and were applied sequentially for 1 h. Three 5-min washing steps with staining solution were performed between the primary and secondary antibody incubations. Three 5-min sequential washes with blocking solution (PBS + 5% BSA + 5% tryptone peptone), high-salt PBS (PBS + 500 mM NaCl), and PBS were performed at the end of the staining procedure, to remove thoroughly any unspecific binding of the antibodies. The coverslips were then embedded in Mowiol (Calbiochem, Billerica, MA, USA) and were allowed to dry overnight at room temperature, before imaging.

The probes used in this study are as follows: TOM20 (rabbit, Proteintech), ANK-G (mouse, Antibodies incorporated), HOMER1 (mouse, Synaptic Systems), VGLUT1 nanobody conjugated to STAR 580 (Nanotag), goat anti-rabbit Alexa Fluor Plus 488 (Thermo Fisher), donkey anti-mouse conjugated to Cy3 (Dianova), goat anti-rabbit STAR 580 (Abberior), goat anti-rabbit ATTO 647N (ATTO-TEC), and goat anti-guinea pig Alexa Fluor 546 (Thermo Fisher).

Labeling of mitochondrial-encoded peptides with [^{35}S] methionine

Radioactive labeling of mitochondrial translation products was performed according to a previously published protocol (Chomyn, 1996) with minor modifications. Cytosolic translation was inhibited with Harringtonine (200 μM) for 20 min. Then, 200 μCi/ml [^{35}S] methionine was added to the cells and was incubated at 37°C for 1 h. The cell lysate was loaded on a 10–18% Tris-Tricine gradient gel, and the radioactive signal was detected using Phosphor Screens and a Typhoon scanner (GE Healthcare).

Quantification of the autoradiography images in Fig 3A and B was performed with ImageJ as follows: First, a manual threshold was determined to separate the background from the regions of interest. Then, in each lane, the integrated density (sum of values) of the pixels over the threshold was obtained.

Click chemistry on extracted mitochondria

Cells were incubated in methionine-free medium with 200 μM Harringtonine for 20 min, and 500 μM HPG was added to the cells for 4 h. After harvesting the cells, mitochondria were isolated by differential centrifugation, as previously described (Lazarou *et al*, 2009). Briefly, cells were dissolved in isolation buffer (300 mM trehalose, 10 mM KCl, 10 mM HEPES pH 7.4, 2 mg/ml BSA and 2mM PMSF). Cells were subsequently homogenized on ice using a Potter S homogenizer. After a first centrifugation step at 400 ×*g* for 10 min at 4°C and a second one at 800 ×*g* for 7 min at 4°C to remove cell debris, mitochondria were collected by centrifugation at 10,000 ×*g* for 10 min at 4°C. Freshly isolated mitochondria were washed in isolation buffer lacking BSA, and protein concentrations were subsequently determined by Bradford assay. 100 μg of mitochondria proteins was pelleted and dissolved in 25 μl 50 mM Tris (pH 8.8) containing 1 mM PMSF and 1% SDS. A click reaction was performed on ice using a commercial kit (Click-iT Cell Reaction Buffer Kit; Thermo Fisher), with 80 μM Alexa Fluor 488-azide (Sigma). According to the manufacturer's protocol, proteins were purified from the mixture using a MeOH/chloroform approach, after the end of the click reaction. The extracted pellet was completely dried by heating up to 50°C and was then dissolved in loading buffer containing 8 M Urea, 100 mM Dithiothreitol (DTT), and 1% benzonase. It was then incubated at 37°C for 20 min and was then loaded on a 10–18% Tris-Tricine gradient gel. Fluorescent signals in the gels were analyzed using a FLA-9000 Starion image scanner (Fujifilm).

Membrane staining with DiO for visualizing neurites

The cell's membrane was stained with the carbocyanine dye, DiO (3,3′-dioctadecyloxacarbocyanine perchlorate, Molecular Probes). The DiO staining procedure results in sparse labeling if used in low concentration. This dye is poorly soluble in water and is only soluble in membranes. Neurons on which DiO crystals land will be abundantly labeled, with all of their neurites becoming fluorescent, because DiO dissolves and spreads in their membranes. Neighboring neurons, which did not receive DiO crystals, remain invisible in the DiO (green) channel. For the staining, the DiO crystals were dissolved in dimethylformamide (DMF) to a stock concentration of 2 mg/ml, by mixing for 10 min at 50°C. The stock was kept at 4°C, in the dark, until use. A working concentration of 1 μg/ml was prepared in PBS and was thoroughly mixed and sonicated. It was applied to the coverslips for 20 min at 37°C. The coverslips were washed with PBS briefly and were left overnight in PBS at room temperature. The next day, the coverslips were embedded in Mowiol, as above, and were dried overnight before imaging.

Image acquisition

Epifluorescent images were taken with an inverted Nikon Ti epifluorescence microscope (Nikon Corporation, Chiyoda, Tokyo, Japan)

© 2021 The Authors

equipped with a Plan Apochromat 60×, 1.4 NA oil immersion objective, an HBO-100W Lamp, and an IXON X3897 Andor (Belfast, Northern Ireland, UK) camera, operated via the NIS-Elements AR software (version 4.20; Nikon).

Confocal images were taken using an Abberior microscope operated with Imspector imaging software (Abberior Instruments, Göttingen, Germany). This setup was built on an Olympus IX83 base, equipped with a UPlanSApo 100× oil immersion objective (Olympus Corporation, Shinjuku, Tokyo, Japan) and an EMCCD iXon Ultra camera (Andor, Belfast, Northern Ireland, UK). Pulsed 561-nm and 640-nm lasers were used for excitation of ATTO 590 and STAR 580 and Alexa Fluor 647, respectively. For stimulated depletion, lasers emitting at 595 and 775 nm were employed. Where mentioned, images were deconvolved using Huygens software (Scientific Volume Imaging, WWW.svi.nl).

Image analysis

To analyze the mitochondrial translation signal, we used a self-written script in Matlab. First, the area of single cells was separated. Then, in each cell, mitochondria were identified by applying an empirically determined threshold in the TOM20 channel. The HPG signal was then averaged inside the mitochondrial area. Different statistical tests were used and mentioned in the respective figure legends. A P-value of < 0.05 was considered statistically significant.

To make the correlation maps in Figs 2C and EV2B, we calculated the Pearson correlation coefficient for the respective images. This procedure calculates for each pixel, identified by coordinates i and j, the following value:

$$Value i,j = (Ai,j - \alpha) \times (Bi,j - \beta) \div \left(\sqrt{\sum (Ai,j - \propto)^2} \times \sqrt{\sum (Bi,j - \beta)^2} \right)$$

where A and B are the two original images (meaning intensity matrices), and α and β are the average intensities of the two images, respectively.

The value obtained at a particular pixel is high when the original pixel intensities in the A and B images correlate (if they are both higher than the respective averages, or both lower). In contrast, if the intensity at the respective pixel is low in one of the original images and is high in the other, then the correlation value will be low (negative). This calculation provides an optimal view of the correlation between the channels, and indicates, pixel by pixel, the regions of low or high correlation.

Data availability

This study includes no data deposited in external repositories. All Matlab analysis routines are available upon request from SOR (srizzol@gwdg.de).

Expanded View for this article is available online.

Acknowledgements

Funded by the European Research Council (ERC) Advanced Grant (ERCAdG No. 339580) to PR and (ERCAdG No. 835102) to SJ, the Sonderforschungsbereiche (SFB) 1286 (projects Z03 (SOR), A05 (SJ), A06 (PR)), the SFB 1002 S01 (LC) and CY 90/1-1 (LC), supported by the Deutsche Forschungsgemeinschaft (DFG, German Research Foundation) under Germany's Excellence Strategy—EXC 2067/1-390729940, the German Federal Ministry of Education and Research (BMBF)/DZHK (LC), Instituto de Salud Carlos III (grant PI17/00021) to JM, the Max Planck Institute for Biophysical Chemistry (PR), and the PhD program Molecular Biology—International Max Planck Research School and the Göttingen Graduate School for Neurosciences and Molecular Biosciences (GGNB; DFG grant GSC 226/1) (RY). Open Access funding enabled and organized by ProjektDEAL.

Author contributions

RY performed the experiments, analyzed and interpreted the data, and edited the manuscript. EFF provided technical advice and edited the manuscript. LC and JM provided resources for the manuscript. SJ participated in conceptualization of the work and edited the manuscript. SOR participated in data analysis and interpretation, design and conceptualization of the work, and wrote and edited the manuscript. PR participated in design and conceptualization of the work, wrote and edited the manuscript, and was involved in supervision during the project. DP-G performed experiments, analyzed and interpreted the data, was involved in supervision during the project, and wrote and edited the manuscript.

Conflict of interest

The authors declare that they have no conflict of interest.

References

Antonicka H, Østergaard E, Sasarman F, Weraarpachai W, Wibrand F, Pedersen AMB, Rodenburg RJ, van der Knaap MS, Smeitink JAM, Chrzanowska-Lightowlers ZM *et al* (2010) Mutations in C12orf65 in patients with encephalomyopathy and a mitochondrial translation defect. *Am J Hum Genet* 87: 115–122

Area-Gomez E, Guardia-Laguarta C, Schon EA, Przedborski S (2019) Mitochondria, OxPhos, and neurodegeneration: cells are not just running out of gas. *J Clin Invest* 129: 34–45

Banker GA, Cowan WM (1977) Rat hippocampal neurons in dispersed cell culture. *Brain Res* 126: 397–425

Bartolomeo FD, Malina C, Campbell K, Mormino M, Fuchs J, Vorontsov E, Gustafsson CM, Nielsen J (2020) Absolute yeast mitochondrial proteome quantification reveals trade-off between biosynthesis and energy generation during diauxic shift. *Pro Natl Acad Sci USA* 117: 7524–7535

Boczonadi V, Horvath R (2014) Mitochondria: Impaired mitochondrial translation in human disease. *Int J Biochem Cell Biol* 48: 77–84

Bruno C, Martinuzzi A, Tang Y, Andreu AL, Pallotti F, Bonilla E, Shanske S, Fu J, Sue CM, Angelini C *et al* (1999) A Stop-Codon mutation in the human mtDNA cytochrome c oxidase I gene disrupts the functional structure of complex IV. *Am J Hum Genet* 65: 611–620

Chomyn A (1996) In vivo labeling and analysis of human mitochondrial translation products. *Methods Enzymol* 264: 197–211

Cioni JM, Lin JQ, Holtermann AV, Koppers M, Jakobs MAH, Azizi A, Turner-Bridger B, Shigeoka T, Franze K, Harris WA *et al* (2019) Late endosomes act as mRNA translation platforms and sustain mitochondria in axons. *Cell* 176: 56–72

Cyganek L, Tiburcy M, Sekeres K, Gerstenberg K, Bohnenberger H, Lenz C, Henze S, Stauske M, Salinas G, Zimmermann WH *et al* (2018) Deep phenotyping of human induced pluripotent stem cell–derived atrial and ventricular cardiomyocytes. *JCI Insight.* 3: 12

 © 2021 The Authors

Dennerlein S, Wang C, Rehling P (2017) Plasticity of mitochondrial translation. *Trends Cell Biol* 27: 712–721

Dieterich DC, Hodas JJL, Gouzer G, Shadrin IY, Ngo JT, Triller A, Tirrell DA, Schuman EM (2010) In situ visualization and dynamics of newly synthesized proteins in rat hippocampal neurons. *Nat Neurosci* 13: 897–905

DiMauro S (2019) A brief history of mitochondrial pathologies. *Int J Mol Sci* 20: 5643

Emperador S, Bayona-Bafaluy MP, Fernández-Marmiesse A, Pineda M, Felgueroso B, López-Gallardo E, Artuch R, Roca I, Ruiz-Pesini E, Couce ML *et al* (2017) Molecular-genetic characterization and rescue of a TSFM mutation causing childhood-onset ataxia and nonobstructive cardiomyopathy. *Eur J Hum Genet* 25: 153–156

Estell C, Stamatidou E, El-Messeiry S, Hamilton A (2017) In situ imaging of mitochondrial translation shows weak correlation with nucleoid DNA intensity and no suppression during mitosis. *J Cell Sci* 130: 4193–4199

Ghezzi D, Zeviani M (2018) Human diseases associated with defects in assembly of OXPHOS complexes. *Essays Biochem* 62: 271–286

Gioio AE, Eyman M, Zhang H, Lavina ZS, Giuditta A, Kaplan BB (2001) Local synthesis of nuclear-encoded mitochondrial proteins in the presynaptic nerve terminal. *J Neurosci Res* 64: 447–453

Gómez-Durán A, Pacheu-Grau D, López-Gallardo E, Díez-Sánchez C, Montoya J, López-Pérez MJ, Ruiz-Pesini E (2010) Unmasking the causes of multifactorial disorders: OXPHOS differences between mitochondrial haplogroups. *Hum Mol Genet* 19: 3343–3353

Graham LC, Eaton SL, Brunton PJ, Atrih A, Smith C, Lamont DJ, Gillingwater TH, Pennetta G, Skehel P, Wishart TM (2017) Proteomic profiling of neuronal mitochondria reveals modulators of synaptic architecture. *Mol Neurodegener* 12: 1–16

Grevel A, Pfanner N, Becker T (2019) Coupling of import and assembly pathways in mitochondrial protein biogenesis. *Biol Chem* 401: 117–129

Hafner AS, Donlin-Asp PG, Leitch B, Herzog E, Schuman EM (2019) Local protein synthesis is a ubiquitous feature of neuronal pre- and postsynaptic compartments. *Science* 364: 6441

Hansen KG, Herrmann JM (2019) Transport of proteins into mitochondria. *Protein J* 38: 330–342

Harris JJ, Jolivet R, Attwell D (2012) Synaptic energy use and supply. *Neuron* 75: 762–777

Haute LV, Pearce SF, Powell CA, D'Souza AR, Nicholls TJ, Minczuk M (2015) Mitochondrial transcript maturation and its disorders. *J Inherit Metab Dis* 38: 655–680

Hollander JM, Thapa D, Shepherd DL (2014) Physiological and structural differences in spatially distinct subpopulations of cardiac mitochondria: influence of cardiac pathologies. *Am J Physiol Heart Circ Physiol* 307: H1–H14

Kaech S, Banker G (2006) Culturing hippocampal neurons. *Nat Protoc* 1: 2406–2415

Kaplan BB, Gioio AE, Hillefors M, Aschrafi A (2009) Axonal protein synthesis and the regulation of local mitochondrial function. *Results Probl Cell Differ* 48: 225–242

King MP, Attardi G (1989) Human cells lacking mtDNA: repopulation with exogenous mitochondria by complementation. *Science* 246: 500–503

Kuzniewska B, Cysewski D, Wasilewski M, Sakowska P, Milek J, Kulinski TM, Winiarski M, Kozielewicz P, Knapska E, Dadlez M *et al* (2020) Mitochondrial protein biogenesis in the synapse is supported by local translation. *EMBO Rep* 21: e48882

Lazarou M, Smith SM, Thorburn DR, Ryan MT, McKenzie M (2009) Assembly of nuclear DNA-encoded subunits into mitochondrial complex IV, and their preferential integration into supercomplex forms in patient mitochondria. *FEBS J* 276: 6701–6713

Mootha VK, Bunkenborg J, Olsen JV, Hjerrild M, Wisniewski JR, Stahl E, Bolouri MS, Ray HN, Sihag S, Kamal M *et al* (2003) Integrated analysis of protein composition, tissue diversity, and gene regulation in mouse mitochondria. *Cell* 115: 629–640

Morgenstern M, Stiller SB, Lübbert P, Peikert CD, Dannenmaier S, Drepper F, Weill U, Höß P, Feuerstein R, Gebert M *et al* (2017) Definition of a high-confidence mitochondrial proteome at quantitative scale. *Cell Rep* 19: 2836–2852

Nottia MD, Marchese M, Verrigni D, Mutti CD, Torraco A, Oliva R, Fernandez-Vizarra E, Morani F, Trani G, Rizza T *et al* (2020) A homozygous MRPL24 mutation causes a complex movement disorder and affects the mitoribosome assembly. *Neurobiol Disease* 141: 104880

Pacheu-Grau D, Bareth B, Dudek J, Juris L, Vögtle FN, Wissel M, Leary SC, Dennerlein S, Rehling P, Deckers M (2015) Cooperation between COA6 and SCO2 in COX2 maturation during cytochrome c oxidase assembly links two mitochondrial cardiomyopathies. *Cell Metab* 21: 823–833

Pacheu-Grau D, Callegari S, Emperador S, Thompson K, Aich A, Topol SE, Spencer EG, McFarland R, Ruiz-Pesini E, Torkamani A *et al* (2018) Mutations of the mitochondrial carrier translocase channel subunit TIM22 cause early-onset mitochondrial myopathy. *Hum Mol Genet* 27: 4135–4144

Pacheu-Grau D, Gómez-Durán A, Iglesias E, López-Gallardo E, Montoya J, Ruiz-Pesini E (2013) Mitochondrial antibiograms in personalized medicine. *Hum Mol Genet* 22: 1132–1139

Pacheu-Grau D, Wasilewski M, Oeljeklaus S, Gibhardt CS, Aich A, Chudenkova M, Dennerlein S, Deckers M, Bogeski I, Warscheid B *et al* (2020) COA6 facilitates cytochrome c oxidase biogenesis as thiol-reductase for copper metallochaperones in mitochondria. *J Mol Bio* 432: 2067–2079

Palmer JW, Tandler B, Hoppel CL (1977) Biochemical properties of subsarcolemmal and interfibrillar mitochondria isolated from rat cardiac muscle. *J Biol Chem* 252: 8731–8739

Pivovarova NB, Nguyen HV, Winters CA, Brantner CA, Smith CL, Andrews SB (2004) Excitotoxic calcium overload in a subpopulation of mitochondria triggers delayed death in hippocampal neurons. *J Neurosci* 24: 5611–5622

Richter JD, Klann E (2009) Making synaptic plasticity and memory last: mechanisms of translational regulation. *Genes Dev* 23: 1–11

Richter-Dennerlein R, Dennerlein S, Rehling P (2015) Integrating mitochondrial translation into the cellular context. *Nat Rev Mol Cell Biol* 16: 586–592

Richter-Dennerlein R, Oeljeklaus S, Lorenzi I, Ronsör C, Bareth B, Schendzielorz AB, Wang C, Warscheid B, Rehling P, Dennerlein S (2016) Mitochondrial protein synthesis adapts to influx of nuclear-encoded protein. *Cell* 167: 471–483

Sasarman F, Shoubridge EA (2012) Radioactive labeling of mitochondrial translation products in cultured cells. *Methods Mol Biol* 837: 207–217

Sickmann A, Reinders J, Wagner Y, Joppich C, Zahedi R, Meyer HE, Schönfisch B, Perschil I, Chacinska A, Guiard B *et al* (2003) The proteome of Saccharomyces cerevisiae mitochondria. *Proc Natl Acad Sci USA* 100: 13207–13212

Smith HL, Bourne JN, Cao G, Chirillo MA, Ostroff LE, Watson DJ, Harris KM (2016) Mitochondrial support of persistent presynaptic vesicle mobilization with age-dependent synaptic growth after LTP. *Elife* 5: e15275

Smits P, Smeitink J, van den Heuvel L (2010) Mitochondrial translation and beyond: processes implicated in combined oxidative phosphorylation deficiencies. *J Biomed Biotechnol* 2010: 1–24

© 2021 The Authors

Soma S, Morgada MN, Naik MT, Boulet A, Roesler AA, Dziuba N, Ghosh A, Yu Q, Lindahl PA, Ames JB *et al* (2019) COA6 is structurally tuned to function as a thiol-disulfide oxidoreductase in copper delivery to mitochondrial cytochrome c oxidase. *Cell Rep* 29: 4114–4126

Stroud DA, Maher MJ, Lindau C, Vögtle FN, Frazier AE, Surgenor E, Mountford H, Singh AP, Bonas M, Oeljeklaus S *et al* (2015) COA6 is a mitochondrial complex IV assembly factor critical for biogenesis of mtDNA-encoded COX2. *Hum Mol Genet* 24: 5404–5415

Suomalainen A, Battersby BJ (2018) Mitochondrial diseases: the contribution of organelle stress responses to pathology. *Nat Rev Mol Cell Biol* 19: 77–92

Truckenbrodt S, Viplav A, Jähne S, Vogts A, Denker A, Wildhagen H, Fornasiero EF, Rizzoli SO (2018) Newly produced synaptic vesicle proteins are preferentially used in synaptic transmission. *EMBO J* 37: e98044

Völgyi K, Gulyássy P, Háden K, Kis V, Badics K, Kékesi KA, Simor A, Györffy B, Tóth EA, Lubec G *et al* (2015) Synaptic mitochondria: a brain mitochondria cluster with a specific proteome. *J Proteomics* 120: 142–157

Wiedemann N, Pfanner N (2017) Mitochondrial machineries for protein import and assembly. *Annu Rev Biochem* 86: 685–714

Williams EG, Wu Y, Ryu D, Kim JY, Lan J, Hasan M, Wolski W, Jha P, Halter C, Auwerx J *et al* (2018) Quantifying and localizing the mitochondrial proteome across five tissues in a mouse population. *Mol Cell Proteomics* 17: 1766–1777

License: This is an open access article under the terms of the Creative Commons Attribution-NonCommercial-NoDerivs 4.0 License, which permits use and distribution in any medium, provided the original work is properly cited, the use is non-commercial and no modifications or adaptations are made.

 © 2021 The Authors

Expanded View Figures

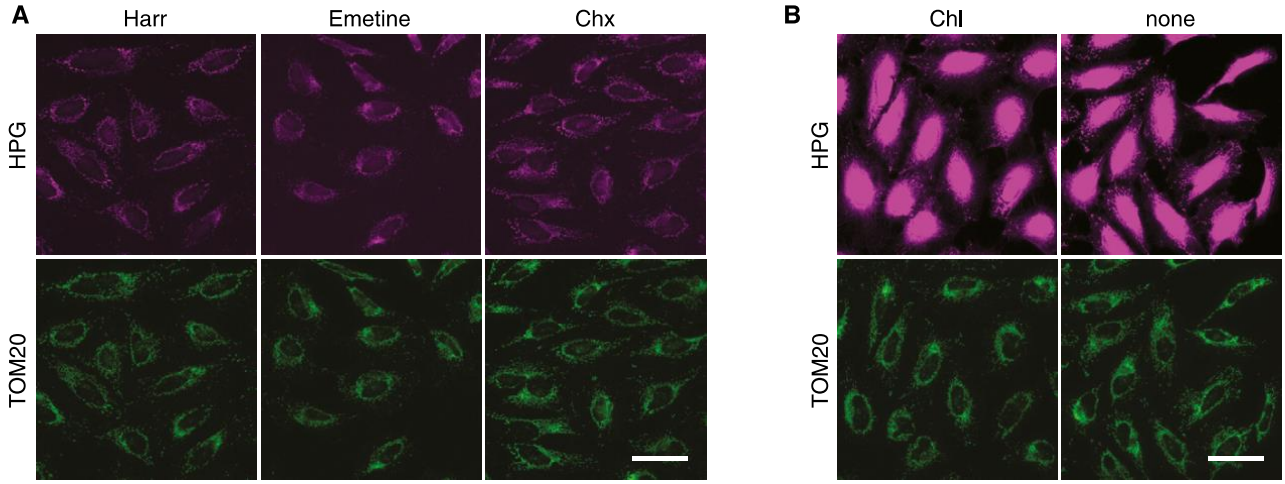

Figure EV1. Visualizing mitochondrial translation in the cellular context.

A Mitochondrial translation was labeled in WT HeLa cells for 30 min using indicated antibiotics for inhibiting cytosolic translation (magenta). Cells were then immunostained for TOM20 (green). Using Emetine and Cycloheximide (Chx) revealed no difference to Harringtonine (Harr).

B HPG labeling of HeLa cells in the presence of mitochondrial translation inhibitor Chloramphenicol (Chl) and the absence of all antibiotics (none). The brightness is scaled to the level of panels in A. Scale bars, 50 μm.

Figure EV2. Different levels of gene expression in mitochondria of a single cell.

A Mitochondrial translation products were labeled with HPG in different cell types and 25 random cells, from $N = 3$ independent experiments, were analyzed and plotted for each cell type. Coefficients of variations (CV) are indicated on each graph. Error bars show mean ± SEM.

B Representative epifluorescent images of HEK and HeLa cells labeled for mitochondrial translation products with HPG and TOM20. Correlation of HPG and TOM20 channels is represented in fire lookup table, after calculating the Pearson correlation values over each pixel of the images. Scale bars, 25 μm.

C Representative images of different cell types, in which the ratio of HPG to TOM20 is calculated in each pixel and scaled in the fire lookup table. The same cells are shown as in Fig 2C and in B, where a correlation map between the two channels is plotted. The background color (blue or magenta) represents the baseline. Brighter pixels (yellow/orange/white) indicate high HPG to TOM20 ratios, while darker pixels (dark blue/black) indicate low ratios. Scale bars, 25 μm.

© 2021 The Authors

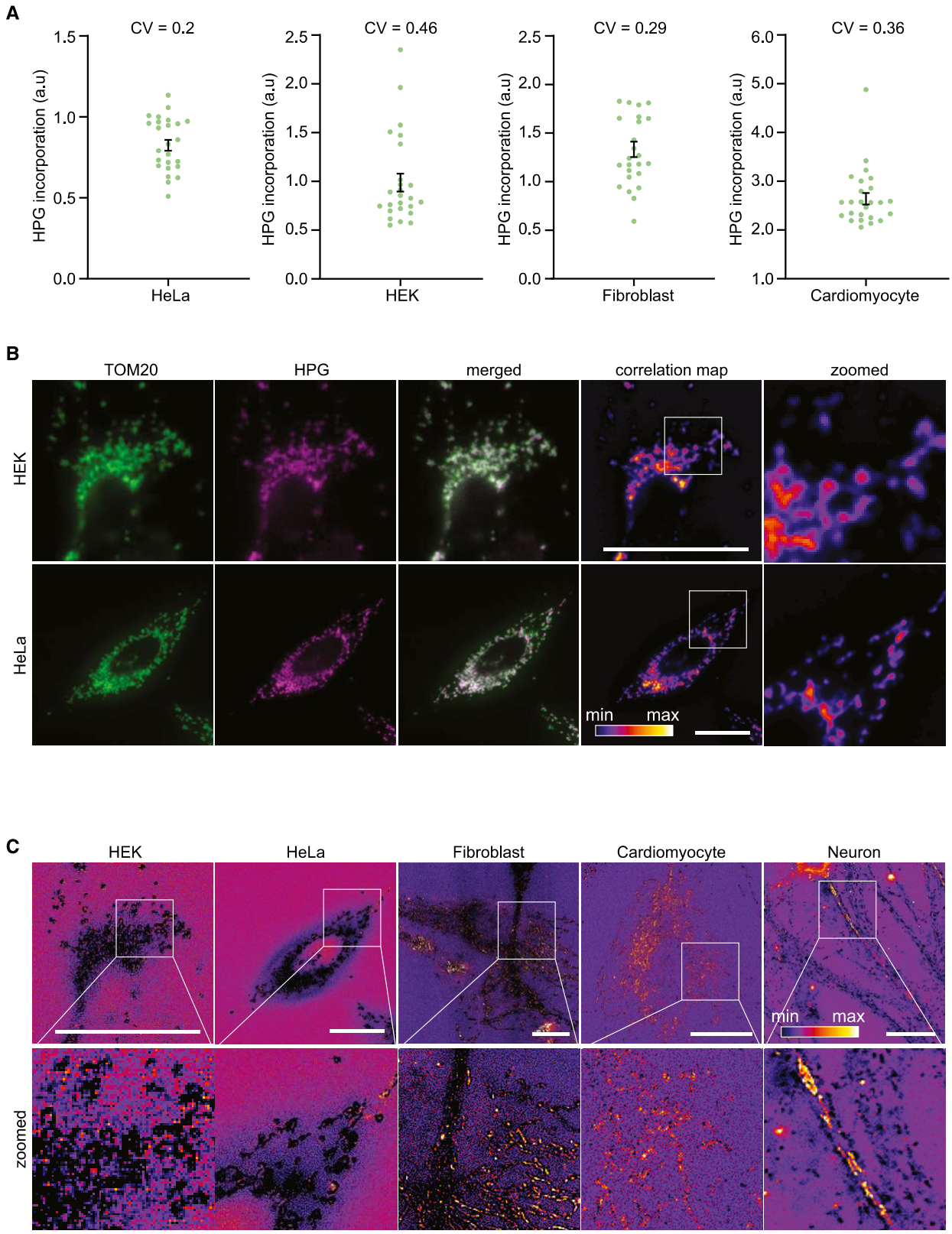

Figure EV2.

© 2021 The Authors

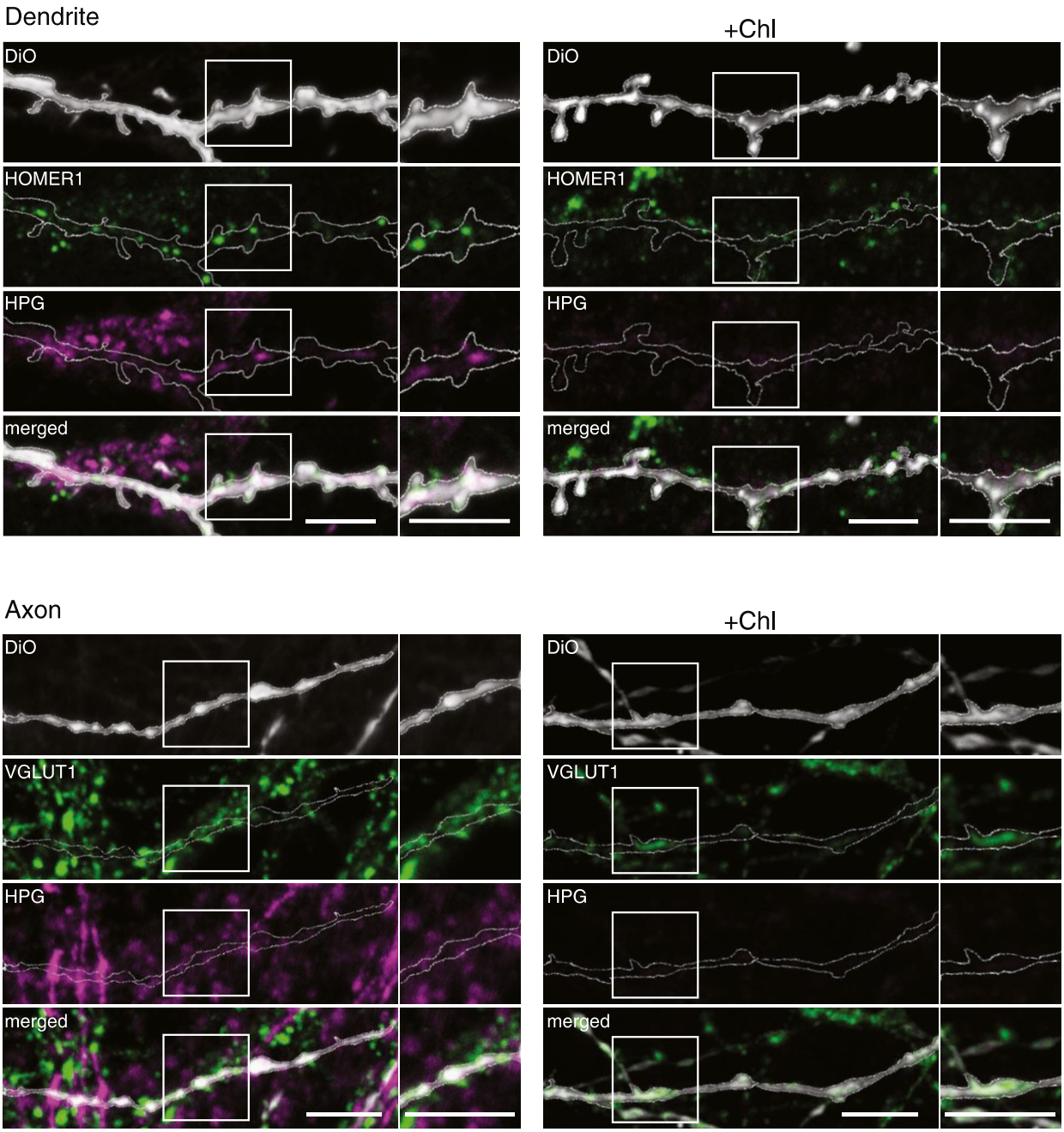

Figure EV3. Mitochondrial translation in neurons.

Representative confocal images of a dendrite (top) and an axon (bottom) in which mitochondrial translation products were labeled with HPG (magenta). HOMER1 and VGLUT1 were used as post- and pre-synapse markers, respectively (green) and DiO-stained randomly neurites (gray). In each neurite, the DiO was outlined to mark the outer edge of the region. As a control, cells were treated with Chloramphenicol (Chl) to inhibit mitochondrial translation. Scale bars, 5 μm.

© 2021 The Authors

Chapter 3: Second Manuscript

“A high throughput mitochondrial-FUNCAT to screen cellular kinases affecting mitochondrial translation”

A high throughput mitochondrial-FUNCAT to screen cellular kinases affecting mitochondrial translation

Manuscript prepared for publication

Roya Yousefi[1], Anusha Valpadashi[1], Silvio O. Rizzoli[2,3], Luis Daniel Cruz-Zaragoza[1], David Pacheu-Grau[4,5,6], Peter Rehling[1,3,7*]

[1]Department of Cellular Biochemistry, University Medical Center Göttingen, Göttingen, Germany

[2]Department of Neuro- and Sensory Physiology, University Medical Center Göttingen, Göttingen, Germany

[3]Cluster of Excellence "Multiscale Bioimaging: from Molecular Machines to Networks of

[4]Departamento de Bioquímica, Biología Molecular y Celular, Universidad de Zaragoza. C/ Miguel Servet, 177, 50013 Zaragoza, Spain.

[5]Instituto de Investigación Sanitaria (IIS) de Aragón, Av. San Juan Bosco, 13, 50009 Zaragoza, Spain.

[6]Centro de Investigaciones Biomédicas en Red de Enfermedades Raras (CIBERER), Av. Monforte de Lemos, 3-5, 28029 Madrid, Spain

Excitable Cells" (MBExC), University of Goettingen, Göttingen, Germany

[7]Max-Planck Institute for Biophysical Chemistry, Göttingen, Germany

Personal contribution: I contributed in designing the experiments, performed them, analyzed and interpreted the data, prepared the figures, and wrote the manuscript.

3.1. Introduction

Mitochondria supply the majority of cellular ATP via oxidative phosphorylation (OXPHOS). In humans, almost all protein complexes of the OXPHOS system are composed of subunits of dual genetic origin. The majority of proteins are synthesized by cytosolic ribosomes and then imported into mitochondria. Only a small fraction of the OXPHOS subunits (13 proteins) are encoded on mitochondrial DNA (mtDNA) along with 2 rRNAs and 22 tRNAs (Anderson et al., 1981; Ojala et al., 1981). mtDNA-encoded mRNAs are translated by mitochondrial ribosomes (mitoribosomes), and the synthesized polypeptides are co-translationally inserted to the inner mitochondrial membrane (Dennerlein et al., 2017; Grevel et al., 2019; Itoh et al., 2021; Wiedemann et al., 2017). Nuclear- and mitochondrial-encoded subunits assemble to form functional OXPHOS complexes in a precise stoichiometry. Many assembly factors are necessary to assist in this process (Dennerlein et al., 2021; Weraarpachai et al., 2012). In addition, translational plasticity maintains the balance between the synthesis of mitochondrial-encoded proteins and the availability of imported subunits in different organisms (Couvillion et al., 2016; Richter-Dennerlein et al., 2015, 2016). Considering the importance of the OXPHOS complexes, malfunctions in the mitochondrial gene expression system are associated with several diseases (Area-Gomez et al., 2019; Brischigliaro et al., 2021; Dimauro, 2019; Gorman et al., 2016). Mitochondrial gene expression is integrated into the cellular context and is modulated in response to various cellular stimuli. For example, mitochondrial protein synthesis is decreased in response to cellular stress pathways such as integrated stress response (ISR) and mitochondrial unfolded protein response (mtUPR) (Mick et al., 2020; Münch et al., 2016; G. Zhang et al., 2021). However, many of the cellular regulatory mechanisms that modulate mitochondrial protein synthesis are not well understood.

Reversible phosphorylation is one of the important mechanisms regulating protein interaction, stability, and function. Recent advances in proteomics have provided new insights into the phosphorylation status of mitochondrial proteins (Kotrasová et al., 2021; Lucero et al., 2019). Approximately 40 percent of the mitochondrial proteome is phosphorylated (Giorgianni et al., 2014; Kruse et al., 2017; Padrão et al., 2013). Phosphorylation has been reported to play a role in modulating various processes in mitochondria (Kotrasová et al., 2021; Lucero et al., 2019). Phosphorylation of proteins at the outer mitochondrial membrane

modulates protein import, mitochondrial fission/fusion, and mitophagy (Kotrasová et al., 2021; Tsushima et al., 2018; Walter et al., 2021). The activity of individual OXPHOS complexes changes as a result of phosphorylation (Pan et al., 2009). Phosphorylation is found on proteins involved in the various steps of mitochondrial gene expression. DNA binding of mitochondrial transcription factor A (TFAM) is decreased by phosphorylation and consequently, mitochondrial transcription is increased (Lu et al., 2013; Wang et al., 2014). Mitochondrial transcription termination factor (mTERF) is active only when phosphorylated (Prieto-Martín et al., 2004). Mitochondrial translation elongation factor (mtEF-Tu) is phosphorylated in rabbit ischemic myocardium (He et al., 2001). In addition, phosphorylation has been detected in nearly one third of mitoribosomal proteins, and in vitro phosphorylation reduces the translational activity of mitoribosomes (Miller et al., 2009). Overall, the importance of phosphorylation as a regulatory mechanism in mitochondrial gene expression has become clearer. However, neither the protein kinases responsible for phosphorylation of mitochondrial proteins nor the enzymes regulating other cellular processes that could have an impact on mitochondrial gene expression have been precisely described. Although the number of known kinases that are either localized to mitochondria (permanently or transiently) or have mitochondrial substrates is increasing, the precise functions of many of these kinases need to be determined (Kotrasová et al., 2021).

Here, we introduced a high-throughput screening approach to identify new factors regulating mitochondrial gene expression in human cells. We used labeling of nascent protein synthesis in mitochondria with fluorescent non-canonical amino acid tagging (FUNCAT) and microscopy (Dieterich et al., 2010; Yousefi et al., 2021; Zorkau et al., 2021) for screening a siRNA library of human kinases. Using this technique, we identified novel factors involved in the regulation of mitochondrial gene expression. Interestingly, we recovered kinases that both down- and upregulated mitochondrial gene expression. Thus, these findings have not only broadened the spectrum of mitochondrial gene expression regulation but also identified potential candidates to be incorporated into therapeutical strategies for mitochondrial disorders.

3.2. Results

3.2.1. Depletion of cellular kinases affects mitochondrial translation.

To investigate cellular kinases that modulate gene expression in mitochondria, we developed a high-throughput method to monitor mitochondrial translation. For that purpose, we established a screening approach in a 96-well plate format, based on our previously described method which uses FUNCAT and fluorescence microscopy (Yousefi et al., 2021). HeLa cells were first transfected with the Silencer™ Human Kinase siRNA Library (Ambion) in a 96-well plate. After 72 hours of transfection, the newly synthesized mitochondrial-encoded proteins were specifically labeled with homopropargylglycine (HPG) and coupled to an azide-containing fluorophore. Plates were then imaged with an automated fluorescence microscope. HPG incorporation (measured from the fluorescence signal) was determined as a measure of mitochondrial translation (Fig. 1-A).

To determine the specificity and sensitivity of the high-throughput setup, we analyzed the HPG incorporation when HeLa cells were plated for 72 hours without further treatment and we found an error of 4.2 percent (Fig. S1-A). To verify that the HPG incorporation signal was specific for mitochondrial protein synthesis, we treated the cells with chloramphenicol, a mitochondrial translation inhibitor, before the addition of HPG. The signal was sensitive to chloramphenicol and localized exclusively to mitochondria (Fig. 1-B and C). Previous studies have shown that disruption of the mitochondrial membrane potential is followed by a reduction in translation (Richter et al., 2015). Therefore, in order to further validate the ability of our method to address changes in mitochondrial translation upon cell distress, we measured HPG incorporation after addition of the proton gradient uncoupler, carbonyl cyanide-m-chlorophenylhydrazone (CCCP) and as expected, HPG incorporation responded in a dose-dependent manner to CCCP (Fig. S1-B and C). Then, in order to address if downregulating the expression of a mitochondrial translation related gene for 72 hours was rendering a detectable decrease in HPG incorporation using our approach, we used an siRNA against DHX30 (DExH-box helicase 30), a mitochondrial ATP-dependent RNA helicase, required for proper levels of mitochondrial translation (Antonicka et al., 2015; Cruz-Zaragoza et al., 2021). As expected, we found depletion of DHX30 resulted in decreased HPG incorporation (Fig. 1-D and E) to a similar extent that was observed using [^{35}S]-methionine labeling (Fig. S1-D).

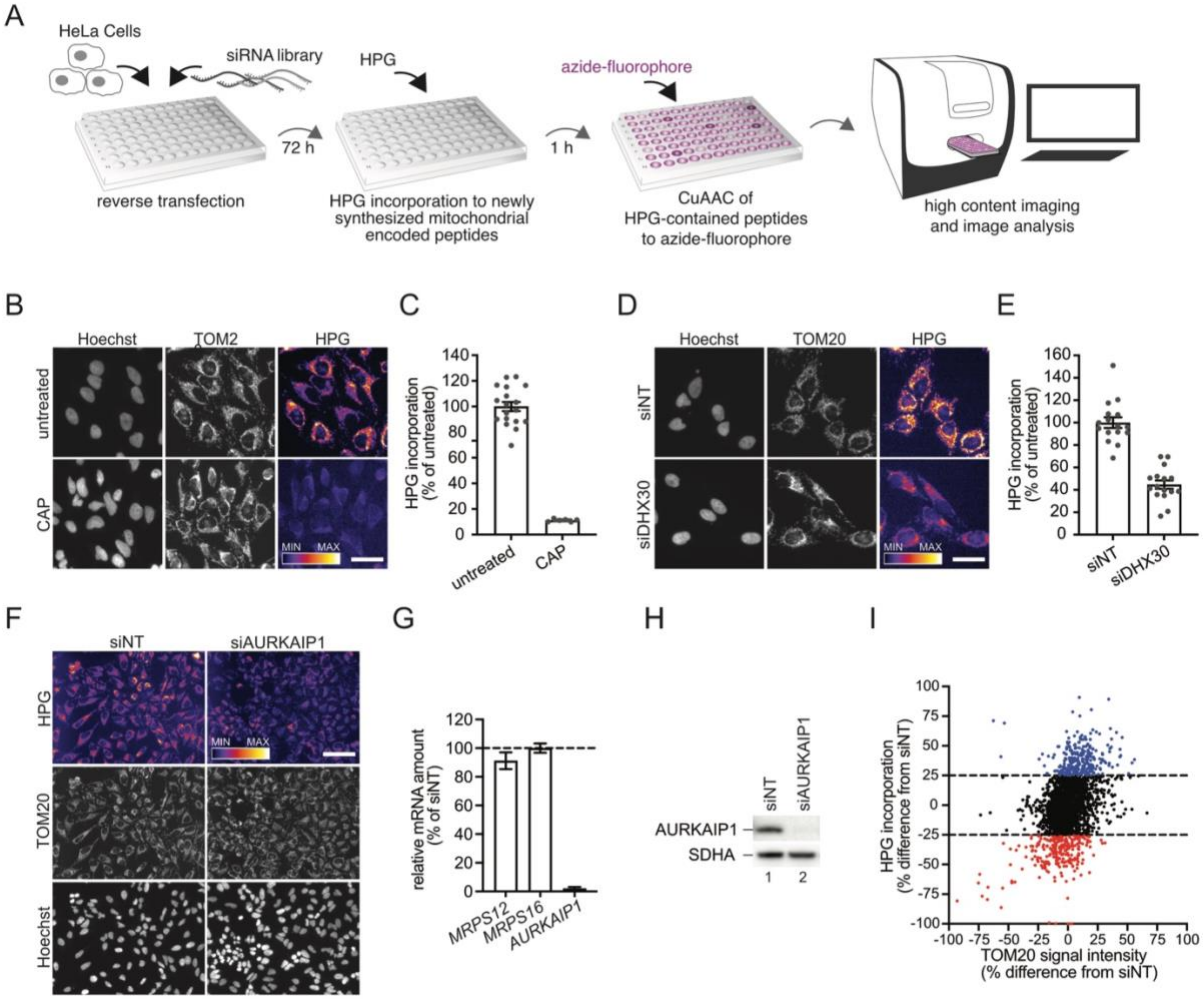

Figure 1. Depletion of cellular kinases affects mitochondrial translation. (A) Schematic representation of the screening approach in which HeLa cells are transfected with the siRNAs from the human kinase library in a 96-well plate for 72 hours, followed by mitochondrial-FUNCAT. HPG is incorporated into the encoded peptides after inhibition of cytosolic ribosomes. Fixed cells are coupled to an azide- fluorophore via copper-catalyzed alkyne-azide cycloaddition (CuAAC). Mitochondria and nuclei were stained and plates were imaged with an automated microscope. The level of translation in mitochondria (HPG incorporation) was measured by automated image analysis. **(B)** Representative fluorescent images of mitochondrial-FUNCAT in control and chloramphenicol treated cells (CAP). HPG incorporation is shown in the fire lookup table. Hoechst and TOM20 in gray show nuclei and mitochondria, respectively. Scale bar, 40 µm. **(C)** Quantitative analysis of HPG incorporation in chloramphenicol treated (CAP) and control cells. For each replicate, approximately 2000 cells were analyzed in 20 images. Error bars show SEM. **(D)** Representative fluorescent images of cells transfected with siDHX30 and the non-targeting control siRNA (siNT) followed by mitochondrial-FUNCAT. Scale bar, 40µm. **(E)** Quantitative analysis of HPG incorporation in cells transfected with siNT and siDHX30. In each replicate, approximately 2000 cells were analyzed in 20 images. Error bars show SEM. **(F)** Representative fluorescent images of cells transfected with siNT and siAURKAIP1 followed by mitochondrial-FUNCAT. Scale bar, 100 µm. **(G)** qRT-PCR analysis of mRNA levels for AURKAIP1 and two mitochondrial ribosomal subunits (MRPS12 and MRPS16) after siRNA-mediated knockdown of AURKAIP1. *RPL28* was used as an internal control mRNA to normalize CT values. N = 3 independent replicates. Error bars show SEM. **(H)** Western blotting analysis of the cells transfected with either siAURKAIP1 or siNT with antibodies against AURKAIP1 and SDHA (a component of the OXPHOS complex I, loading control). **(I)** HPG incorporation is plotted against TOM20 values for all human kinase library siRNAs transfected and labeled according to the protocol in A (see Methods).

We then proceeded with the screening of the human kinase siRNA library. We analyzed the changes in HPG incorporation for the 2127 siRNAs targeting all 709 known human kinase genes (3 siRNA per gene contained in the library). The decreased of HPG incorporation observed when we downregulated aurora kinase A-interacting protein 1 (AURKAIP1) was presented as a representative example for candidates identified with this screening strategy (Fig. 1-F). AURKAIP1 (also known as mS38) was detected as a component of the mitoribosome (Koc et al., 2013). The efficiency of knockdown of AURKAIP1 was confirmed at both mRNA and protein levels (Fig. 1-G and H). The data obtained for all siRNAs from the library are shown in Fig. 1-I. For each siRNA, HPG incorporation is plotted against TOM20 level. HPG incorporation showed only a low to moderate correlation with TOM20 staining (Pearson correlation coefficient, PCC=0.39). Interestingly, 25 percent of the siRNAs showed a change in mitochondrial translation greater than 25 percent of control: 13 percent increased and 12 percent decreased the mitochondrial translation. Overall, after validating the strength of the method for high-throughput analysis, we obtained a comprehensive view of the effect of various kinase knockdowns on mitochondrial translation.

3.2.2. Ablation of kinases affects mitochondrial function and ATP levels.

In order to determine which candidates have significant effects on mitochondrial translation, we focused on genes for which more than two of their siRNAs produced a change of at least 20 percent (either increase or decrease) in the first screening. A total of 225 siRNAs were selected and tested in three biological replicates for more thorough analysis (Fig. 2-A, Table S1). Nearly 50 percent of siRNAs showed a significant change compared to the non-targeting control (p-value < 0.05), whereas TOM20 level remained unchanged under most knockdown conditions and showed little correlation with HPG incorporation signal (Pears. 0.29, Fig. S2-A). However, a drastically low TOM20 level was often associated with a sharp decrease in HPG incorporation. For example, when Polo like kinase 1 (PLK1) was knocked down, both TOM20 and HPG incorporation signals were decreased and the cells appeared to be very unhealthy (Fig. 2A). These points were excluded from further analysis. We then focused on the siRNAs that showed significant effects on mitochondrial translation (a p-value of less than 0.05) for further investigation. With this filter, 90 siRNAs targeting 65 cellular kinases were selected. To start dissecting the possible modulating roles of these kinases on mitochondrial translation, we analyzed the location of these proteins among the different cellular

compartments. Subcellular localizations were extracted from data available in UniProt, the Human Protein Atlas (HPA) (Thul et al., 2018)), Mitocarta 3.0 (Rath et al., 2021), and the Kinome Atlas (H. Zhang et al., 2021). While most kinases were assigned to cytosolic, nuclear, and plasma membrane localizations, 9 kinases in this list were assigned to a mitochondrial localization/association in at least one database (Fig. 2-B and Table S2). Some of them were metabolic kinases with well-described functions such as hexokinase 1 (HK1), glucokinase (GCK), and mitochondrial creatine kinase 2 (CKMT2) (Table S2). In all three cases, translation in mitochondria was decreased after knockdown. Another protein shown to be associated to the mitochondrial outer membrane is FKBP12-rapamycin-associated protein 1 (FRAP1, also known as mTOR). The role of FRAP1 in regulating the expression of various nuclear-encoded mitochondrial proteins, mitochondrial function, and ATP production has been investigated in several studies (Cunningham et al., 2007; de la Cruz López et al., 2019). Here, we observed decreased mitochondrial translation after its silencing.

Mitochondrial translation products are essential components of the OXPHOS complexes which produce ATP in mitochondria via oxidative phosphorylation. In order to analyze how defects in the synthesis of OXPHOS subunits are associated with mitochondrial energy production, we measured cellular ATP levels and oxygen consumption rate (OCR) after downregulation of selected kinases. The cellular ATP level was significantly decreased in 30 percent of the cases (Fig. 2-C) and showed a moderate correlation with the level of mitochondrial translation (Fig. S2-C). Interestingly, we did not detect an increase in cellular ATP level in the cases with increased mitochondrial translation, therefore showing a low correlation between ATP content and mitochondrial translation (Fig. 2-C and Fig. S2-C). A larger number of siRNAs (60 percent) caused a significant decrease in oxygen consumption rates (OCR), whereas only two of them slightly increased OCR. Therefore, we could find a moderate/high correlation between mitochondrial translation and OCR level that was higher than cellular ATP. (Fig 2-D and Fig. S2-D).

In conclusion, we evaluated the effects of 90 siRNAs targeting 65 cellular kinases on mitochondrial translation. Cellular ATP and OCR partially correlate with the level of mitochondrial translation under these knockdown conditions.

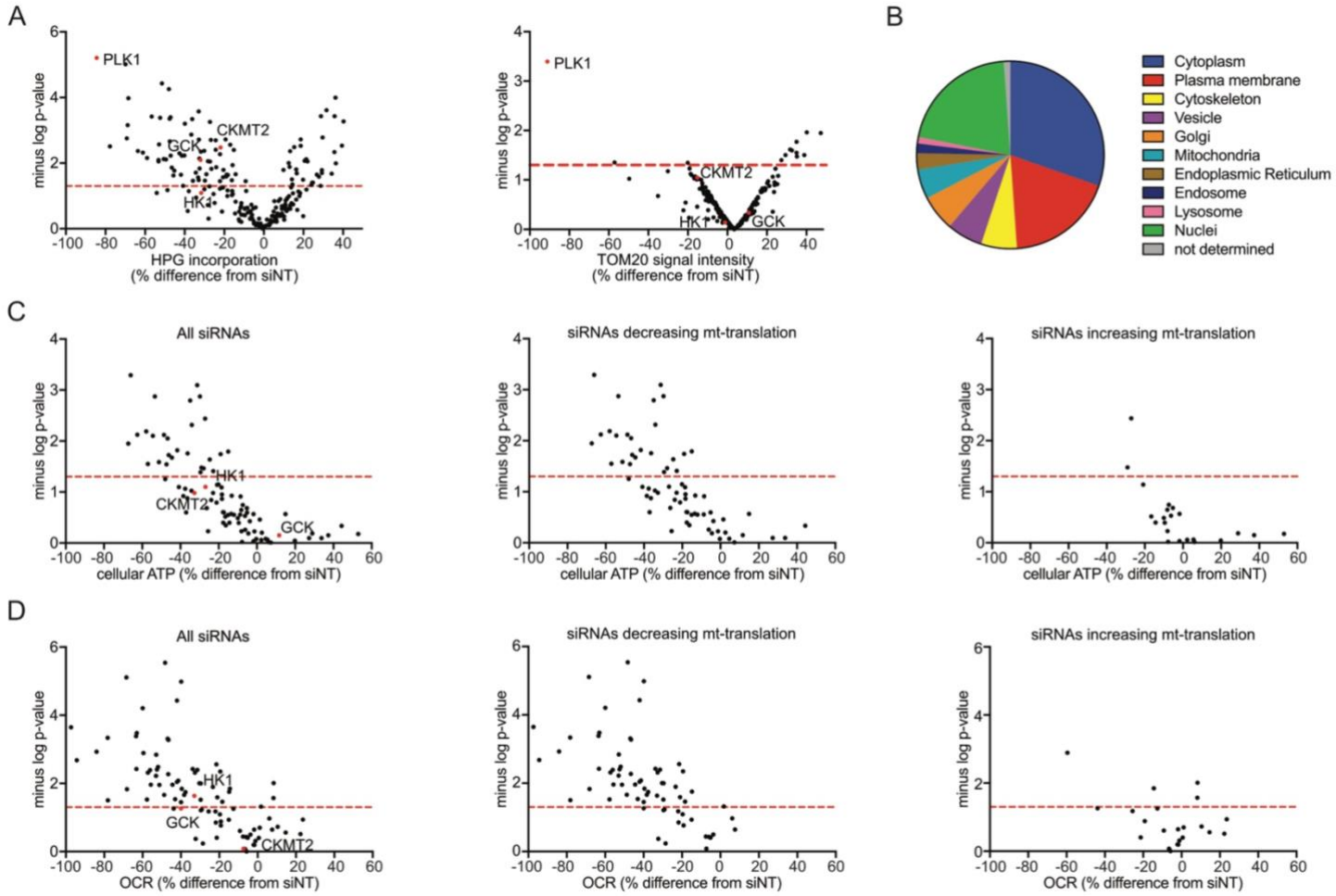

Figure 2. Ablation of kinases affects mitochondrial function and ATP levels. (A) HPG incorporation and TOM20 were measured in 3 independent replicates after knockdown with 225 selected siRNAs. Student *t*-test. The points with p-value above 0.05 (red dashed line) were considered significant. **(B)** Subcellular localization of kinases whose siRNA knockdown affected mitochondrial translation. Data were extracted from 4 different databases (see Table S2). **(C)** Cellular ATP level was measured after downregulation of the selected kinases. Separate plots show knockdown conditions with a decreasing or an increasing effect on mitochondrial translation. N = 3 independent replicates. Student *t*-test, Dashed line shows $*P = 0.05$. **(D)** Basal oxygen consumption rate (OCR) was measured after downregulation of the selected kinases. Separate plots show siRNAs with decreasing or increasing effect on mitochondrial translation. N = 3 independent replicates. Student *t*-test, Dashed line shows $*P = 0.05$.

3.2.3. Downregulation of selected kinases show changes in energetic state and mitoribosome integrity.

From the 65 kinases with a significant effect on mitochondrial translation we selected 8 kinases with less described functions to perform a deeper characterization: The aarF domain containing kinase 2 (ADCK2), Dual Specificity Tyrosine Phosphorylation Regulated Kinase 4 (DYRK4), Uridine-Cytidine Kinase 2 (UCK2), TANK Binding Kinase 1 (TBK1), AURKAIP1, Fructosamine 3 Kinase (FN3K), MOK Protein Kinase (MOK), and mitogen-activated protein kinase 11 (MAPK11, also known as p38). With the exception of MAPK11, knockdown of these kinases resulted in a decreased HPG incorporation. In order to verify the specificity of the effect of these factors on mitochondrial translation, we measured the knockdown efficiency at both mRNA and protein levels and observed a prominent decrease of both mRNA and protein levels (Fig. S3-B and C).

We then further investigated the association of altered mitochondrial translation on the energetic function of the organelle in the selected candidates. For that, we plotted and analyzed individually the values obtained for cellular ATP and OCR levels (Fig. 3-A). In some cases, low cellular ATP level was associated with lower OCR (UCK2, TBK1, AURKAIP1, FN3K, MOK), suggesting a possible impairment of mitochondrial OXPHOS function. In other cases (ADCK2 and DYRK4), siRNA knockdown did not alter ATP level or OCR compared to the non-targeting control. Interestingly, knockdown of MAPK11 showed a slight insignificant increase in the OCR (Fig. 3-A).

The two major cellular sources of ATP production are glycolysis in the cytosol and OXPHOS in the mitochondria. To examine how downregulation of selected kinases influences ATP production from the two sources, we performed a real time ATP production rate assay that quantifies the rate of ATP produced by glycolysis and mitochondrial OXPHOS. Consistent with cellular ATP and OCR measurements, siADCK2 had no effect on ATP production rate. In the case of siDYRK4, ATP production from OXPHOS appeared to have a minor defect that was compensated by the increase in glycolytic ATP. In siUCK2 and siTBK1, ATP production from both sources was decreased. ATP production by OXPHOS was significantly impaired in siAURKAIP1 and siFN3K, whereas the rate of glycolytic ATP was unchanged. Upon siRNA knockdown against MOK, the ATP production rate showed no significant change, although cellular ATP and OCR were slightly but significantly reduced. Surprisingly, ATP production rate

was slightly lower in the case of MAPK11 knockdown, whereas cellular ATP and OCR were comparable to the non-targeting control.

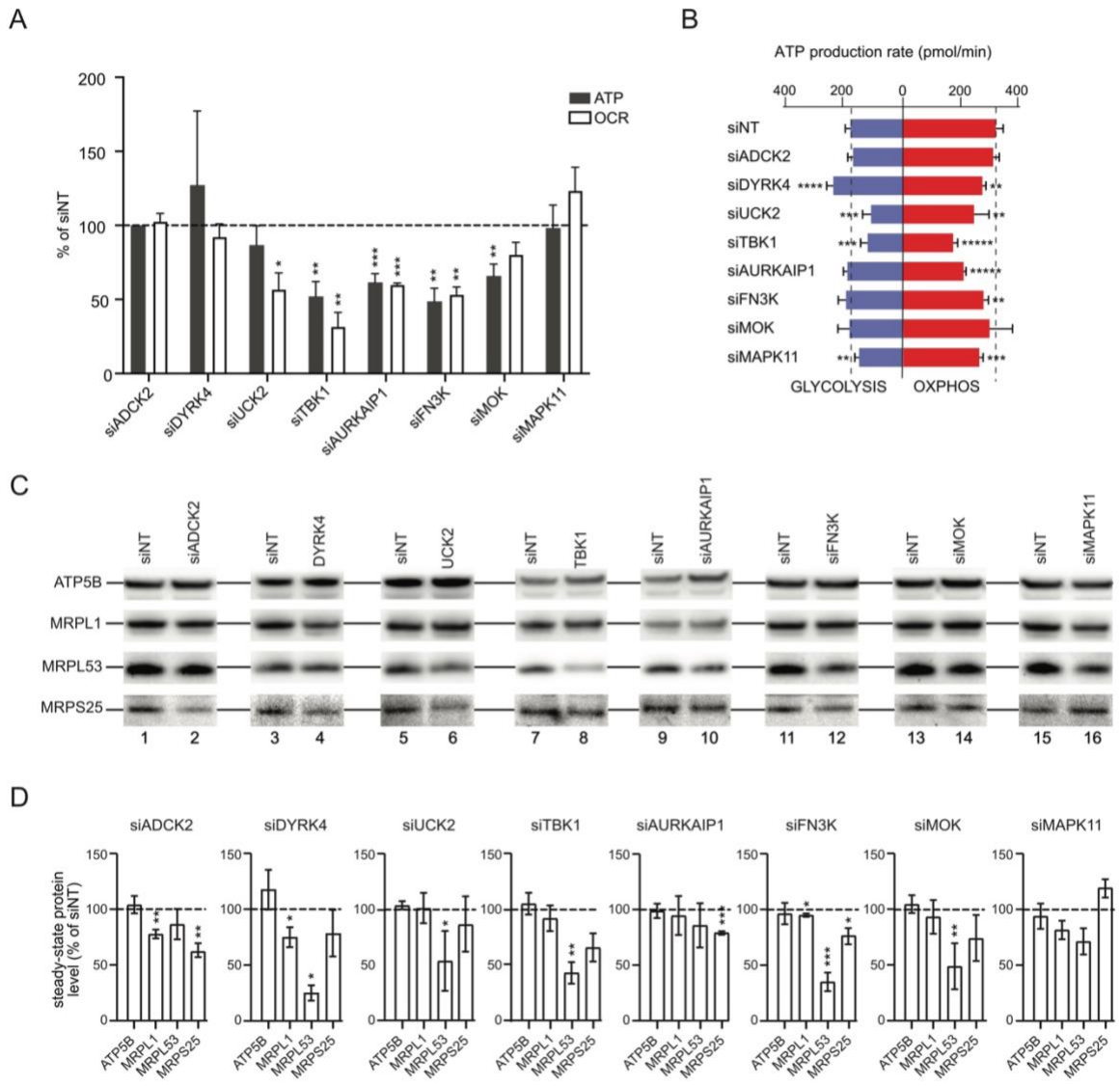

Figure 3. Downregulation of selected kinases changes the cellular energetic state and mitoribosome integrity. (A) Cellular ATP and OCR values were extracted for selected siRNAs from the data in Fig. 2-C and D, respectively. **(B)** Glycolysis and mitochondrial ATP production rates were calculated after knockdown with selected siRNAs. N=3 independent replicates. **(C)** The steady state level of ATP5B, MRPL53, MRPL1, and MRPS25 was analyzed by Western blotting in the cells after knockdown with respective siRNAs. **(D)** Quantitative analysis of the steady-state level of ATP5B, MRPL53, MRPL1, and MRPS25 was performed after knockdown of each kinase in 3 independent experiments. Error bars show SEM. Student *t*-test, **P*<0.05, ***P*<0.01, ****P*<0.001, *****P*<0.0001, ******P*<0.00001.

Any changes in mitochondrial ribosome assembly and function could change the protein synthesis. Therefore, we assessed whether the observed changes in mitochondrial translation were related to the steady-state level of mitoribosomal subunits after silencing of selected candidate kinases. The steady-state level of MRPL53 from the large subunit and MRPS25 from the small subunit was reduced in most of the knockdown conditions, whereas the level of

MRPL1 was unchanged or only slightly reduced. Interestingly, downregulation of MAPK11 with an increased mitochondrial translation phenotype, differently affected the mitoribosome subunits, decreasing the components of the large subunit and increasing the component of the small subunit. Overall, downregulation of the kinases with a reduced mitochondrial translation phenotype, showed a general reduction in the mitoribosome subunits.

3.2.4. Effect of downregulation of selected kinases on individual proteins

Labeling mitochondrial translation with FUNCAT does not provide resolution to individual peptides. To test whether the observed changes in translation were due to specific or general effects, we labeled mitochondrial translation products with radioactive [^{35}S]-methionine after knockdown of the selected kinases (Fig. 4-A).

Consistent with FUNCAT labeling, siMAPK11 increased total mitochondrial translation and the other selected siRNAs decreased it (Fig. 4-A and B). Accordingly, the radioactive signal was analyzed for each band representing a specific mitochondrial-encoded protein (Fig. 4-C). Exceptions were COX2/COX3 and ATP8/ND4L, for which the bands were difficult to resolve.

Overall, the observed change on mitochondrial translation was rather a general effect and not due to the change of mitochondrial polypeptide belonging to a specific OXPHOS complex. However, in some cases specific mt-encoded proteins are more affected than others. For example, ND2, COX1, and CYTB were most prominently affected by knockdown of TBK1. Downregulation of FN3K, UCK2, and MOK affected ND3 and ND6 more than the other proteins. Knockdown of MAPK11, increased the synthesis of CYTB, COX2, COX3, and to some extent COX1, whereas the other proteins were or slightly lower than in the control.

In conclusion, we studied the changes in mitochondrial translation after silencing 8 selected candidate kinases using [^{35}S]-methionine labeling. Using this approach, we could not only confirm the most interesting results of the screening but also analyze the synthesis of each individual mitochondrial peptide. Interestingly, changes in mitochondrial translation were not due to the increased or decreased synthesis of the same polypeptides in all studied kinases, but showed rather a differential pattern for each kinase.

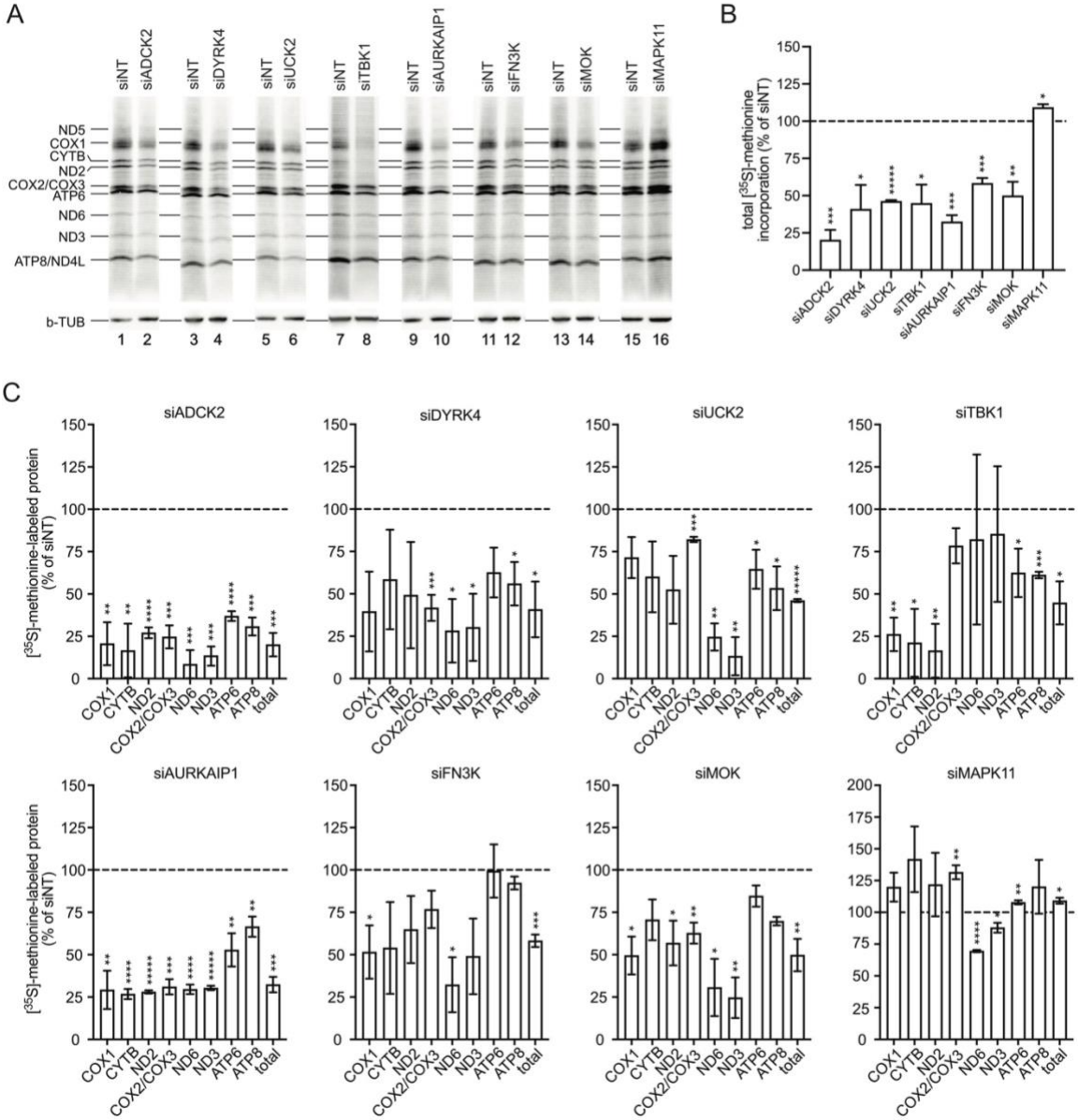

Figure 4. Effect of downregulation of selected kinases on individual mitochondrial proteins. (A) Radiolabeling of mitochondrial translation in cells with [^{35}S]-methionine after knockdown of selected kinases. Western blotting with b-tubulin antibody served as loading control. **(B)** Quantitative analysis of total mitochondrial translation labeled with [^{35}S]-methionine after downregulation of the respective kinases. **(C)** Quantitative analysis of individual proteins labeled with [^{35}S]-methionine. N = 3 independent replicates. Error bars show SEM. Student t-test, *P<0.05, **P<0.01, ***P<0.001, ****P<0.0001, *****P<0.00001.

3.3. Discussion

Recent structural analysis of mitochondrial RNA polymerase (POLRMT) and mitoribosomes have provided insights into the mechanisms of gene expression in mitochondria (Amunts et al., 2015; Hillen et al., 2017; Kummer et al., 2018, 2021). Several molecular mechanisms for modulating gene expression in mitochondria at the level of RNA stability and RNA turnover

have been described (Jedynak-Slyvka et al., 2021; Jourdain et al., 2017; Ruzzenente et al., 2012). In addition, phosphorylation of various transcription and translation factors as well as components of mitoribosomes has been demonstrated in vitro and in the native state in cells (He et al., 2001; Lu et al., 2013; Wang et al., 2014). At the same time, the number of kinases discovered in association with mitochondria or having mitochondrial targets is growing. Some of the kinases transiently enter mitochondria, while others phosphorylate their target proteins in the cytosol before translocating to mitochondria (Kotrasová et al., 2021). How phosphorylation alters protein activity and modulates translation in mitochondria is not well understood. Therefore, we aimed to screen cellular kinases to elucidate their putative role in mitochondrial translation. This would allow us to identify new players and potential pathways in regulating mitochondrial gene expression. FUNCAT provided the tool for developing a high throughput approach to measure mitochondrial translation. We have shown that the method is robust and accurate enough to detect even small changes in mitochondrial translation (Fig. 1 and Fig. S1). This setup can be used to test various treatments, substrates, and inhibitors for their effect on mitochondrial translation.

By combining the FUNCAT method with siRNA-mediated knockdown, we screened the siRNA library containing all 709 human kinases. Of these, knockdown of 65 kinases affected mitochondrial translation (Fig. 2 and Table S1). Among them were 9 kinases whose mitochondrial localization has been described in various databases. In that way, the strategy that we designed is validated by the identification of known mitochondrial kinases with functions that could possibly modify mitochondrial gene expression.

Impaired mitochondrial translation may lead to decreased concentration and activity of OXPHOS complexes and therefore energy production (Bhatti et al., 2017). On the other hand, the decrease in mitochondrial translation may be an indirect effect triggered by alteration of another cellular mechanism and activation of mechanisms such as the integrated stress response (G. Zhang et al., 2021). Decreased cellular ATP was observed in 45 percent of cases with decreased mitochondrial translation. In addition, the effects on oxygen consumption rate (OCR) were more pronounced (82 percent of cases). However, in several cases decreased mitochondrial translation did not correlate with cellular ATP and OCR levels, suggesting that either different mechanisms compensate for decreased mitochondrial translation or OXPHOS malfunction and decrease of mitochondrial translation are not directly associated.

Among all identified kinases modulating mitochondrial translation, we selected 8 of them focusing on putative mitochondrial localizations and less-described functions. ADCK2 was found with high confidence in proteomic data of human mitochondria (Morgenstern et al., 2021). Its deficiency was shown to be associated with impaired fatty acid oxidation in mitochondria resulted from reduced biosynthesis of coenzyme Q (CoQ) (Vázquez-Fonseca et al., 2019). Here, we found a general decrease in synthesis of all mitochondrial-encoded proteins and a reduction in the steady-state levels the mitoribosome subunits upon deletion of ADCK2, whereas no effect was observed in the OXPHOS, and glycolysis ATP production. Whether impaired biosynthesis of CoQ is responsible for reduced mitochondrial protein synthesis or vice versa requires further investigation.

DYRK4 is assigned to cytosolic and vesicular localizations in several databases, but its function has not yet been described. Previous studies with other kinases in its protein family have shown that DYRK1A phosphorylates the mitochondrial import receptor TOM70 and modulates translocation of the protein into mitochondria (Walter et al., 2021). Despite the significant reduction in mitochondrial translation and OXPHOS activity, the increase in glycolysis appeared to compensate for this reduction. Interestingly, a decreased on the steady-state levels of components of the mitoribosome was found upon DYRK4 silencing, probably explaining the downregulation of mitochondrial translation.

UCK2 is the rate-limiting enzyme in the salvage pathway of pyrimidine synthesis. Therefore, it may have a direct effect on nucleic acid synthesis. Its upregulation has been found in many cancers (Cai et al., 2020; Malami et al., 2019). Its depletion resulted in decreased mitochondrial translation, lowered mitochondrial and glycolytic ATP production, and decreased MRPL53 level. Surprisingly, synthesis of ND3 and ND6 was more affected than other mitochondrial-encoded proteins. Whether this effect is due to altered RNA synthesis remains to be elucidated.

Microscopy studies have postulated FN3K to be localized inside mitochondria, but to date no mitochondria-related function has been described for this protein. FN3K phosphorylates the glycan moiety on glycated proteins and therefore reverses the deleterious effects of spontaneous glycation by destabilizing the proteins (Szwergold et al., 2001). Interestingly, silencing of this factor decreased mitochondrial translation (with a differential pattern for each polypeptide), decreased levels of mitoribosome components and also OXPHOS function.

A similar phenotype was observed after the depletion of MOK protein kinase. Interestingly, MOK was recently found to be localized in the intermembrane space of mitochondria and its CRISPR-mediated knockout altered mitochondrial length and cristae morphology (H. Zhang et al., 2021).

Since AURKAIP1 has been described as a component of the mitoribosome small subunit (Koc et al., 2013), the observed decrease in mitochondrial translation and OXPHOS activity was expected. Interestingly, no significant change in the steady-state levels of large mitoribosomal subunits of MRPL53 and MRPL1 was observed, however, MRPS25 was decreased upon AURKAIP1 knockdown. In the study by Koc et al., where they characterized AURKAIP1 and several other proteins as components of the mitoribosomes, they reported no significant change in the steady state levels of two other proteins of large and small subunits upon downregulation of AURKAIP1 (Koc et al., 2013).

MAPK11 has been reported to be involved in several signaling pathways related to mitochondrial biogenesis and mitochondria-mediated apoptosis (Gräb et al., 2019; Gui et al., 2020). We observed an increase in mitochondrial translation after knockdown of MAPK11 (Fig. S3-A and Table S1). Interestingly, we could identify some polypeptides whose synthesis was increased to higher extent than the others (COX1, COX2, and COX3 from complex IV, and CYTB versus ND3, ND3, and ND6 from complex I) although no changes in ATP levels or OCR was observed. In that way, either a different time frame is required for such an extra effect or it may be that OXPHOS capacity adapts to the maximum cell demand and it remains independent of mitochondrial translation levels until a higher energy production is required.

In conclusion, the screening provided unprecedented information on potential factors involved in the regulation of mitochondrial translation. Although, a first characterization of these factors has been performed in this study in terms of OXPHOS capacity after silencing, further studies are needed to decipher the mechanism behind the mitochondrial translation modulation phenotype.

3.4. Material and Methods

3.4.1. Cell line and cell culture

HeLa cells were purchased from the DSMZ collection at the Leibnitz institute and were cultured in Dulbecco's modified Eagle's medium (DMEM, ThermoFischer), supplemented with

10% (V/V) fetal bovine serum (FBS, Biochrom), 1 mM sodium pyruvate, 2 mM L-glutamine, and 50 µg/ml uridine. Cells were cultured at 37°C in the incubator with 5% CO_2 and passaged regularly. For imaging purposes, glass coverslips or glass-bottom Sensoplates (Greiner) were coated with poly L-lysine (PLL, 0.1 mg/ml) for one hour and washed thoroughly before the start of the experiments.

3.4.2. Transfection of HeLa cells with Human Kinase siRNA library

Silencer™ Human Kinase siRNA Library was purchased from ThermoFischer. Nuclease-free water was added to the original plates to make a concentration of 2 µM. Running plates of 166 nM were prepared in 96-well PCR plates and were used for transfection. Reverse transfection was performed according to the manufacturer's protocol with slight modifications. Briefly, for each well of 96-well Sensoplate, 0.2 µl of Lipofectamine® RNAiMAX (Invitrogen) was diluted in 20 µl of OptiMEM (Gibco), mixed and incubated for 5 min. From the siRNA running plate, 5 µl was added to the OptiMEM-Lipofectmaine mixture and incubated for 20 minutes. Meanwhile, 4000 cells per well were counted in 100 µl of media and were added to the plate after the incubation. For respirometry analysis, the transfection was performed in Seahorse 96-well microplates (Agilent) with 2500 cells. The plates were then incubated for 72 hours in the incubator, wrapped in humid tissues to minimize evaporation.

3.4.3. HPG-labeling of mitochondrial translation in 96-well plate

To label mitochondrial translation in 96-well plate, we adapted a click-chemistry based method that was previously introduced by us and the others (Estell et al., 2017; Yousefi et al., 2021; Zorkau et al., 2021). Cells were incubated with methionine-free DMEM medium containing the antibiotic harringtonine (200 µM, Carbosynth) for 10 minutes. The medium was changed to methionine-free DMEM containing harringtonine and 500 µM of L-Homopropargylglycine (HPG, ThermoFisher). The labeling was done for 1 hour and then the medium was exchanged with an ice-cold permeabilizing buffer containing 10mM HEPES, 10mM NaCl, 5mM KCl, 300 mM sucrose, and 0.015% digitonin, for 2 minutes. A quick wash with the same buffer, only without digitonin was performed for 15 seconds. The buffer was removed and 4% PFA solution (pH 7.5, in PBS) was added to fix the cells for 30 minutes at room temperature. In negative control samples, 150 µg/ml chloramphenicol, freshly

prepared in ethanol, was used 50 minutes before the labeling to stop mitochondrial translation. To maintain the timing and the solution volumes precise in all the wells, an automated pipetting system was used (Biomek FX^P).

3.4.4. Click-chemistry and immunostaining of fixed cells

After PFA fixation, cells were washed for 5 minutes with PBS and quenched for 15 minutes with 100 mM NH_4Cl in PBS. Cells were blocked and permeabilized with the staining solution (PBS + 5% BSA + 5% tryptone peptone + 0.1% Triton X-100) 3 x 5 minutes. After a brief wash with 3% BSA in PBS, cells were clicked with 1.5 µM AlexaFluor 647-azide (ThermoFisher) for 40 minutes using Click-iT Cell Reaction Buffer Kit (ThermoFisher). Cells were quickly washed with 3% BSA in PBS again and then primary and secondary antibodies were applied sequentially for 1 hour. Between antibody incubations, cells were washed with staining solution 3 x 5 minutes. Same number of washes with blocking solution (PBS + 5% BSA + 5% tryptone peptone), high-salt PBS (PBS + 500 mM NaCl), and normal PBS were performed after the secondary antibody, to thoroughly remove unspecific staining of the antibodies. For cells on coverslips, embedding was performed in Mowiol (Calbiochem, Billerica, MA, USA) and the coverslips were allowed to dry overnight at room temperature before imaging. For the library screening experiments, the nuclei were stained with Hoechst (Thermo Fisher) diluted 1:10000 in PBS for 5 minutes and the glass-bottom Sensoplates were washed once more with PBS, kept at 4°C in dark and were imaged within 24 hours.

The antibodies used for fluorescent microscopy are as follows: TOM20 (1:800, Proteintech, 11802-1-AP), goat anti-rabbit Alexa Fluor Plus 488 (1:800, ThermoFisher, A32731).

3.4.5. Image acquisition and analysis

For the library screening, the 96-well Sensoplates were imaged using a Cytation 5™ Cell Imaging Multi-Mode Reader BioTek (Winooski, VT, USA) equipped with a Sony CCD 16-bit grayscale camera. At least 20 images were acquired per well with a 20×, 0.45 NA objective. We used a custom macro written in MATLAB (The Mathworks, Inc., Natick, MA, USA) to analyze the images. The nuclei staining was used to spot the cells by applying a threshold. The selected regions of the nuclei were dilated to cover the whole cell area. HPG and TOM20 signals were measured for each cell area. The signals from all the cells were then averaged and normalized to the signal from the controls. The script is available upon request.

3.4.6. Radioactive-labeling of mitochondrial translation products

Mitochondrial translation products were labeled with radioactive [^{35}S]-methionine according to a previously published protocol (Chomyn, 1996) with minor modifications. Briefly, the medium of the cells was changed twice with the methionine-free DMEM deprived of FBS, each time incubated at 37°C for 10 minutes. The methionine-free DMEM, supplemented with 10% FBS and containing antibiotic emetine (100 µg/ml, Merck) was added to the cells for 10 minutes. Then, the cells were treated with 200 µCi/ml [^{35}S]-methionine and were incubated at 37°C for 1 hour. After the incubation, the cells were lysed and equal amounts were loaded on a 10-18% Tris-Tricin gradient gel. The proteins were transferred to PVDF membranes and exposed to Phosphor Screens for digital radiography. The radioactive signal was detected on a Typhoon scanner (GE Healthcare). Quantification of the autoradiography images in Figure 4 was performed using FIJI software as follows: First, a manual threshold was determined to separate the background from the regions of interest. The values of background pixels were set to zero. Then, for the individual band or the total lane, the sum of the values over the threshold (integrated density) was obtained.

3.4.7. Steady-state analysis of protein level with western blotting

The cells were harvested and lysed. Whole cell lysates were loaded on NuPage Bis-Tris 4-10% SDS gels and the proteins were transferred on PVDF membranes. Western blotting was performed according to the standard protocols. Primary antibodies were incubated overnight and were as follows: ATP5B (custom-made raised in rabbit); SDHA (Thermo, 459200); MRPL1 (Proteintech, 16254-1-AP); MRPL53 (Proteintech, 16142-1-AP); MRPS25 (Proteintech, 67903-1-Ig); b-tubulin (abcam, AB6046). Secondary antibodies were goat anti-Rabbit and anti-mouse conjugated to horse-raddish peroxidase (Dianova).

3.4.8. RNA extraction, cDNA synthesis and qRT-PCR

RNA was extracted from cells using RNA Clean&Concentrator kit (Zymo Reseach, R1091) according to the manufacturer's protocol with minor changes. Adequate amount of TRIzol (Invitrogen) was added to the cells, incubated for 5 minutes at 24°C. Chloroform was added one fifth of the TRIzol volume to the cells, then vigorously vortexed for 15 seconds. After a 3-minute incubation at 24°C, samples were pelleted down at 4°C, 12000xg for 15 minutes. The aqueous upper phase was separated and mixed with 1:1 volume of pure ethanol, mixed well

and loaded to the columns. From here, the manufacture's protocol was precisely followed and RNA was eluted in RNAse/DNase free water and the concentration was measured with Nanodrop (Thermo). The samples were stored at -80 until use. cDNA was synthesized from 1 µg of RNA, using the First Strand cDNA Synthesis kit (Thermo Scientific, K1612) and random hexamer primers. The qRT-PCR was performed using the SensiMix^{TM} SYBR Low-Rox Obe Step kit (Bioline, QT625-02), in a QuantStudio 6 flex cycler (Applied Biosystems). The sequence of the primers is available upon request.

3.4.9. Real-time respirometry

Real-time respirometry for oxygen consumption rate (OCR) was performed with a XF96 Extracellular Flux Analyzer (Seahorse Bioscience, Billerica, MA, USA) as previously described (Pacheu-Grau et al., 2020). Briefly, cell media was changed to Seahorse assay media and was calibrated at 37°C for 1 hour in an incubator without CO_2. The sensors were calibrated and the cell plate was placed into the analyzer. Three periodic measurements of oxygen level were captured before and after addition of different inhibitors/uncouplers and the OCR was calculated from the slope of oxygen level change over the course of time. The inhibitors/uncouplers were added in this order: 3 µM oligomycin, 1.6 µM FCCP, and 1 µM antimycin A plus 1 µM rotenone.

In order to measure the real-time ATP production rate from mitochondrial respiration and glycolysis, similar approach was performed with a slightly different order of inhibitors: 3 µM oligomycin followed by 1 µM antimycin A plus 1 µM rotenone. Extracellular acidification rate (ECAR) and OCR measurements were used using the Agilent Seahorse analytics software (WAVE) to calculate the ATP production rate.

3.4.10. Cellular ATP detection assay

The cellular ATP was measured using Luminescent ATP Detection Assay Kit (abcam, ab113849) according to the manufacturer's protocol. Briefly, cells were lysed using the kit detergent and then, the substrate was added. The luminescent light was detected using a plate reader (Agilent BioTek). The values were normalized to the number of cells measured by parallel CyQuant cell proliferation assay (Thermo, C7026).

3.5. Acknowledgement

This project was funded by the European Research Council (ERC) Advanced Grant (ERCAdG No. 339580), the Sonderforschungsbereiche (SFB) 1286, the Max Planck Institute for Biophysical Chemistry, and the PhD program Molecular Biology-International Max Planck Research School and the Göttingen Graduate School for Neurosciences and Molecular Biosciences (GGNB; DFG grant GSC 226/1).

3.6. References

Amunts, A., Brown, A., Toots, J., Scheres, S. H. W., & Ramakrishnan, V. (2015). Ribosome. The structure of the human mitochondrial ribosome. *Science (New York, N.Y.)*, *348*(6230), 95–98. doi: 10.1126/SCIENCE.AAA1193

Anderson, S., Bankier, A. T., Barrell, B. G., de Bruijn, M. H. L., Coulson, A. R., Drouin, J., Eperon, I. C., Nierlich, D. P., Roe, B. A., Sanger, F., Schreier, P. H., Smith, A. J. H., Staden, R., & Young, I. G. (1981). Sequence and organization of the human mitochondrial genome. *Nature*, *290*(5806), 457–465. doi: 10.1038/290457a0

Antonicka, H., & Shoubridge, E. A. (2015). Mitochondrial RNA Granules Are Centers for Posttranscriptional RNA Processing and Ribosome Biogenesis. *Cell Reports*, *10*(6), 920–932. doi: 10.1016/J.CELREP.2015.01.030

Area-Gomez, E., Guardia-Laguarta, C., Schon, E. A., & Przedborski, S. (2019). Mitochondria, OxPhos, and neurodegeneration: cells are not just running out of gas. *The Journal of Clinical Investigation*, *129*(1). doi: 10.1172/JCI120848

Bhatti, J. S., Bhatti, G. K., & Reddy, P. H. (2017). Mitochondrial dysfunction and oxidative stress in metabolic disorders — A step towards mitochondria based therapeutic strategies. *Biochimica et Biophysica Acta (BBA) - Molecular Basis of Disease*, *1863*(5), 1066–1077. doi: 10.1016/J.BBADIS.2016.11.010

Brischigliaro, M., & Zeviani, M. (2021). Cytochrome c oxidase deficiency. *BBA-Bioenergetics*, *1862*, 148335. doi: 10.1016/j.bbabio.2020.148335

Cai, J., Sun, X., Guo, H., Qu, X., Huang, H., Yu, C., Wu, H., Gao, Y., Kong, X., & Xia, Q. (2020). Non-metabolic role of UCK2 links EGFR-AKT pathway activation to metastasis enhancement in hepatocellular carcinoma. *Oncogenesis 2020 9:12*, *9*(12), 1–14. doi: 10.1038/s41389-020-00287-7

Chomyn, A. (1996). [18] In vivo labeling and analysis of human mitochondrial translation products. *Methods in Enzymology*, *264*, 197–211. doi: 10.1016/S0076-6879(96)64020-8

Couvillion, M. T., Soto, I. C., Shipkovenska, G., & Stirling, & L. (2016). Synchronized mitochondrial and cytosolic translation programs. *Nature*. doi: 10.1038/nature18015

Cruz-Zaragoza, L. D., Dennerlein, S., Linden, A., Yousefi, R., Lavdovskaia, E., Aich, A., Falk, R. R., Gomkale, R., Schöndorf, T., Bohnsack, M. T., Richter-Dennerlein, R., Urlaub, H., & Rehling, P. (2021). An in vitro system to silence mitochondrial gene expression. *Cell*, *184*(23), 5824-5837.e15. doi: 10.1016/j.cell.2021.09.033

Cunningham, J. T., Rodgers, J. T., Arlow, D. H., Vazquez, F., Mootha, V. K., & Puigserver, P. (2007). mTOR controls mitochondrial oxidative function through a YY1–PGC-1α transcriptional complex. *Nature 2007 450:7170*, *450*(7170), 736–740. doi: 10.1038/nature06322

de la Cruz López, K. G., Toledo Guzmán, M. E., Sánchez, E. O., & García Carrancá, A. (2019). mTORC1 as a Regulator of Mitochondrial Functions and a Therapeutic Target in Cancer. *Frontiers in Oncology*, *9*, 1373. doi: 10.3389/FONC.2019.01373/BIBTEX

Dennerlein, S., Poerschke, S., Oeljeklaus, S., Wang, C., Richter-Dennerlein, R., Sattmann, J., Bauermeister, D., Hanitsch, E., Stoldt, S., Langer, T., Jakobs, S., Warscheid, B., & Rehling, P. (2021). Defining the interactome of the human mitochondrial ribosome identifies SMIM4 and TMEM223 as respiratory chain assembly factors. *ELife*, *10*. doi: 10.7554/ELIFE.68213

Dennerlein, S., Wang, C., & Rehling, P. (2017). Plasticity of Mitochondrial Translation. *Trends in Cell Biology*, *27*(10), 712–721. doi: 10.1016/J.TCB.2017.05.004

Dieterich, D. C., Hodas, J. J. L., Gouzer, G., Shadrin, I. Y., Ngo, J. T., Triller, A., Tirrell, D. A., & Schuman, E. M. (2010). In situ visualization and dynamics of newly synthesized proteins in rat hippocampal neurons. *Nature Neuroscience*, *13*(7), 897. doi: 10.1038/NN.2580

Dimauro, S. (2019). A Brief History of Mitochondrial Pathologies. *International Journal of Molecular Sciences 2019, Vol. 20, Page 5643*, *20*(22), 5643. doi: 10.3390/IJMS20225643

Estell, C., Stamatidou, E., El-Messeiry, S., & Hamilton, A. (2017). In situ imaging of mitochondrial translation shows weak correlation with nucleoid DNA intensity and no suppression during mitosis. *Journal of Cell Science*, *130*(24), 4193–4199. doi: 10.1242/JCS.206714

Giorgianni, F., Koirala, D., Weber, K., & Beranova-Giorgianni, S. (2014). Proteome Analysis of Subsarcolemmal Cardiomyocyte Mitochondria: A Comparison of Different Analytical Platforms. *International Journal of Molecular Sciences*, *15*(6), 9285–9301. doi: 10.3390/ijms15069285

Gorman, G. S., Chinnery, P. F., DiMauro, S., Hirano, M., Koga, Y., McFarland, R., Suomalainen, A., Thorburn, D. R., Zeviani, M., & Turnbull, D. M. (2016). Mitochondrial diseases. *Nature Reviews Disease Primers 2016 2:1*, *2*(1), 1–22. doi: 10.1038/nrdp.2016.80

Gräb, J., & Rybniker, J. (2019). The Expanding Role of p38 Mitogen-Activated Protein Kinase in Programmed Host Cell Death. *Microbiology Insights*, *12*, 1178636119864594. doi: 10.1177/1178636119864594

Grevel, A., Pfanner, N., & Becker, T. (2019). Coupling of import and assembly pathways in mitochondrial protein biogenesis. *Biological Chemistry*, *401*(1). doi: 10.1515/HSZ-2019-0310

Gui, C., Ren, Y., Chen, J., Wu, X., Mao, K., Li, H., Yu, H., Zou, F., & Li, W. (2020). p38 MAPK-DRP1 signaling is involved in mitochondrial dysfunction and cell death in mutant A53T α-synuclein model of Parkinson's disease. *Toxicology and Applied Pharmacology*, *388*, 114874. doi: 10.1016/J.TAAP.2019.114874

He, H., Chen, M., Scheffler, N. K., Gibson, B. W., Spremulli, L. L., & Gottlieb, R. A. (2001). Phosphorylation of Mitochondrial Elongation Factor Tu in Ischemic Myocardium. *Circulation Research*, *89*(5), 461–467. doi: 10.1161/HH1701.096038

Hillen, H. S., Morozov, Y. I., Sarfallah, A., Temiakov, D., & Cramer, P. (2017). Structural Basis of Mitochondrial Transcription Initiation. *Cell*, *171*(5), 1072-1081.e10. doi: 10.1016/j.cell.2017.10.036

Itoh, Y., Andréll, J., Choi, A., Richter, U., Maiti, P., Best, R. B., Barrientos, A., Battersby, B. J., & Amunts, A. (2021). Mechanism of membrane-tethered mitochondrial protein synthesis. *Science*, *371*(6531), 846–849. doi: 10.1126/SCIENCE.ABE0763/SUPPL_FILE/ABE0763S1.MOV

Koc, E. C., Cimen, H., Kumcuoglu, B., Abu, N., Akpinar, G., Haque, M. E., Spremulli, L. L., & Koc, H. (2013). Identification and characterization of CHCHD1, AURKAIP1, and CRIF1 as new members of the mammalian mitochondrial ribosome. *Frontiers in Physiology*, *4 JUL*, 183. doi: 10.3389/FPHYS.2013.00183/ABSTRACT

Kotrasová, V., Keresztesová, B., Ondrovičová, G., Bauer, J. A., Havalová, H., Pevala, V., Kutejová, E., & Kunová, N. (2021). Mitochondrial Kinases and the Role of Mitochondrial Protein Phosphorylation in Health and Disease. *Life*, *11*(2), 82. doi: 10.3390/life11020082

Kruse, R., & Højlund, K. (2017). Mitochondrial phosphoproteomics of mammalian tissues. *Mitochondrion*, *33*, 45–57. doi: 10.1016/j.mito.2016.08.004

Kummer, E., & Ban, N. (2021). Mechanisms and regulation of protein synthesis in mitochondria. In Nature Reviews Molecular Cell Biology (Vol. 22, Issue 5, pp. 307–325). Nature Research. doi: 10.1038/s41580-021-00332-2

Kummer, E., Leibundgut, M., Rackham, O., Lee, R. G., Boehringer, D., Filipovska, A., & Ban, N. (2018). Unique features of mammalian mitochondrial translation initiation revealed by cryo-EM. *Nature 2018 560:7717*, *560*(7717), 263–267. doi: 10.1038/s41586-018-0373-y

Lu, B., Lee, J., Nie, X., Li, M., Morozov, Y. I., Venkatesh, S., Bogenhagen, D. F., Temiakov, D., & Suzuki, C. K. (2013). Phosphorylation of Human TFAM in Mitochondria Impairs DNA Binding and Promotes Degradation by the AAA+ Lon Protease. *Molecular Cell*, *49*(1), 121–132. doi: 10.1016/j.molcel.2012.10.023

Lucero, M., Suarez, A. E., & Chambers, J. W. (2019). Phosphoregulation on mitochondria: Integration of cell and organelle responses. *CNS Neuroscience & Therapeutics*, cns.13141. doi: 10.1111/cns.13141

Malami, I., & Abdul, A. B. (2019). Involvement of the uridine cytidine kinase 2 enzyme in cancer cell death: A molecular crosstalk between the enzyme and cellular apoptosis induction. *Biomedicine & Pharmacotherapy*, *109*, 1506–1510. doi: 10.1016/J.BIOPHA.2018.10.200

Mick, E., Titov, D. v., Skinner, O. S., Sharma, R., Jourdain, A. A., & Mootha, V. K. (2020). Distinct mitochondrial defects trigger the integrated stress response depending on the metabolic state of the cell. *ELife*, *9*. doi: 10.7554/ELIFE.49178

Miller, J. L., Cimen, H., Koc, H., & Koc, E. C. (2009). Phosphorylated Proteins of the Mammalian Mitochondrial Ribosome: Implications in Protein Synthesis. *Journal of Proteome Research*, *8*(10), 4789–4798. doi: 10.1021/pr9004844

Morgenstern, M., Peikert, C. D., Lübbert, P., Suppanz, I., Klemm, C., Alka, O., Steiert, C., Naumenko, N., Schendzielorz, A., Melchionda, L., Mühlhäuser, W. W. D., Knapp, B., Busch, J. D., Stiller, S. B., Dannenmaier, S., Lindau, C., Licheva, M., Eickhorst, C., Galbusera, R., … Warscheid, B. (2021). Quantitative high-confidence human

mitochondrial proteome and its dynamics in cellular context. *Cell Metabolism*, *33*(12), 2464. doi: 10.1016/J.CMET.2021.11.001

Münch, C., & Harper, J. W. (2016). Mitochondrial unfolded protein response controls matrix pre-RNA processing and translation. *Nature 2016 534:7609*, *534*(7609), 710–713. doi: 10.1038/nature18302

Ojala, D., Montoya, J., & Attardi, G. (1981). tRNA punctuation model of RNA processing in human mitochondria. *Nature*, *290*(5806), 470–474. doi: 10.1038/290470a0

Pacheu-Grau, D., Wasilewski, M., Oeljeklaus, S., Gibhardt, C. S., Aich, A., Chudenkova, M., Dennerlein, S., Deckers, M., Bogeski, I., Warscheid, B., Chacinska, A., & Rehling, P. (2020). COA6 Facilitates Cytochrome c Oxidase Biogenesis as Thiol-reductase for Copper Metallochaperones in Mitochondria. *Journal of Molecular Biology*, *432*(7), 2067–2079. doi: 10.1016/J.JMB.2020.01.036

Padrão, A. I., Vitorino, R., Duarte, J. A., Ferreira, R., & Amado, F. (2013). Unraveling the phosphoproteome dynamics in mammal mitochondria from a network perspective. *Journal of Proteome Research*, *12*(10), 4257–4267. doi: 10.1021/PR4003917

Pan, Y., & Shadel, G. S. (2009). Extension of chronological life span by reduced TOR signaling requires down-regulation of Sch9p and involves increased mitochondrial OXPHOS complex density. *Aging*, *1*(1), 131–145. doi: 10.18632/aging.100016

Prieto-Martín, A., Montoya, J., & Martínez-Azorín, F. (2004). Phosphorylation of rat mitochondrial transcription termination factor (mTERF) is required for transcription termination but not for binding to DNA. *Nucleic Acids Research*, *32*(7), 2059–2068. doi: 10.1093/NAR/GKH528

Rath, S., Sharma, R., Gupta, R., Ast, T., Chan, C., Durham, T. J., Goodman, R. P., Grabarek, Z., Haas, M. E., Hung, W. H. W., Joshi, P. R., Jourdain, A. A., Kim, S. H., Kotrys, A. v., Lam, S. S., McCoy, J. G., Meisel, J. D., Miranda, M., Panda, A., … Mootha, V. K. (2021). MitoCarta3.0: an updated mitochondrial proteome now with sub-organelle localization and pathway annotations. *Nucleic Acids Research*, *49*(D1), D1541–D1547. doi: 10.1093/NAR/GKAA1011

Richter, U., Lahtinen, T., Marttinen, P., Suomi, F., & Battersby, B. J. (2015). Quality control of mitochondrial protein synthesis is required for membrane integrity and cell fitness. *Journal of Cell Biology*, *211*(2), 373–389. doi: 10.1083/JCB.201504062

Richter-Dennerlein, R., Dennerlein, S., & Rehling, P. (2015). Integrating mitochondrial translation into the cellular context. *Nature Reviews. Molecular Cell Biology*, *16*(10), 586–592. doi: 10.1038/NRM4051

Richter-Dennerlein, R., Oeljeklaus, S., Lorenzi, I., Ronsör, C., Bareth, B., Schendzielorz, A. B., Wang, C., Warscheid, B., Rehling, P., & Dennerlein, S. (2016). Mitochondrial Protein Synthesis Adapts to Influx of Nuclear-Encoded Protein. *Cell*, *167*(2), 471. doi: 10.1016/J.CELL.2016.09.003

Szwergold, B. S., Howell, S., & Beisswenger, P. J. (2001). Human fructosamine-3-kinase: purification, sequencing, substrate specificity, and evidence of activity in vivo. *Diabetes*, *50*(9), 2139–2147. doi: 10.2337/DIABETES.50.9.2139

Thul, P. J., & Lindskog, C. (2018). The human protein atlas: A spatial map of the human proteome. *Protein Science : A Publication of the Protein Society*, *27*(1), 233. doi: 10.1002/PRO.3307

Tsushima, K., Bugger, H., Wende, A. R., Soto, J., Jenson, G. A., Tor, A. R., McGlauflin, R., Kenny, H. C., Zhang, Y., Souvenir, R., Hu, X. X., Sloan, C. L., Pereira, R. O., Lira, V. A., Spitzer, K. W., Sharp, T. L., Shoghi, K. I., Sparagna, G. C., Rog-Zielinska, E. A., … Abel, E. D. (2018). Mitochondrial Reactive Oxygen Species in Lipotoxic Hearts Induce Post-Translational Modifications of AKAP121, DRP1, and OPA1 That Promote Mitochondrial Fission. *Circulation Research*, *122*(1), 58–73. doi: 10.1161/CIRCRESAHA.117.311307

Vázquez-Fonseca, S., Schaefer, J., Navas-Enamorado, I., Santos-Ocaña, C., Hernández-Camacho, J. D., Guerra, I., Cascajo, M. v., Sánchez-Cuesta, A., Horvath, Z., Siendones, E., Jou, C., Casado, M., Gutiérrez, P., Brea-Calvo, G., López-Lluch, G., Fernández-Ayala, D. J. M., Cortés-Rodríguez, A. B., Rodríguez-Aguilera, J. C., Matté, C., … Navas, P. (2019). ADCK2 Haploinsufficiency Reduces Mitochondrial Lipid Oxidation and Causes Myopathy Associated with CoQ Deficiency. *Journal of Clinical Medicine 2019, Vol. 8, Page 1374*, *8*(9), 1374. doi: 10.3390/JCM8091374

Walter, C., Marada, A., Suhm, T., Ernsberger, R., Muders, V., Kücükköse, C., Sánchez-Martín, P., Hu, Z., Aich, A., Loroch, S., Solari, F. A., Poveda-Huertes, D., Schwierzok, A., Pommerening, H., Matic, S., Brix, J., Sickmann, A., Kraft, C., Dengjel, J., … Meisinger, C. (2021). Global kinome profiling reveals DYRK1A as critical activator of the human mitochondrial import machinery. *Nature Communications*, *12*(1). doi: 10.1038/S41467-021-24426-9

Wang, K. Z. Q., Zhu, J., Dagda, R. K., Uechi, G., Cherra, S. J., Gusdon, A. M., Balasubramani, M., & Chu, C. T. (2014). ERK-mediated phosphorylation of TFAM downregulates mitochondrial transcription: Implications for Parkinson's disease. *Mitochondrion*, *17*, 132–140. doi: 10.1016/J.MITO.2014.04.008

Weraarpachai, W., Sasarman, F., Nishimura, T., Antonicka, H., Auré, K., Rötig, A., Lombs, A., & Shoubridge, E. A. (2012). Mutations in C12orf62, a factor that couples COX I synthesis with cytochrome c oxidase assembly, cause fatal neonatal lactic acidosis. *American Journal of Human Genetics*, *90*(1), 142–151. doi: 10.1016/J.AJHG.2011.11.027

Wiedemann, N., & Pfanner, N. (2017). *Mitochondrial Machineries for Protein Import and Assembly*. doi: 10.1146/annurev

Yousefi, R., Fornasiero, E. F., Cyganek, L., Montoya, J., Jakobs, S., Rizzoli, S. O., Rehling, P., & Pacheu-Grau, D. (2021). Monitoring mitochondrial translation in living cells. *EMBO Reports*, *22*(4), e51635. doi: 10.15252/EMBR.202051635

Zhang, G., Wang, X., Li, C., Li, Q., An, Y. A., Luo, X., Deng, Y., Gillette, T. G., Scherer, P. E., & Wang, Z. v. (2021). Integrated Stress Response Couples Mitochondrial Protein Translation With Oxidative Stress Control. *Circulation*, *144*(18), 1500–1515. doi: 10.1161/CIRCULATIONAHA.120.053125

Zhang, H., Cao, X., Tang, M., Zhong, G., Si, Y., Li, H., Zhu, F., Liao, Q., Li, L., Zhao, J., Feng, J., Li, S., Wang, C., Kaulich, M., Wang, F., Chen, L., Li, L., Xia, Z., Liang, T., … Zhao, B. (2021). A subcellular map of the human kinome. *ELife*, *10*. doi: 10.7554/ELIFE.64943

Zorkau, M., Albus, C. A., Berlinguer-Palmini, R., Chrzanowska-Lightowlers, Z. M. A., & Lightowlers, R. N. (2021). High-resolution imaging reveals compartmentalization of mitochondrial protein synthesis in cultured human cells. *Proceedings of the National Academy of Sciences*, *118*(6). doi: 10.1073/pnas.2008778118

3.7. Supplementary information

3.7.1. Supplementary figures

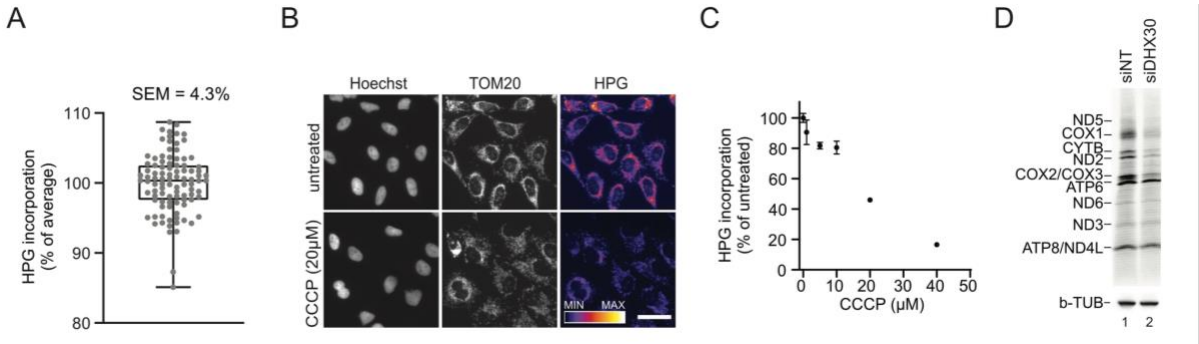

Figure S1. (A) HPG incorporation values of cells in each well of a 96-well plate labeled with mitochondrial-FUNCAT. The standard error of the mean between wells was calculated to be 4.2%. **(B)** Representative fluorescent images of untreated and 20µM CCCP treated cells followed by mitochondrial-FUNCAT. Scale bar, 40 µm. **(C)** Quantitative analysis of HPG incorporation in cells treated with different concentrations of CCCP. Approximately 2000 cells were analyzed in 20 frames in each replicate. N = 3 independent replicates. Error bars show SEM. **(D)** Radiolabeling of mitochondrial translation in cells transfected with siNT and siDHX30. Western blotting analysis of b-tubulin served as loading control.

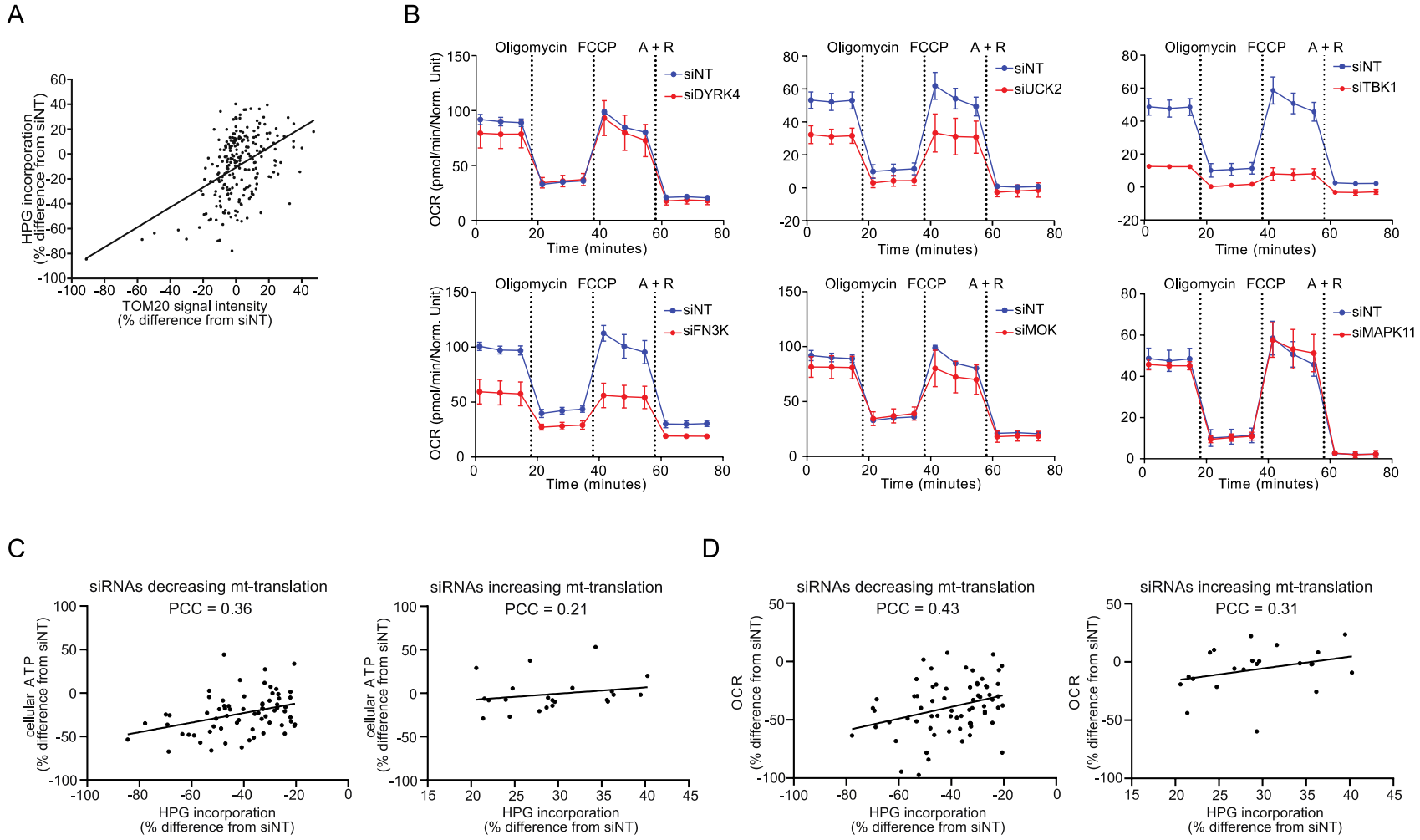

Figure S2. (A) HPG incorporation was plotted against TOM20 values for each siRNA from Fig. 2A. Pearson correlation coefficient (PCC) was calculated as 0.29. **(B)** Example graphs of OCR measurement performed in Fig. 2D after the transfection with selected siRNAs. **(C)** cellular ATP and **(D)** OCR values of Fig 2C and 2D are plotted against HPG incorporation values. PCCs are indicated on the graphs. FCCP, Carbonyl cyanide 4-(trifluoromethoxy)phenylhydrazone. A + R, Anisomycin plus Rotenone.

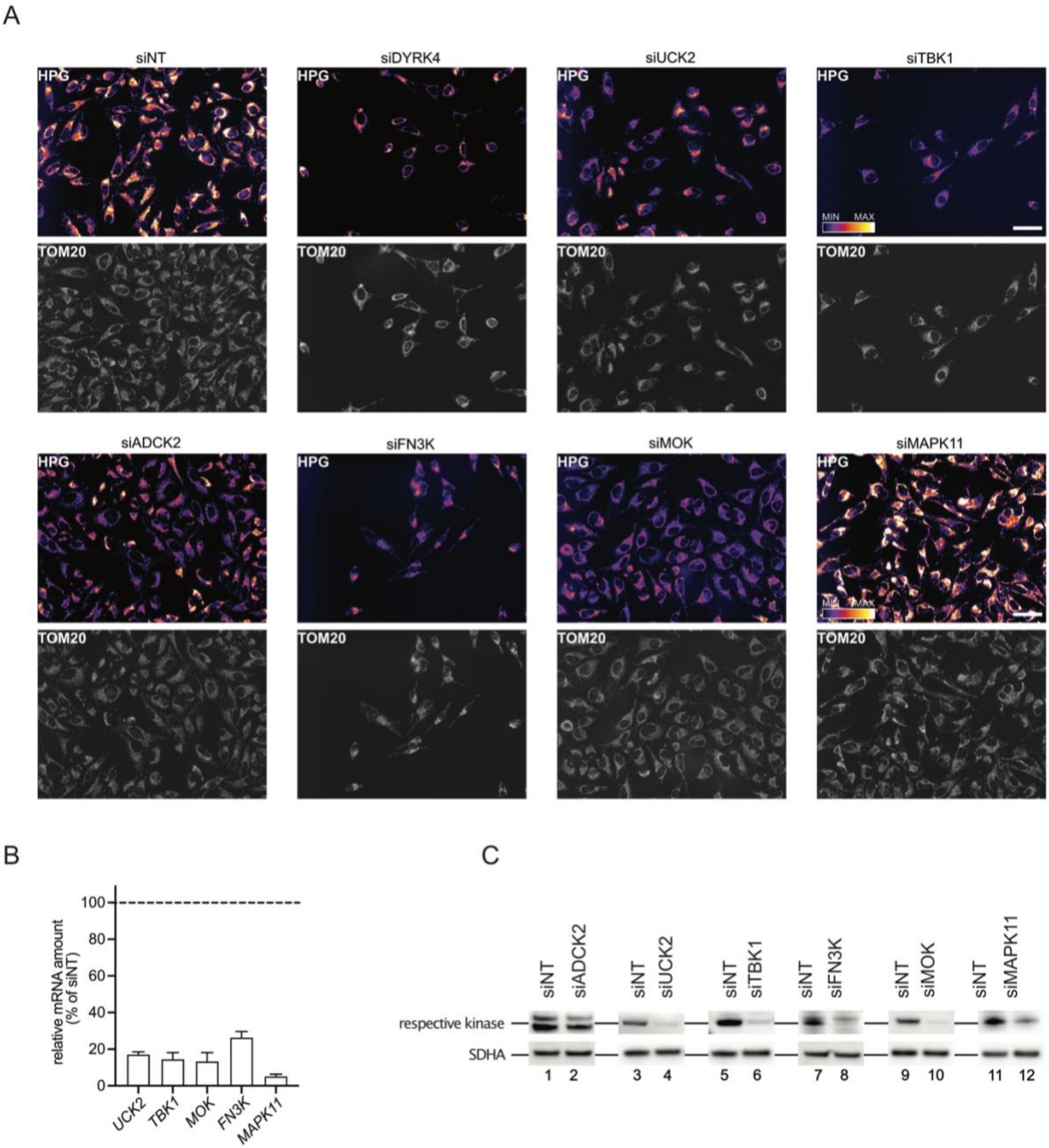

Figure S3. (A) Representative fluorescent images of HPG incorporation and TOM20 immunostaining after knockdown of the selected kinases (images were analyzed as part of the data in Fig. 2A). **(B)** qRT-PCR analysis of the kinase transcripts after knockdown with the respective siRNAs. *RPL28* was used as an internal control mRNA to normalize CT values. N = 3 independent replicates. Error bars show SEM. **(C)** The steady state level of the kinases after knockdown with the respective siRNA and non-targeting (siNT) was detected by Western blotting.

3.7.2. Supplementary tables

Table S1. Related to Figure 2A

Gene Symbol	Full Gene Name	Sense siRNA Sequence	HPG	HPG pvalue	TOM20	TOM20 pvalue
ABL1	c-abl oncogene 1, non-receptor tyrosine kinase	CGACAAGUGGGAGAUGGAAtt	107,99	0,40921469	111,98	0,355422046
ABL1	c-abl oncogene 1, non-receptor tyrosine kinase	GAAGGGAGGGUGUACCAUUtt	114	0,16525811	112,22	0,353079005
ABL2	c-abl oncogene 2, non-receptor tyrosine kinase	CCCUCAAACUCGCAACAAAtt	90,84	0,03542376	135,18	0,033494998
ABL2	c-abl oncogene 2, non-receptor tyrosine kinase	CCCUGUCCUUAAUAACUUAtt	124,44	0,03949225	123,86	0,126085956
ACVR2A	activin A receptor, type IIA	GCCCAGUUGCUUAACGAAUtt	88,66	0,61365592	102,21	0,88977136
ACVR2A	activin A receptor, type IIA	GGAUGAUAUCAACUGCUAUtt	93,17	0,48338275	127,27	0,039747756
ADCK2	aarF domain containing kinase 2	GAUUGACCUGCGUUACGAAtt	85,7	0,02175045	94,33	0,318204619
ADCK2	aarF domain containing kinase 2	GACCAGUCGUUUCUAGAAAtt	106,27	0,53836505	96,41	0,430355111
ADRBK2	adrenergic, beta, receptor kinase 2	GCAAGCUGUAGAACACGUAtt	83,01	0,00274188	96,41	0,440727207
ADRBK2	adrenergic, beta, receptor kinase 2	GCUACUUGAUUGCGACCAAtt	113,26	0,19591595	96,17	0,433815558
ADRBK2	adrenergic, beta, receptor kinase 2	GCAGCAAGAAGUAACGGAAtt	131,64	0,00024421	102,54	0,903234782
ALPK1	alpha-kinase 1	GAGAUGUUGUGGUCGAUUUtt	93,74	0,18661545	94,71	0,351017254
ALPK1	alpha-kinase 1	CCAUGAGCAAGAACGAUUAtt	110,23	0,24299342	103,76	0,982376485
ARAF	v-raf murine sarcoma 3611 viral oncogene homolog	CGAGAUCUCAAGUCUAACAtt	111,95	0,11456871	119,37	0,148785043
ARAF	v-raf murine sarcoma 3611 viral oncogene homolog	GUGUUGACAUGAGUACCAAtt	129,35	0,01631193	131,78	0,024300243
AURKAIP1	aurora kinase A interacting protein 1	CCACCGCAAUCCUACCAGUtt	30,74	0,00176586	106,84	0,721172785
AURKAIP1	aurora kinase A interacting protein 1	GCAGAUCAAGUUCGAGAAAtt	48,46	3,73E-05	90,14	0,201472209
BLK	B lymphoid tyrosine kinase	UGAUGGAAGUUGUCACUUAtt	53,5	0,01364091	116,85	0,166965263
BLK	B lymphoid tyrosine kinase	UCUACGCAGUGGUCACCAAtt	129,63	0,00165792	100,92	0,756579401
BMX	BMX non-receptor tyrosine kinase	CAGACUAUGAUGAAACUCAtt	84,2	0,01144815	94,34	0,376976729
BMX	BMX non-receptor tyrosine kinase	GUACCAGUCUAGCGCAAUAtt	98,14	0,81829637	93,21	0,293776719
CALM1	calmodulin 1 (phosphorylase kinase, delta)	UGACAAACUUAGGAGAAAAtt	75,15	0,16419686	92,81	0,268661365

CALM1	calmodulin 1 (phosphorylase kinase, delta)	AGGCAUUCCGAGUCUUUGAtt	128,85	0,00037108	102,37	0,906560662
CALM2	calmodulin 2 (phosphorylase kinase, delta)	CAAAGAAGCUUUUUCACUAtt	54,26	0,02379753	102,48	0,928465691
CALM2	calmodulin 2 (phosphorylase kinase, delta)	GCACAAUUGACUUCCCUGAtt	96,74	0,77139791	99,61	0,683568789
CAMK2A	calcium/calmodulin-dependent protein kinase II alpha	GGACUUCCAUCGAUUCUAUtt	59,8	0,00581489	103,07	0,958876276
CAMK2A	calcium/calmodulin-dependent protein kinase II alpha	ACAUCGUCCGACUACAUGAtt	84,33	0,0870377	113,11	0,469402332
CAMK2D	calcium/calmodulin-dependent protein kinase II delta	GGGAUGGAUUUUCACCGAUtt	97,71	0,79826139	93,4	0,310010917
CAMK2D	calcium/calmodulin-dependent protein kinase II delta	GCGACUUCAUGAUAGCAUAtt	127,85	0,02600559	99,8	0,657367155
CAMK2D	calcium/calmodulin-dependent protein kinase II delta	GCAUAGCAUAUAUUAGGCUtt	129,34	0,02008141	98,44	0,559249932
CAMK2G	calcium/calmodulin-dependent protein kinase II gamma	ACCAGAAACUAGAACGUGAtt	93,69	0,48646038	99,98	0,701061575
CAMK2G	calcium/calmodulin-dependent protein kinase II gamma	GAUCAUUAAGAUUACAGAAtt	102,75	0,78568522	105,99	0,796766567
CAMK4	calcium/calmodulin-dependent protein kinase IV	GCAGAUGCCGUUAAACAAAtt	58,52	0,00592695	106,18	0,827065083
CAMK4	calcium/calmodulin-dependent protein kinase IV	CUCUCAAAGUGUUAAAGAAtt	114,74	0,08341313	90,53	0,192991256
CDC2L5	cell division cycle 2-like 5 (cholinesterase-related cell division controller)	CAGAUUGUCUAGAUCCAGAtt	47,03	0,00267488	88,02	0,178261747
CDC2L5	cell division cycle 2-like 5 (cholinesterase-related cell division controller)	GGAACUUGCACAACUAGAAtt	67,07	0,03296362	94,85	0,675588201
CDC7	cell division cycle 7 homolog (S. cerevisiae)	GGCUAUUUCUACGAAAGUUtt	47,59	0,000414	84,73	0,346521502
CDC7	cell division cycle 7 homolog (S. cerevisiae)	GCAUUGUUUUGAUGAGUAUtt	64,17	0,0348242	108,15	0,646145217
CDK10	cyclin-dependent kinase 10	GUUUCCAACUUGCUCAUGAtt	78,83	0,29757449	99,18	0,608788967
CDK10	cyclin-dependent kinase 10	GGCCUAUGGUGUCCCAGUAtt	95	0,68929679	91,32	0,205467477
CDK5	cyclin-dependent kinase 5	CCUCGAUCCUGAGAUUGUAtt	77,88	0,00537776	85,97	0,151108679
CDK5	cyclin-dependent kinase 5	CGGGAGAUCUGCCUACUCAtt	94,72	0,23906407	102,36	0,91199871
CDK5	cyclin-dependent kinase 5	GCAAUGAUGUCGAUGACCAtt	98,24	0,88386387	108,59	0,633227202
CKMT2	creatine kinase, mitochondrial 2 (sarcomeric)	GAGGCAAUAUGAAACGAGUtt	78,14	0,00333319	111,66	0,380829318
CKMT2	creatine kinase, mitochondrial 2 (sarcomeric)	GACCCACGCUUUUCUAAGAtt	87,62	0,57739119	110,54	0,466714268

CKMT2	creatine kinase, mitochondrial 2 (sarcomeric)	GGAUAAAUGAGGAGGAUCAtt	93,26	0,29852097	84,67	0,088308413
CLK3	CDC-like kinase 3	GCCGGUAUGUGAAGGAGAAtt	54,74	0,01700016	109,67	0,631776896
CLK3	CDC-like kinase 3	CUACAGUCGGGAACAUGAAtt	69,84	0,00420043	93,6	0,304710477
CSNK1D	casein kinase 1, delta	GGAUUAGCGAGAAGAAAAUtt	43,35	0,00038166	92,97	0,575113209
CSNK1D	casein kinase 1, delta	CACGCACCUUGGAAUUGAAtt	52,5	0,00216829	92,03	0,236670091
CSNK1G2	casein kinase 1, gamma 2	GCUUCGUGUUCGACUAUGAtt	88,63	0,37432211	101,99	0,871878456
CSNK1G2	casein kinase 1, gamma 2	GCCUGGACUUCUUCGAGAAtt	113,8	0,05514069	94,58	0,390104203
DDR2	discoidin domain receptor tyrosine kinase 2	CCUAUGAUCCAAUGCUUAAtt	97,27	0,70622432	117,75	0,148869677
DDR2	discoidin domain receptor tyrosine kinase 2	GGUUAUUGAGAAUACUGGAtt	103,2	0,68497963	101,74	0,83515448
DDR2	discoidin domain receptor tyrosine kinase 2	GCACUGUCAGUUACACCAAtt	114,19	0,03149218	129,4	0,03144146
DGKB	diacylglycerol kinase, beta 90kDa	GACAUUGUCUGUUACCUGUtt	72,49	0,05076634	92,07	0,230221852
DGKB	diacylglycerol kinase, beta 90kDa	GGUUUUGGAUUGCAUAGAAtt	90,58	0,23812613	111,18	0,394706787
DGKB	diacylglycerol kinase, beta 90kDa	GGCUUAGAAAAUAACGUGAtt	93,09	0,28956057	101,59	0,824932392
DGKG	diacylglycerol kinase, gamma 90kDa	GUGUCAAAACGUACUCAAAtt	106,48	0,60651724	97,42	0,505871228
DGKG	diacylglycerol kinase, gamma 90kDa	CAGAUACUAAUAUACAGAAtt	107,44	0,14206175	101,12	0,772138121
DMPK	dystrophia myotonica-protein kinase	AGAUCGUCCACUACAAGGAtt	88,65	0,16509584	114,66	0,245099295
DMPK	dystrophia myotonica-protein kinase	GGUGUAUUCGCCUAUGAAAtt	96,53	0,72034764	96,84	0,463185676
DMPK	dystrophia myotonica-protein kinase	ACAGGGACAUCAAACCCGAtt	101,59	0,52422394	81,39	0,07538943
DYRK4	dual-specificity tyrosine-(Y)-phosphorylation regulated kinase 4	CCUACAAUGUGGUGCAUAUtt	52,97	0,00590848	109,82	0,587675645
DYRK4	dual-specificity tyrosine-(Y)-phosphorylation regulated kinase 4	GUAUACACGUACAUCCAAAtt	68,12	0,00451722	92,38	0,285023758
EEF2K	eukaryotic elongation factor-2 kinase	GCGACGAUGAGGAAGGUUAtt	61,54	0,28771292	101,87	0,853075934
EEF2K	eukaryotic elongation factor-2 kinase	GCUCGAACCAGAAUGUCAAtt	121,38	0,00756986	113,42	0,281722535
EGFR	epidermal growth factor receptor	CCAUAAAUGCUACGAAUAUtt	89,73	0,38084805	107,36	0,666082392

EGFR	epidermal growth factor receptor	GAUCUUUCCUUCUUAAAGAtt	110,99	0,13655266	94,69	0,332805908
EIF2AK2	eukaryotic translation initiation factor 2-alpha kinase 2	GGUGAAGGUAGAUCAAAGAtt	94,09	0,38095118	94,43	0,382999748
EIF2AK2	eukaryotic translation initiation factor 2-alpha kinase 2	GACGGAAAGACUUACGUUAtt	119,83	0,03214539	91,82	0,250477948
EPHA1	EPH receptor A1	CUACCUCAGUAAUCACAAUtt	90,38	0,24849161	88,8	0,175041326
EPHA1	EPH receptor A1	GAAACAUCUUGGUGAAUCAtt	94,2	0,49271452	124,33	0,059150749
EPHA3	EPH receptor A3	GGAUGUACUGCAGUACAGAtt	106,8	0,34253709	93,71	0,29110292
EPHA3	EPH receptor A3	CACCUGUCCUGACGAUUAAtt	110,22	0,41682303	98,68	0,572495044
EPHA4	EPH receptor A4	CAGUAAUGAUCAUAACAGAtt	83,8	0,03332227	106,85	0,708306352
EPHA4	EPH receptor A4	GAAUCAAGGUGUAAGAACAtt	121,53	0,06403668	89,01	0,140909619
EPHB1	EPH receptor B1	CGACCAUCCUAACAUCAUUtt	112,56	0,00991029	101,78	0,862980513
EPHB1	EPH receptor B1	GAAACGGGCUUAUAGCAAAtt	135,71	0,00037085	105,95	0,798349875
FER	fer (fps/fes related) tyrosine kinase	GAAUUAUGUCAGCAACGUAtt	93,32	0,29677474	103,01	0,949554865
FER	fer (fps/fes related) tyrosine kinase	GAACAACGGCUGCUAAAGAtt	98,56	0,91931391	96,73	0,436984871
FGFR2	fibroblast growth factor receptor 2	GAACAGUAUUCACCUAGUUtt	58,06	0,02247933	89,59	0,213908542
FGFR2	fibroblast growth factor receptor 2	GUAGGACUGUAGACAGUGAtt	84,82	0,00396117	88,17	0,190870578
FGFR4	fibroblast growth factor receptor 4	CAUUGACUACUAUAAGAAAtt	100,1	0,92339154	107,75	0,643854192
FGFR4	fibroblast growth factor receptor 4	UCAAGAUGCUCAAAGACAAtt	105,54	0,51064968	135,02	0,028166428
FGR	feline Gardner-Rasheed sarcoma viral oncogene homolog	GCAUCCUCAUUUGCCCACAtt	70,98	0,02170115	107,51	0,676271068
FGR	feline Gardner-Rasheed sarcoma viral oncogene homolog	CCCUGUUCAUUGCCCUGUAtt	105,46	0,4272513	114,46	0,274733676
FGR	feline Gardner-Rasheed sarcoma viral oncogene homolog	GCAUUACAAGAUCCGCAAAtt	124,76	0,03937625	94,95	0,368182322
FN3K	fructosamine 3 kinase	CAGUGUUCGUCAAAGUCAAtt	63,82	0,00045189	97,73	0,689570646
FN3K	fructosamine 3 kinase	CCGCCUUUGUGAUGGAGCAtt	99,36	0,99440894	95,9	0,454171965
FRAP1	FK506 binding protein 12-rapamycin associated protein 1	GCUCGUAGUUGGGAUAACAtt	52,05	5,52E-05	84,47	0,097755284

FRAP1	FK506 binding protein 12-rapamycin associated protein 1	GGAGCCUUGUUGAUCCUUAtt	77,86	0,06018701	81,89	0,080136679
FRK	fyn-related kinase	GCAGACAAGUCAACCGUGAtt	77,83	0,0357182	115,42	0,221042085
FRK	fyn-related kinase	CCAUUUGAUUUGUCGUAUAtt	106,06	0,48840235	89,96	0,169077625
GALK2	galactokinase 2	GGAGAGUUGAUGAACCAGAtt	95,99	0,78153558	125,22	0,121283606
GALK2	galactokinase 2	CGAGUGCUCCAGUUUAAGAtt	114,77	0,18126013	97,84	0,526093937
GCK	glucokinase (hexokinase 4)	GCAUGUGCGUCAAUACCGAtt	67,96	0,00803983	110,54	0,506398192
GCK	glucokinase (hexokinase 4)	GGUCAGCAGCUGUAUGAGAtt	109,15	0,34349802	95,24	0,411521655
GCKR	glucokinase (hexokinase 4) regulator	GAACAUUGUUCGACUGCUAtt	96	0,74637554	123,91	0,111681584
GCKR	glucokinase (hexokinase 4) regulator	GGCAUUGCAGCAUCUCAAAtt	103,97	0,61757057	95,23	0,426825113
GRK5	G protein-coupled receptor kinase 5	GAAGGACCAUAGACAGAGAtt	84,04	0,07055146	100,92	0,807374176
GRK5	G protein-coupled receptor kinase 5	CGUCUACCGAGAUCUGAAAtt	108,3	0,12413938	98,08	0,591291207
HIPK3	homeodomain interacting protein kinase 3	CAGUUCCACUUGUAACUCAtt	113,3	0,00433875	120,61	0,105898845
HIPK3	homeodomain interacting protein kinase 3	CGAAUAGUAUGUCAGAUGAtt	116,88	0,26621375	106,94	0,694450644
HK1	hexokinase 1	CAUCCACACUUCUCCAGAAtt	68,37	0,08164966	98,91	0,725367357
HK1	hexokinase 1	GAUCGAGAGUGACCGAUUAtt	109,1	0,20403162	97,08	0,514077824
IKBKB	inhibitor of kappa light polypeptide gene enhancer in B-cells, kinase beta	GAAUGGAACGGUGAAGUUUtt	73,25	0,00196961	94,55	0,373037163
IKBKB	inhibitor of kappa light polypeptide gene enhancer in B-cells, kinase beta	GGAUGACAUCUUAAACUUAtt	88,54	0,20517186	112,2	0,411192429
INSR	insulin receptor	CUACGUGACAGACUAUUUAtt	71,72	0,18935399	120,18	0,116336434
INSR	insulin receptor	GAAUGACCAGAGACAUCUAtt	81,88	0,02286381	96,13	0,560247535
INSR	insulin receptor	GAACGAUGUUGGACUCAUAtt	94,88	0,58789641	123,58	0,175140506
INSRR	insulin receptor-related receptor	GGAUGACUCGGGACGUGUAtt	103,42	0,55045064	100,35	0,712214342
INSRR	insulin receptor-related receptor	GCUUCAUCGUGUACUACAAtt	110,27	0,53059851	135	0,016932138
IRAK1	interleukin-1 receptor-associated kinase 1	GGUUGUCCUUGAGUAAUAAtt	31,21	0,00069901	42,89	0,044234263

IRAK1	interleukin-1 receptor-associated kinase 1	CAAGUCAGGUUUCAUGUAAtt	80,65	0,00188677	111,98	0,489159673
ITPK1	inositol 1,3,4-triphosphate 5/6 kinase	GAUUGAGGCCUACAUGGAAtt	111,42	0,2886493	89,65	0,184869519
ITPK1	inositol 1,3,4-triphosphate 5/6 kinase	GAAGCCGACCAGAAUGAUAtt	113,02	0,01306395	102,87	0,934954962
ITPK1	inositol 1,3,4-triphosphate 5/6 kinase	GUUGUGCAGCUGAACCUUAtt	118,02	0,10058323	147,25	0,011285408
ITPKA	inositol 1,4,5-trisphosphate 3-kinase A	GAAGGACAUGUACAAGAAAtt	36,39	0,00429596	50,36	0,094285534
ITPKA	inositol 1,4,5-trisphosphate 3-kinase A	GGACUUACCUAGAGGAGGAtt	91,7	0,22896196	85,67	0,09644708
KHK	ketohexokinase (fructokinase)	GGUAAGGCCUUAUAAUGUAtt	45,92	0,08165276	103,44	0,989902815
KHK	ketohexokinase (fructokinase)	GCCUGAAAGUCUCACCCUUtt	52,82	0,000402	115,16	0,30439346
KHK	ketohexokinase (fructokinase)	GUAUGGUCGUGUGAGGAAAtt	81,6	0,10085166	121,28	0,131690194
MAK	male germ cell-associated kinase	GGACGUACUUAUAAUCCUAtt	65,85	0,11193385	90,28	0,623476006
MAK	male germ cell-associated kinase	GGAGGACUAUGAUUUCGGAtt	103,51	0,63302998	90,48	0,17491754
MAP2K7	mitogen-activated protein kinase kinase 7	GCAUUGAGAUUGACCAGAAtt	31,61	0,00010523	69,84	0,066680638
MAP2K7	mitogen-activated protein kinase kinase 7	GACAGUUUCCCUACAAGAAtt	87,41	0,51509408	107,92	0,620849618
MAP3K3	mitogen-activated protein kinase kinase kinase 3	GGAAUACUCAGAUCGGGAAtt	96,74	0,67937304	83,19	0,092939327
MAP3K3	mitogen-activated protein kinase kinase kinase 3	CGAGGGCUAUGGAAGGAAAtt	105,66	0,59993568	106,38	0,767527536
MAP3K4	mitogen-activated protein kinase kinase kinase 4	CUAACGAACUGAUCUGGUUtt	97,6	0,4915921	113,68	0,426836286
MAP3K4	mitogen-activated protein kinase kinase kinase 4	GCUUCGCCUUUGUUAGAGAtt	115,37	0,00323168	90,04	0,182346988
MAPK11	mitogen-activated protein kinase 11	GCGACUACAUUGACCAGCUtt	112,2	0,25504381	119,03	0,161040388
MAPK11	mitogen-activated protein kinase 11	GAACACGCCCGGACAUAUAtt	139,47	0,00291946	99,82	0,659580993
MAST2	microtubule associated serine/threonine kinase 2	GAUACUAGCUAUUUUGACAtt	116,37	0,01560562	99,05	0,599609041
MAST2	microtubule associated serine/threonine kinase 2	CGUCUAUACUUUGCGGAAAtt	122,03	0,00887434	99,96	0,696585768
MAST3	microtubule associated serine/threonine kinase 3	GGAGUACCUGCAUAACUAUtt	67,52	0,01462516	79,91	0,044965785
MAST3	microtubule associated serine/threonine kinase 3	GAAGAGCGGCAACAAGAUAtt	90,4	0,39035303	99,64	0,700177064

MATK	megakaryocyte-associated tyrosine kinase	AGUGUGAUGUGACAGCCCAtt	22,21	0,00309272	97,51	0,729836661
MATK	megakaryocyte-associated tyrosine kinase	CGAUAAAGACGGAUUCUAAtt	67,41	0,00726967	110,44	0,534305162
MELK	maternal embryonic leucine zipper kinase	GAAACGGAUUUCUAUGAAAtt	75,67	0,00201911	105,63	0,825708043
MELK	maternal embryonic leucine zipper kinase	CCUGGAUCAUGCAAGAUUAtt	87,55	0,29701743	124,53	0,117998294
MELK	maternal embryonic leucine zipper kinase	GGUUGUCUUCCGUCAGAUAtt	120,59	0,00849417	100,47	0,716930314
MET	met proto-oncogene	GCACUAGCAAAGUCCGAGAtt	112,71	0,1019017	99,1	0,608842991
MET	met proto-oncogene	GCUACUUAUGUGAACGUAAtt	135,61	0,00462713	105,04	0,881001572
MKNK2	MAP kinase interacting serine/threonine kinase 2	GCAGCGGCAUCAAACUCAAtt	134,29	0,02096932	90,57	0,273354503
MKNK2	MAP kinase interacting serine/threonine kinase 2	GCCUUGGACUUUCUGCAUAtt	136,37	0,01011222	109,03	0,541101925
MOK	MOK protein kinase	CACUAAUAUGUGAACUUAUtt	69,93	0,06217248	87,67	0,161846772
MOK	MOK protein kinase	GGAAUACCUCUACUAACAAtt	85,45	0,34289286	122,98	0,440523189
MPP6	membrane protein, palmitoylated 6 (MAGUK p55 subfamily member 6)	CAUUACUCCUCAACAGGUAtt	79,42	0,02682833	95,23	0,413150383
MPP6	membrane protein, palmitoylated 6 (MAGUK p55 subfamily member 6)	CCUAAUACCUUGCAAAGAAtt	88,18	0,22965359	89,55	0,173103391
MRC2	mannose receptor, C type 2	GAUCUUCGGUGAAUCAGAAtt	49,41	0,00754926	96,89	0,562937374
MRC2	mannose receptor, C type 2	CCUGCCCAAUGUGACCUUUtt	66,85	0,02729567	104,64	0,927251417
MST1R	macrophage stimulating 1 receptor (c-met-related tyrosine kinase)	GCGUAGAUGGUGAAUGUCAtt	63,35	0,00134878	112,84	0,316593024
MST1R	macrophage stimulating 1 receptor (c-met-related tyrosine kinase)	GGCCCAGAAUCGAAUCCAAtt	102,7	0,73852299	102,02	0,865811143
MYLK2	myosin light chain kinase 2	CAACAGACAAGGCACCUAAtt	67,11	0,00026389	125,65	0,082594774
MYLK2	myosin light chain kinase 2	GGGCAUUUGGUGAAGAUCAtt	72,82	0,0089117	87,26	0,116389573
MYLK2	myosin light chain kinase 2	GGUGGUGAAUUAUGACCAAtt	83,96	0,09434793	97,77	0,541843779
NME5	NME/NM23 family member 5	CAGAUAUUGUUGACAAAGAtt	109,06	0,2462341	98,72	0,640557739
NME5	NME/NM23 family member 5	GAACUUUUGGGACCAAAUAtt	118,64	0,00296094	110,97	0,441121298
NRGN	neurogranin (protein kinase C substrate, RC3)	GCCGGACGACGACAUUCUAtt	73,51	0,01505059	108,41	0,60058884

NRGN	neurogranin (protein kinase C substrate, RC3)	UGCUCUGACCGGAAGAGAAtt	74,58	0,0878462	107,32	0,750087687
NTRK2	neurotrophic tyrosine kinase, receptor, type 2	GCUCCUUAAGGAUAACUAAtt	79,57	0,01622838	80,88	0,058749455
NTRK2	neurotrophic tyrosine kinase, receptor, type 2	GAAUUGACGAUGGUGCAAAtt	109,94	0,01621502	94,39	0,350224843
PACSIN1	protein kinase C and casein kinase substrate in neurons 1	CCACCACCAAGAAGGAGAAtt	46,76	0,00889507	98,87	0,649825847
PACSIN1	protein kinase C and casein kinase substrate in neurons 1	GCGGCAGUGUUAGCAGCUAtt	81,05	0,02574284	83,66	0,084857202
PAK6	p21 protein (Cdc42/Rac)-activated kinase 6	GGACAGCUACGUGAAGAUUtt	46,77	0,00795281	103,34	0,985563457
PAK6	p21 protein (Cdc42/Rac)-activated kinase 6	GGCUAUUCCGAAGCAUGUUtt	59,19	0,04898586	100,85	0,925681514
PDGFRA	platelet-derived growth factor receptor, alpha polypeptide	GGCCUUACUUUAUUGGAUUtt	106,07	0,22762118	105,52	0,816805362
PDGFRA	platelet-derived growth factor receptor, alpha polypeptide	CUCUAGGAAUGACGGAUUAtt	114,47	0,04430432	93,72	0,283425262
PDGFRB	platelet-derived growth factor receptor, beta polypeptide	GGCUAGACACGGGAGAAUAtt	101,22	0,78933825	112,87	0,312866437
PDGFRB	platelet-derived growth factor receptor, beta polypeptide	GAGCAACUUUGAUCAACGAtt	126,78	0,02229228	103,95	0,964088051
PDK1	pyruvate dehydrogenase kinase, isozyme 1	GAGUCGCAUUUCAAUUAGAtt	105,26	0,14366408	93,89	0,287816257
PDK1	pyruvate dehydrogenase kinase, isozyme 1	CAGAUACUGUGAUACGGAUtt	113,38	0,24613859	110,83	0,449078653
PHKG1	phosphorylase kinase, gamma 1 (muscle)	GGACUUCUAUGAGAAUUAUtt	71,77	0,00877173	116,99	0,176240695
PHKG1	phosphorylase kinase, gamma 1 (muscle)	GGAUGAUCAUGAGCGGCAAtt	104,16	0,40926687	105,18	0,87300757
PHKG2	phosphorylase kinase, gamma 2 (testis)	AGAUCCUGAUGUUACGCAUtt	91,06	0,07111481	104,64	0,911187767
PHKG2	phosphorylase kinase, gamma 2 (testis)	AAGGAAACCAGGUCCAUCAtt	111,46	0,12526836	95,74	0,387972836
PIK3C3	phosphatidylinositol 3-kinase, catalytic subunit type 3	GCAUGGAGAUGAUUUACGUtt	110,93	0,20235548	100,24	0,715374387
PIK3C3	phosphatidylinositol 3-kinase, catalytic subunit type 3	GAGAUGUACUUGAACGUAAtt	128,68	0,04893529	96,93	0,467450103
PIK3CD	phosphoinositide-3-kinase, catalytic, delta polypeptide	ACAACAUCAUGAUCCGAGAtt	62,13	0,07123202	90,28	0,408710884
PIK3CD	phosphoinositide-3-kinase, catalytic, delta polypeptide	GCACUUCCGAGUGAAGUUUtt	79,29	0,05596168	103,51	0,99494961
PLK1	polo-like kinase 1	CAACCAAAGUCGAAUAUGAtt	15,55	6,20E-06	8,92	0,000400558
PLK1	polo-like kinase 1	GCAAUUACAUGAGCGAGCAtt	40,99	0,00694843	77,76	0,410562136

PRKCDBP	protein kinase C, delta binding protein	GCUCCAAAUGGAGAGUGUAtt	72,06	0,49349371	115,52	0,231365023
PRKCDBP	protein kinase C, delta binding protein	CGAAUCCUACAUCCACCAAtt	97,97	0,88073359	112,23	0,366486066
PRKD1	protein kinase D1	CCUCAUUGUUUCGAAAUCAtt	30,12	9,77E-06	89,02	0,25765284
PRKD1	protein kinase D1	CGAAGUUUUUAAUUACUCAtt	104,8	0,40595628	96,43	0,470262117
PRKDC	protein kinase, DNA-activated, catalytic polypeptide	CAAGCGACUUUAUAGCCUUtt	65,6	0,01948633	112,69	0,318500031
PRKDC	protein kinase, DNA-activated, catalytic polypeptide	GCGCUUUUCUGGGUGAACUtt	75,98	0,01331666	109,11	0,51980932
PSKH2	protein serine kinase H2	CCAGGUGAAGAGUCGAAAAtt	102,76	0,69833138	96,61	0,441208742
PSKH2	protein serine kinase H2	GGAUCUGCACAGUCUUCUAtt	116,32	0,12976947	117,59	0,172809031
PSKH2	protein serine kinase H2	GGACUUUAUAGACAAACUAtt	123,98	0,04601543	98,31	0,541069368
RIOK2	RIO kinase 2 (yeast)	CAAUCAAGCUUUAGAAGAAtt	50,58	0,00775015	99,78	0,727874845
RIOK2	RIO kinase 2 (yeast)	GGUUGACAAAUGCAGGAUAtt	117,45	0,07306034	104,19	0,941480529
RIOK2	RIO kinase 2 (yeast)	GAAUCAGUAUAGAACAAGAtt	136,18	0,00010084	114,28	0,316142901
ROCK1	Rho-associated, coiled-coil containing protein kinase 1	CCUUCAAGCUCGAAUUACAtt	75,7	0,00391273	93,18	0,293396712
ROCK1	Rho-associated, coiled-coil containing protein kinase 1	GUAUGAAGAUGAAUAAGGAtt	106,43	0,40661915	99,52	0,695423299
ROR1	receptor tyrosine kinase-like orphan receptor 1	GGAUGAAAACUUUAAGUCUtt	99,93	0,83154162	100,39	0,719456893
ROR1	receptor tyrosine kinase-like orphan receptor 1	GUACUGCGAUGAAACUUCAtt	104,93	0,29882796	140,17	0,010887285
RPS6KA2	ribosomal protein S6 kinase, 90kDa, polypeptide 2	GAGUAUGCCGUGAAGAUCAtt	67,14	0,00191847	87,41	0,135694868
RPS6KA2	ribosomal protein S6 kinase, 90kDa, polypeptide 2	CGAUAUCUGACGCAGCUAAtt	93,85	0,37266697	100,51	0,766465549
RPS6KB2	ribosomal protein S6 kinase, 70kDa, polypeptide 2	GCAAGGAGUCUAUCCAUGAtt	98,33	0,6909824	100,24	0,707992501
RPS6KB2	ribosomal protein S6 kinase, 70kDa, polypeptide 2	CCCUUUUUCCGGCACAUGAtt	118,61	0,00190042	98,62	0,611542361
TBK1	TANK-binding kinase 1	GGCACAACAUUUCCCUAAAtt	38,9	0,00479224	64,94	0,211225199
TBK1	TANK-binding kinase 1	GAACGUAGAUUAGCUUAUAtt	51,32	0,06617644	80,6	0,58435898
TBK1	TANK-binding kinase 1	GGAACCUCUGAAUACCAUAtt	81,24	0,02243621	112,54	0,462757127

TGFBR1	transforming growth factor, beta receptor 1	GGUACUACGUUGAAAGACUtt	91,87	0,31776822	102,47	0,897342328
TGFBR1	transforming growth factor, beta receptor 1	GCAAUGGGCUUAGUAUUCUtt	95,86	0,22363882	122,94	0,08628794
TGFBR1	transforming growth factor, beta receptor 1	GCCUUAUUAUGAUCUUGUAtt	108,81	0,40366455	110,11	0,497898914
TK1	thymidine kinase 1, soluble	GGGCCGAUGUUCUCAGGAAtt	70,27	0,03422984	86,74	0,099612724
TK1	thymidine kinase 1, soluble	GUCGCUUCCAGAUUGCUCAtt	119,84	0,4139803	78,85	0,287964068
TK2	thymidine kinase 2, mitochondrial	GCUCUGUGAUACCCAAUAAtt	93,1	0,50092215	118,93	0,14594226
TK2	thymidine kinase 2, mitochondrial	CUGUUGAUUUGAUAGUUUAtt	116,64	0,02058734	99,38	0,624448551
TLK1	tousled-like kinase 1	GCGACUAUUUUGAAUACCAtt	57,35	0,00501526	132,68	0,02534643
TLK1	tousled-like kinase 1	CCUCAUCUGUUCGACCGAAtt	60,14	0,00062617	90,86	0,235094605
TNNI3K	TNNI3 interacting kinase	CCAUCUCGACUGACAAGAAtt	81,66	0,06773758	138,93	0,031472547
TNNI3K	TNNI3 interacting kinase	GCAUUGACCUAGUCAAAUUtt	85,71	0,15061125	91,69	0,210367757
TSSK6	testis-specific serine kinase 6	GGGAAACUGUACAUCGUGAtt	110,79	0,17797883	99,77	0,657031048
TSSK6	testis-specific serine kinase 6	CAGUUGCCCUUGUUCGGAAtt	140,25	0,00053476	99,6	0,644971313
TXNDC3	thioredoxin domain containing 3 (spermatozoa)	CAACUUCUAUAGUCGAAUAtt	103,32	0,68264544	95,45	0,430723488
TXNDC3	thioredoxin domain containing 3 (spermatozoa)	GACAAGUAGUAUUAUCGGAtt	107,86	0,3601872	92,82	0,274464206
UCK2	uridine-cytidine kinase 2	GUACGAGACCUGUUCCAGAtt	52,39	0,00044479	95,57	0,467077033
UCK2	uridine-cytidine kinase 2	AGCUUCUACCGUGUCCUUAtt	72,8	0,00055692	106,3	0,826719801
ULK1	unc-51-like kinase 1 (C. elegans)	CGCCUGUUCUACGAGAAGAtt	113,29	0,23192805	102,77	0,927792108
ULK1	unc-51-like kinase 1 (C. elegans)	GCAUCGGCACCAUCGUCUAtt	118,38	0,08201938	97,91	0,541659176

Table S2. Related to Figure 2-B and C

Symbol	Sense siRNA Sequence	HPG	TOM20	Cellular ATP	ATP_pvalue	OCR	OCR-pvalue	UNIPROT	HPA database	Zhang et al	MitoCarta3.0
ABL2	CCCUGUCCUUAAUAACUUAtt	124,44	123,86	72,87	0,00365015	110,45	0,18809197	Cytoplasm Cytoplasmic vesicle	Nucleoplasm	Cytosol Cytoskeleton	
ADRBK2	GCAGCAAGAAGUAACGGAAtt	131,64	102,54	106,08	0,96302172	114,60	0,27570304	Cytoplasmic vesicle			
ARAF	GUGUUGACAUGAGUACCAAtt	129,35	131,78	91,94	0,58783686	40,42	0,00128509	Cytoplasmic vesicle	Nucleoli fibrillar center	Cytosol Cytoskeleton Plasma membrane	
AURKAIP1	CCACCGCAAUCCUACCAGUtt	30,74	106,84	63,67	0,13321596	57,97	3,7271E-05	Cytoplasmic vesicle Mitochondrion Nucleus	Mitochondria Nucleoplasm		Matrix
AURKAIP1	GCAGAUCAAGUUCGAGAAAtt	48,46	90,14	61,54	0,12041778	60,16	1,04E-05	Cytoplasmic vesicle Mitochondrion Nucleus	Mitochondria Nucleoplasm		Matrix
BLK	UGAUGGAAGUUGUCACUUAtt	53,50	116,85	73,80	0,2077694	37,00	0,00033123	Cytoplasmic vesicle	Nucleoplasm	Cytosol Plasma membrane Golgi	
BLK	UCUACGCAGUGGUCACCAAtt	129,63	100,92	90,01	0,32474161	100,66	0,39694867	Cytoplasmic vesicle	Nucleoplasm	Cytosol Plasma membrane Golgi	
CALM1	AGGCAUUCCGAGUCUUUGAtt	128,85	102,37	94,75	0,20708856	101,07	0,19876955	Cytoplasm Cytoplasmic vesicle	Vesicles		

CALM2	CAAAGAAGCUUUUUCACUAtt	54,26	102,48	84,91	0,28115758	80,35	0,08126793	Cytoplasm Cytoplasmic vesicle			
CAMK2A	GGACUUCCAUCGAUUCUAUtt	45,92	103,07	77,02	0,10408282	70,36	0,06123282	Cytoplasmic vesicle	Plasma membrane	Cytosol Plasma membrane	
CAMK2D	GCGACUUCAUGAUAGCAUAtt	127,85	99,80	79,19	0,07207977	93,50	0,84507527	Cytoplasm Cytoplasmic vesicle	Plasma membrane	Cytosol Plasma membrane	
CAMK2D	GCAUAGCAUAUAUUAGGCUtt	129,34	98,44	85,60	0,39934395	98,32	0,64104794	Plasma membrane Cytoplasm Cytoplasmic vesicle	Plasma membrane	Cytosol Plasma membrane	
CAMK4	GCAGAUGCCGUUAAACAAAtt	58,52	106,18	114,93	0,27097979	107,55	0,22557795	Cytoplasm Cytoplasmic vesicle Nucleus	Nucleoli fibrillar center; Nucleoplasm	Nuclei Cytosol Plasma membrane	
CDC2L5	CAGAUUGUCUAGAUCCAGAtt	47,03	88,02	55,50	0,02115751	70,38	0,01007768	Cytoplasmic vesicle Nucleus			
CDC2L5	GGAACUUGCACAACUAGAAtt	67,07	94,85	82,27	0,2483658	47,11	0,00143299	Cytoplasmic vesicle Nucleus			
CDC7	GGCUAUUUCUACGAAAGUUtt	47,59	84,73	33,97	0,0005126	2,65	0,00022502	Cytoplasmic vesicle Nucleus	Nucleoplasm	Nuclei	
CDC7	GCAUUGUUUUGAUGAGUAUtt	64,17	108,15	76,05	0,14291992	31,52	7,7525E-06	Cytoplasmic vesicle Nucleus	Nucleoplasm	Nuclei	

EEF2K	GCUCGAACCAGAAUGUCAAtt	121,38	113,42	70,97	0,03336198	56,21	0,05522784	Cytoplasmic vesicle	Nucleoplasm	Cytosol Plasma membrane	
EPHA4	GAAUCAAGGUGUAAGAACAtt	121,53	89,01	93,78	0,29491582	87,37	0,05542627	Plasma membrane Cytoplasmic vesicle Early endosome		Cytosol Endoplasmic reticulum	
EPHB1	GAAACGGGCUUAUAGCAAAtt	135,71	105,95	90,46	0,40401969	98,26	0,22738187	Cytoplasmic vesicle Early endosome	Cytosol Endoplasmic reticulum Plasma membrane	Plasma membrane Golgi Endoplasmic reticulum	
FGFR2	GAACAGUAUUCACCUAGUUtt	58,06	89,59	68,70	0,00080232	76,69	0,01275058	Cytoplasm Cytoplasmic vesicle Golgi	Cell Junctions		
FGR	GCAUCCUCAUUUGCCCACAtt	70,98	107,51	99,70	0,8340035	69,62	0,0098919	Cytoplasm Cytoplasmic vesicle Mitochondrion	Plasma membrane	Cytosol Cytoskeleton Plasma membrane Golgi	
FGR	GCAUUACAAGAUCCGCAAAtt	124,76	94,95	105,52	0,86337161	78,73	0,39337873	Plasma membrane Cytoplasm Cytoplasmic vesicle Mitochondrion	Plasma membrane	Cytosol Cytoskeleton Plasma membrane Golgi	
FN3K	CAGUGUUCGUCAAAGUCAAtt	63,82	97,73	48,72	0,02581588	53,35	0,00535864	Cytoplasmic vesicle	Mitochondria		
FRAP1	GCUCGUAGUUGGGAUAACAtt	52,05	84,47	91,42	0,12293541	42,78	0,00483024	Cytoplasm Cytoplasmic vesicle Endoplasmic reticulum Golgi Lysosome Mitochondrion Nucleus			
FRAP1	GGAGCCUUGUUGAUCCUUAtt	77,86	81,89	72,14	0,0345165	70,24	0,03028651	Cytoplasm Cytoplasmic vesicle Endoplasmic reticulum Golgi Lysosome Mitochondrion Nucleus			

FRK	GCAGACAAGUCAACCGUGAtt	77,83	115,42	94,83	0,25308206	80,77	0,17114946	Cytoplasm Cytoplasmic vesicle Nucleus	Nucleoplasm	Cytoskeleton Plasma membrane Golgi	
GCK	GCAUGUGCGUCAAUACCGAtt	67,96	110,54	111,69	0,70655766	60,08	0,05421897	Cytoplasm Cytoplasmic vesicle Mitochondrion Nucleus	Cytosol; Golgi apparatus		
HK1	CAUCCACACUUCUCCAGAAtt	68,37	98,91	73,13	0,0790659	67,02	0,02310327	Cytoplasm Cytoplasmic vesicle Mitochondrion	Mitochondria		
IKBKB	GAAUGGAACGGUGAAGUUUtt	73,25	94,55	98,72	0,59490738	79,02	0,02556866	Cytoplasm Cytoplasmic vesicle Nucleus	Cytosol	Nuclei Cytosol Plasma membrane	
IRAK1	GGUUGUCCUUGAGUAAUAAtt	31,21	42,89	32,68	0,0112632	43,87	0,0040467	Cytoplasm Cytoplasmic vesicle Nucleus	Cytosol	Cytosol	
ITPKA	GAAGGACAUGUACAAGAAAtt	36,39	50,36	52,73	0,02871011	48,06	0,00327179	Cytoplasmic vesicle	Vesicles		
KHK	GCCUGAAAGUCUCACCCUUtt	52,82	115,16	82,40	0,39915573	66,14	0,00376205	Cytoplasmic vesicle	Cytosol		
KHK	GGUAAGGCCUUAUAAUGUAtt	59,80	103,44	81,65	0,13652643	53,09	0,00048936	Cytoplasmic vesicle	Cytosol		
MAP2K7	GCAUUGAGAUUGACCAGAAtt	31,61	69,84	74,47	0,58697229	67,68	0,42588737	Cytoplasm Cytoplasmic vesicle Nucleus	Cytosol; Plasma membrane	Nuclei Cytosol Plasma membrane	

MAPK11	GAACACGCCCGGACAUAUAtt	139,47	99,82	98,24	0,92284473	123,67	0,1156249	Cytoplasm Cytoplasmic vesicle Nucleus	Mitochondria	Cytosol Plasma membrane	
MAST2	CGUCUAUACUUUGCGGAAAtt	122,03	99,96	91,84	0,225611	85,59	0,01419159	Plasma membrane Cytoplasm Cytoplasmic vesicle	Cytosol	Cytosol Plasma membrane	
MAST3	GGAGUACCUGCAUAACUAUtt	67,52	79,91	53,83	0,01888479	44,34	0,01092015	Cytoplasmic vesicle	Nuclear speckles		
MATK	AGUGUGAUGUGACAGCCCAtt	22,21	97,51	65,10	0,00160107	36,61	0,00041347	Cytoplasm Cytoplasmic vesicle	Microtubules	Nuclei Cytosol Plasma membrane	
MATK	CGAUAAAGACGGAUUCUAAtt	67,41	110,44	81,73	0,1114117	46,96	0,00597171	Cytoplasm Cytoplasmic vesicle	Microtubules	Nuclei Cytosol Plasma membrane	
MELK	GAAACGGAUUUCUAUGAAAtt	75,67	105,63	78,93	0,16153667	67,32	0,004853	Cytoplasmic vesicle		Cytosol Plasma membrane	
MELK	GGUUGUCUUCCGUCAGAUAtt	120,59	100,47	128,98	0,65127746	80,81	0,13045065	Plasma membrane Cytoplasmic vesicle		Cytosol Plasma membrane	
MET	GCUACUUAUGUGAACGUAAtt	135,61	105,04	92,25	0,95232268	97,96	0,63539031	Cytoplasmic vesicle Nucleus	Cytosol; Plasma membrane	Cytosol Plasma membrane	
MKNK2	GCAGCGGCAUCAAACUCAAtt	134,29	90,57	153,04	0,66487485	98,87	0,48570448	Cytoplasmic vesicle	Nuclear bodies	Nuclei Cytosol Plasma membrane	

MKNK2	GCCUUGGACUUUCUGCAUAtt	136,37	109,03	98,25	0,27134109	108,34	0,00974688	Cytoplasmic vesicle	Nuclear bodies	Nuclei Cytosol Plasma membrane	
MOK	CACUAAUAUGUGAACUUAUtt	69,93	87,67	65,96	0,00485583	80,48	0,00451715	Cytoplasm Cytoplasmic vesicle Nucleus	Endoplasmic reticulum	Cytosol Mitochondria	
MPP6	CAUUACUCCUCAACAGGUAtt	79,42	95,23	62,44	0,08610954	21,93	0,03151198	Cytoplasm Cytoplasmic vesicle Nucleus			
MRC2	GAUCUUCGGUGAAUCAGAAtt	49,41	96,89	70,53	0,04088303	101,74	0,04822635	Cytoplasmic vesicle			
MRC2	CCUGCCCAAUGUGACCUUUtt	66,85	104,64	70,23	0,00134145	58,55	0,00826562	Cytoplasmic vesicle			
MST1R	GCGUAGAUGGUGAAUGUCAtt	63,35	112,84	58,31	0,01512746	42,32	0,02978137	Cytoplasmic vesicle	Cytosol	Cytosol Plasma membrane	
MYLK2	CAACAGACAAGGCACCUAAtt	67,11	125,65	86,57	0,26926138	36,79	0,00375652	Cytoplasm Cytoplasmic vesicle	Endoplasmic reticulum		
MYLK2	GGGCAUUUGGUGAAGAUCAtt	72,82	87,26	82,67	0,2500559	55,64	0,01087122	Cytoplasm Cytoplasmic vesicle	Endoplasmic reticulum		
NRGN	UGCUCUGACCGGAAGAGAAtt	57,35	107,32	65,74	0,09488813	68,57	0,00400498	Cytoplasmic vesicle			

NRGN	GCCGGACGACGACAUUCUAtt	73,51	108,41	93,83	0,54983137	78,20	0,14016669	Cytoplasmic vesicle			
NTRK2	GCUCCUUAAGGAUAACUAAtt	79,57	80,88	63,72	0,01748627	62,36	0,01804338	Cytoplasm Cytoplasmic vesicle Early endosome	Cytosol	Golgi Vesicles	
PACSIN1	CCACCACCAAGAAGGAGAAtt	46,76	98,87	95,49	0,64864214	48,74	0,01109175	Cytoplasm Cytoplasmic vesicle	Nucleoplasm; Vesicles		
PAK6	GGACAGCUACGUGAAGAUUtt	46,77	103,34	102,57	0,62996189	84,95	0,11661516	Cytoplasm Cytoplasmic vesicle Nucleus	Nucleoli fibrillar center; Nucleoplasm	Plasma membrane	
PAK6	GGCUAUUCCGAAGCAUGUUtt	59,19	100,85	37,47	0,00749927	40,07	6,2198E-05	Cytoplasm Cytoplasmic vesicle Nucleus	Nucleoli fibrillar center; Nucleoplasm	Plasma membrane	
PDGFRB	GAGCAACUUUGAUCAACGAtt	126,78	103,95	137,37	0,70537134	94,25	0,99942302	Cytoplasm Cytoplasmic vesicle Lysosome	Vesicles	Cytosol	
PHKG1	GGACUUCUAUGAGAAUUAUtt	71,77	116,99	79,85	0,07101419	85,13	0,017628	Cytoplasmic vesicle		Cytosol Plasma membrane	
PIK3C3	GAGAUGUACUUGAACGUAAtt	128,68	96,93	83,41	0,304381	122,33	0,30489995	Cytoplasm Cytoplasmic vesicle			
PIK3CD	ACAACAUCAUGAUCCGAGAtt	62,13	90,28	45,60	0,00790727	51,76	2,8966E-06	Cytoplasm Cytoplasmic vesicle	Vesicles		

PIK3CD	GCACUUCCGAGUGAAGUUUtt	79,29	103,51	133,80	0,80327565	96,28	0,31928741	Cytoplasm Cytoplasmic vesicle	Vesicles		
PLK1	CAACCAAAGUCGAAUAUGAtt	15,55	8,92	46,60	0,00134035	-51,02	8,4167E-05	Cytoplasm Cytoplasmic vesicle Nucleus		Nuclei Cytosol Centrosome	
PLK1	GCAAUUACAUGAGCGAGCAtt	40,99	77,76	51,31	0,00757563	5,62	0,002104	Cytoplasm Cytoplasmic vesicle Nucleus		Nuclei Cytosol Centrosome	
PRKD1	CCUCAUUGUUUCGAAAUCAtt	30,12	89,02	75,28	0,02299974	60,09	0,03533699	Cytoplasm Cytoplasmic Vesicle Golgi	Plasma membrane	Cytosol Plasma membrane Golgi	
PRKDC	CAAGCGACUUUAUAGCCUUtt	65,60	112,69	77,16	0,038904	94,81	0,39158084	Cytoplasmic vesicle Nucleus	Nucleoplasm		
PRKDC	GCGCUUUUCUGGGUGAACUtt	75,98	109,11	83,74	0,45124498	106,16	0,10688678	Cytoplasmic vesicle Nucleus	Nucleoplasm		
PSKH2	GGACUUUAUAGACAAACUAtt	123,98	98,31	92,59	0,18039632	108,23	0,02708108	Cytoplasmic vesicle	Nucleoplasm	Cytosol Plasma membrane	
RIOK2	CAAUCAAGCUUUAGAAGAAtt	50,58	99,78	81,47	0,0813135	21,81	0,00046044	Cytoplasm Cytoplasmic vesicle	Cytosol	Nuclei Cytosol Plasma membrane	
RIOK2	GAAUCAGUAUAGAACAAGAtt	136,18	114,28	102,28	0,87375612	74,41	0,06678557	Cytoplasm Cytoplasmic vesicle	Cytosol	Nuclei Cytosol Plasma membrane	

ROCK1	CCUUCAAGCUCGAAUUACAtt	75,70	93,18	53,24	0,008873	47,47	0,00389468	Cytoplasm Cytoplasmic vesicle Golgi		Cytosol Plasma membrane	
RPS6KA2	GAGUAUGCCGUGAAGAUCAtt	67,14	87,41	87,98	0,28097583	77,99	0,06622909	Cytoplasm Cytoplasmic vesicle Nucleus	Nucleoplasm	Cytosol Plasma membrane	
TBK1	GGCACAACAUUUCCCUAAAtt	38,90	64,94	52,05	0,05566187	31,82	0,01474134	Cytoplasm Cytoplasmic vesicle	Nucleoplasm		
TBK1	GAACGUAGAUUAGCUUAUAtt	51,32	80,60	59,19	0,07989327	15,98	0,00118404	Cytoplasm Cytoplasmic vesicle	Nucleoplasm		
TK1	GGGCCGAUGUUCUCAGGAAtt	70,27	86,74	107,31	0,98025404	70,84	0,0589207	Cytoplasm Cytoplasmic vesicle			
TLK1	CCUCAUCUGUUCGACCGAAtt	60,14	90,86	96,31	0,3745435	57,95	0,00907887	Cytoplasmic vesicle Nucleus	Nucleoplasm	Nuclei	
TLK1	GCGACUAUUUUGAAUACCAtt	74,58	132,68	62,98	0,25137638	71,45	0,58068268	Cytoplasmic vesicle Nucleus	Nucleoplasm	Nuclei	
TSSK6	GUAGGACUGUAGACAGUGAtt	140,25	99,60	119,84	0,90223703	90,75	0,2468643	Cytoplasmic vesicle		Nuclei Cytosol	
UCK2	GUACGAGACCUGUUCCAGAtt	52,39	95,57	144,25	0,46047557	94,03	0,37178711	Cytoplasmic vesicle	Nucleoplasm		
UCK2	AGCUUCUACCGUGUCCUUAtt	72,80	106,30	86,81	0,11844731	57,00	0,02919522	Cytoplasmic vesicle	Nucleoplasm		

Chapter 4: Discussion

4.1. Mitochondrial-FUNCAT as a versatile tool in studying mitochondrial gene expression with spatial resolution

In the first part of this project, we developed a metabolic labeling technique based on FUNCAT to detect nascent protein synthesis in mitochondria (mitochondrial-FUNCAT). In this method, upon inhibition of cytosolic translation, an amino acid homolog (in this case, HPG) was incorporated to the mitochondrial-encoded proteins during their synthesis at the mitoribosomes. HPG-containing proteins were bound to an azide-fluorophore in fixed cells. We showed that this method is compatible with the gel-based separation systems (Chapter 2, Figure 1) and can replace the use of radioactive labeling. Fluorescent probes allow imaging with different fluorescence microscopy techniques and thus provide spatial resolution within a cell. Zorkau et al. published a similar approach in parallel with ours and studied the suborganellar localization of protein synthesis in mitochondria (Zorkau et al., 2021). Using high-resolution nanoscopy, they showed that mitochondrial translation occurs close to the cristae membrane and outside the mitochondrial RNA granules. Moreover, strong colocalization was observed between the HPG incorporation signal and mitoribosomal proteins and TACO1, the only translational activator found to date in human mitochondria. This further provided evidence that protein synthesis occurs near the membrane and that newly synthesized mitochondrial proteins do not diffuse away from the ribosome, along with their co-translational insertion into the membrane.

Mitochondrial-FUNCAT was shown to be robust, specific, and quantitative in cells even after a brief pulse. However, whether the newly synthesized proteins labeled with mitochondrial-FUNCAT are assembled into the OXPHOS complexes was not answered in neither of our studies. Nonetheless, Zorkau et al. showed that the majority of the proteins were rapidly degraded within 6 hours after the pulse and nearly 20% remained stable throughout the entire 36-hour chase. Excess synthesis and rapid degradation of the unassembled mitochondrial proteins were recently suggested using a pulse-chase SILAC approach (Bogenhagen et al., 2020). However, further experiments are needed to decipher whether HPG-labeled proteins form complexes and whether they are functional.

4.2. Mitochondrial-FUNCAT for studying the heterogeneity of mitochondria

The development of techniques with spatial resolution is particularly important because of intrinsic heterogeneity between mitochondria in a single cell (intracellular) or between cells (intercellular). Similar to us, Zorkau et al. observed heterogeneity in protein synthesis within mitochondria of a single cell (Chapter 2, Figure 1). Regardless of the duration of labeling, about 50% of the mitochondrial network was translationally active, with a higher proportion in mitochondria around the nuclei than in peripheral mitochondria. What causes heterogeneous protein synthesis within mitochondria of a single cell remains to be elucidated.

Mitochondria are responsible for some of the diversity seen among genetically identical cells (das Neves et al., 2010; Johnston et al., 2012). Because each mitochondrion contains multiple mtDNA molecules, differences in copy number and sequence of mtDNA result in genetic variation within individual cells. In addition, nongenetic heterogeneity of mitochondria may arise from subcellular location, morphology, enzymatic activity, protein content, and many other sources (Szabadkai et al., 2019). Highly specialized cells such as cardiomyocytes and neurons even have subpopulations of mitochondria within individual cells.

In cardiomyocytes and muscle cells, subpopulations of mitochondria localized in different subcellular regions have been extensively studied for their distinct properties. Using microscopy techniques and biochemical separation of the different populations, it has been shown that subsarcolemmal and interfibrillar subpopulations of mitochondria within a single cardiomyocyte vary in their morphology, cristae structure, and metabolic activity (Hollander et al., 2014; Lukyanenko et al., 2009; Palmer et al., 1986; Riva et al., 2005). For example, isolated mitochondria from mouse hearts fed with $^{2}H_2O$ for up to 60 days showed a lower rate of protein synthesis in the interfibrillar mitochondria (Kasumov et al., 2013; Sheng et al., 2012), but this includes both mitochondrial- and nuclear-encoded proteins. To monitor the differences in mitochondrial-encoded proteins, the labeling approach established in this project can be applied in future studies.

4.2.1. Heterogeneity of mitochondria in neurons

Applying mitochondrial-FUNCAT to hippocampal neuron culture, we found a high degree of heterogeneity in protein synthesis between mitochondria of a single neuron. Translationally

active mitochondria were distributed in both the axon and dendrite, and we detected new protein synthesis in both pre- and postsynaptic mitochondria (Chapter 2, Figure 4). Neurons have a highly polar morphology and different regions within them are specialized for different functions. Consequently, mitochondria located in these regions may have distinctive features. Characterization of mitochondrial subpopulations as synaptic and non-synaptic has been the focus of many studies for several decades (Hill et al., 2018; Lai et al., 1977; Ly et al., 2006). Various protocols based on density gradient ultracentrifugation have been developed to separate mitochondrial populations located in the synapse (synaptic) from somatic mitochondria (nonsynaptic) (Baranov et al., 2018; Clark et al., 1970; Lai et al., 1976). Two factors could affect the plausibility of studies on synaptic mitochondria. First, the biochemical isolation of synaptic mitochondria could affect their properties. Second, the purity of mitochondria isolated from synaptosomes is controversial. Purification with antibody columns has isolated and characterized purer synaptosomes and synaptic mitochondria (Biesemann et al., 2014; Hafner et al., 2019; Hubbard et al., 2019). Furthermore, microscopic techniques are essential for the study of neuronal organization and function as they allow visualization of neurons and synapses in their natural location.

Recent advances in probe development have enabled spatial analysis of different subpopulations of mitochondria *in vivo* and *in vitro* (Brown et al., 2006; Hill et al., 2018). Accordingly, several differences have been described between the two subpopulations of synaptic and nonsynaptic mitochondria (Hafner et al., 2019; Lai et al., 1977; Smit-Rigter et al., 2016). Synaptic mitochondria are more susceptible to Ca^{2+} overload and more vulnerable to traumatic brain injury (Brown et al., 2006; Hill et al., 2018; Stauch et al., 2014). The proteome of synaptic and nonsynaptic mitochondria from mouse brains differs significantly in proteins involved in pathways of calcium transport, mitochondrial fission/fusion, oxidative phosphorylation, and mtDNA replication and maintenance (Stauch et al., 2014). These studies suggest that synaptic mitochondria undergo some adaptations to perform specific functions at the synapse. It is controversial whether synaptic mitochondria retain the ability to locally renew at least part of their proteome after these adaptations. Several findings have supported this idea. Local synthesis of mitochondrial proteins in the synapse is now well documented and translation of several nuclear-encoded mitochondrial mRNAs has been demonstrated in the synapse (A. Aschrafi et al., 2008; Gioio et al., 2001; Hafner et al., 2019; Natera-Naranjo et al., 2012). In radioactive labeling of translation in mitochondria isolated

from synaptosomes, two of the protein bands were sensitive to chloramphenicol, depicting mitochondrial-encoded proteins (Gioio et al., 2001). In isolated synaptoneurosomes from mouse brains, polyribosomes were detected in association with mitochondrial mRNAs (Kuzniewska et al., 2020). The instant synthesis of many mitochondrial proteins after stimulation of synaptoneurosomes confirmed that mitochondrial protein biogenesis occurs locally (Kuzniewska et al., 2020). Moreover, mtDNA replication was detected in the distal regions of axons and dendrites, even increasing when mitochondrial OXPHOS function was defected (van Laar et al., 2018). In this project, we have provided further evidence for local biogenesis of the mitochondrial proteome in the synapse by demonstrating novel protein synthesis in synaptic mitochondria.

One limitation of mitochondrial-FUNCAT in neurons is labeling time. In neurons, we performed a 30-minute treatment with HPG to obtain a reliable labeling signal. Mitochondria move along neurites at a speed of 0.1-2 µm/s. Considering this, mitochondria can be translocated in a 30-minute labeling pulse. However, mitochondria in axons and dendrites are transported in a very controlled manner depending on local needs (MacAskill et al., 2010; Sheng et al., 2012). In addition, several studies have shown that only a small fraction of mitochondria (15-40%) are motile. *In vivo*, this number is smaller and even more mitochondria become stationary and remain at the synapse over time (Faits et al., 2016; Lewis et al., 2016; Misgeld et al., 2017; Smit-Rigter et al., 2016). Thus, the probability that the signal for protein synthesis in mitochondria at the synapse originates from mitochondria transported from the soma is low. Furthermore, in a preliminary experiment (data not shown), we pharmacologically blocked microtubule polymerization and thus the anterograde movement of mitochondria and observed no change in the distribution of mitochondrial protein synthesis signal along neurites. Shortening the labeling time to 5 minutes also did not change the distribution of translating mitochondria in the neurites. These findings propose that the mitochondrial protein synthesis to happen locally at the synapse.

One question is raised by the demonstration of protein synthesis in synaptic mitochondria: what is the significance of local mitochondrial protein synthesis for synaptic function? Two main tasks have been described for mitochondria at the synapse: ATP production and Ca^{2+} buffering. Because mitochondria are not the only organelles that perform these functions at the synapse, the extent to which the role of mitochondria is critical is still highly controversial. Previously, it was assumed that the role of mitochondria in buffering Ca^{2+} at the synapse was

limited to prolonged synaptic activity because of the relatively low affinity of the mitochondrial Ca^{2+} uniporter (MCU) (Ly et al., 2006). With recent advances in Ca^{2+} biosensors, the importance of mitochondria in neurotransmitter release and Ca^{2+} clearance has become clearer (Gazit et al., 2016; Kwon et al., 2016). The other described role of mitochondria at the synapse is ATP production. ATP drives important molecular processes at the synapse such as maintenance of membrane potential, mobilization of synaptic vesicles, exocytosis and endocytosis, vesicle recycling, and re-acidification. Synaptic activity depends on ATP synthesis from both glycolysis and OXPHOS, and blocking either process affects synaptic transmission in stimulated neurons (Pathak et al., 2015; Rangaraju et al., 2014). Mitochondria-derived ATP is thought to be particularly important during intense stimulation and is thought to drive mobilization of the reserved pool of synaptic vesicles (Verstreken et al., 2005). Several studies have found that approximately 40-50% of synaptic boutons do not contain mitochondria (Kang et al., 2008; Pathak et al., 2015; Shepherd et al., 1998). However, ATP levels and synaptic transmission have been shown to be similar in boutons with and without mitochondria. ATP produced by mitochondria in neighboring boutons is thought to diffuse to the neighboring boutons (Pathak et al., 2015). Moreover, the energy required for local protein synthesis during synaptic plasticity in dendritic spines is driven by mitochondria (Rangaraju et al., 2019). Considering that mitochondrial translation products are components of the OXPHOS system, whether their local synthesis is required to sustain mitochondrial ATP production and to what extent it correlates with the molecular processes of synaptic transmission is an open question that needs to be answered in the future.

4.3. Mitochondrial-FUNCAT as a tool for diagnosis of mitochondrial pathologies

We used mitochondrial-FUNCAT to label mitochondrial protein synthesis in several cellular models, such as iPSC-derived cardiomyocytes, and primary cultures such as hippocampal neurons, hepatocytes (data not shown), and fibroblasts. The compatibility of the technique for labeling mitochondrial protein synthesis in different cell types extends its application not only to study the dynamics and mechanistic of mitochondrial translation in different models but also to assess the changes in protein synthesis in disease models. Using mitochondrial-FUNCAT, we confirmed the described decreased on mitochondrial protein synthesis rate in the fibroblasts of a patient carrying a missense mutation in *TSFM* (a mitochondrial

translational elongation factor). This patient suffers from ataxia and hypertrophic cardiomyopathy, and molecular analysis had revealed a deficiency in the activity of several OXPHOS complexes. Other missense mutations in the *TSFM* gene have been characterized in patients causing a variety of symptoms affecting multiple organs and varying in age of onset and lifespan (Ahola et al., 2014; Smeitink et al., 2006). Complexity increases even further when the same mutation causes a different spectrum of symptoms, suggesting the contribution of other disease determinants (Emperador et al., 2016). This type of complexity is very common in mitochondrial diseases and complicates the diagnosis. However, the development of fast and robust techniques to measure common mitochondrial parameters that could evidence the nature of the molecular defect present, will help the diagnostic process.

Nearly a quarter of the mitochondrial proteome is responsible to maintain, regulate, and express the mitochondrial genome. Of the 213 proteins detected in the human high confidence mitochondrial proteome in the gene expression category, 85 proteins (~40%) have already been associated with mitochondrial pathologies. Moreover, several mutations in mitochondrial tRNAs and rRNAs (which play a critical role in mitochondrial translation) have been shown to cause diseases (Elson et al., 2015; Liu et al., 2014; Prezant et al., 1993; Smith et al., 2014; Yarham et al., 2010). In addition to mitochondrial diseases, impaired mitochondrial function and alteration of factors regulating mitochondrial gene expression have been found in several tumors, and targeting mitochondrial gene expression has been proposed as a potential therapeutic agent against several cancers (Criscuolo et al., 2021; de la Cruz López et al., 2019; Heerma Van Voss et al., 2018; Hu et al., 2019). Therefore, monitoring mitochondrial protein synthesis may serve to assess mitochondrial dysfunction in such diseases. Mitochondrial-FUNCAT is particularly advantageous in this regard as the number of cells required for reliable measurement is much smaller than biochemical approaches. In addition, the method provides single-cell resolution that allows monitoring of heterogeneity within cells of different tissues.

The process of cell extraction from the tissues and culturing the cells can affect cellular processes including mitochondrial gene expression. Therefore, the optimal approach is to label mitochondrial protein synthesis in tissue sections prepared from the affected organs. FUNCAT for labeling cytosolic translation has already been shown to be effective in hippocampal slices (Dieck et al., 2012). Transferring this technique to labeling mitochondrial

protein synthesis is very useful for both research and diagnostic applications. Successful translation of mitochondrial-FUNCAT to tissue sections requires overcoming several challenges: 1) Because the proteins encoded in mitochondria are less abundant, the sensitivity of the technique may need to be increased by optimizing the concentration of reagents and labeling time. 2) Penetration of cytosolic translation inhibitor is more limited in tissue sections due to higher concentration of extracellular matrix. 3) Unincorporated HPG needs to be completely removed from the tissue sections to minimize background noise, which might be more difficult in multilayer tissue sections than in a single-layer cell culture.

4.4. A high throughput mitochondrial-FUNCAT approach

In the second part of this project, we extended the application of mitochondrial-FUNCAT by optimizing the approach in a 96-well plate format. More than one plate (we tested up to three) was transfected and labeled in parallel, further increasing the readout capacity of the method. Processing the same number of samples using conventional approaches such as radiolabeling or even FUNCAT in coverslips dramatically increases the workload and requires much more time. In addition, the much smaller number of cells that it requires, makes this method suitable for primary cells such as neurons and cardiomyocytes. When performed correctly, the error of labeling is very small, allowing detection of small changes in mitochondrial protein synthesis. However, at least 3 biological replicates are required to statistically confirm the results.

Several steps in the labeling protocol are more susceptible to increase noise: 1) the concentration of HPG, 2) the pulse duration, 3) the duration of digitonin permeabilization, and 4) the concentration of fluorophore. By increasing the solution volumes and optimizing the pipetting speed using an automated pipetting system, we were able to minimize the error to ~4%.

Using this approach, we can implement high throughput strategies by testing many compound libraries for their effects on mitochondrial protein synthesis in different cell types. In this project, we combined the labeling approach with gene knockdown by siRNA. There are several certified siRNA libraries for specific organisms that target specific categories of mRNAs such as transcription factors, cancer genes, apoptosis, etc. In addition, custom libraries can be designed and their effect on mitochondrial protein synthesis tested using the established approach to answer specific questions.

4.5. Introducing kinases with potential roles in regulation of mitochondrial gene expression

We focused on human kinase genes with the aim of exploring the proteins and pathways that modulate mitochondrial gene expression by reversible phosphorylation. In several studies, examination of the mitochondrial phosphoproteome has shown that phosphorylation in mitochondrial proteins is not only highly abundant (40-50 percent of the proteome) but also highly variable from tissue to tissue (F. M. Hansen et al., 2022; Kotrasová et al., 2021; Kruse et al., 2017). This suggests an important role for phosphorylation in modulating the tissue-specific functions of mitochondria.

We have identified several kinases whose downregulation significantly altered mitochondrial protein synthesis in a range of 80% decrease to 40% increase compared with the non-targeting control (Manuscript 2, Figure 2 and Table S1). Several identified kinases are involved in general signaling pathways for cell growth and survival, such as the PI3K-AKT and MAPK signaling cascades. In these general signaling pathways, it is particularly difficult to assess whether the effect on mitochondrial protein synthesis is a direct regulatory mechanism, for example, through modification of the transcription factor CREB and subsequent alteration of mitochondrial biogenesis, or whether it is due to a change in the metabolic state of the cells. However, downregulation of many factors identified in these pathways, including PDGFRB, CAMK2D, PIK3C3, CALM1, CAMK2A, ARAF, MET, and MAPK11, resulted in a marked increase in mitochondrial protein synthesis. This may indicate a regulatory effect on mitochondrial protein synthesis that is perturbed by downregulation of these kinases. Further experiments are needed to unravel the underlying relationship by analyzing the upstream and downstream factors and the metabolic state of the cells.

Mitochondrial OXPHOS is an important source of ATP production in cells. However, as we found by measuring cellular ATP, reduced mitochondrial translation does not necessarily correlate with low ATP levels. Of 49 kinases whose downregulation reduced mitochondrial translation, cellular ATP levels were significantly decreased in 22 cases. Under conditions of impaired mitochondrial function, cells may compensate for reduced ATP production by switching to more glycolysis when glycolytic substrates are available. This may explain the knockdown conditions in which cellular ATP remained unchanged despite the reduced mitochondrial translational phenotype (17 Kinases). OCR is a more direct measure of

mitochondrial respiratory function than cellular ATP. Accordingly, in 40 of 49 knockdown conditions, reduction in mitochondrial translation was associated with a significant decrease in OCR. However, if the defect in mitochondrial protein synthesis is below a threshold, it is possible that the corresponding OXPHOS complexes are not affected and no change is reflected in cellular ATP or OCR levels (Bai et al., 2000; ROSSIGNOL et al., 2003). Moreover, cells might compensate for the reduced synthesis by increasing the stability of the proteins present. Whether the steady-state level of OXPHOS components is affected under these knockdown conditions requires further testing.

Overall, knockdown of the siRNA library in combination with high-throughput mitochondrial-FUNCAT served as an initial screening step to identify cellular kinases whose downregulation alters mitochondrial protein synthesis. Other siRNA libraries such as transcription factors and phosphatases can be screened and combined in a similar approach to perform a thorough analysis of signaling pathways associated with mitochondrial protein synthesis.

4.6. Future perspectives

In the first part of this project, we optimized a quantitative approach with single-cell resolution for labeling mitochondrial protein synthesis in cells. Using this approach, heterogeneity in mitochondrial protein synthesis was observed in populations of cells and in mitochondria within a single cell. What causes this heterogeneity and how it relates to various mitochondrial functions are open questions that require further investigation. For example, mitochondrial membrane potential, Ca^{2+}-buffering capacity, and mitochondrial ATP are factors for which single-cell resolution assays are available. In addition, the steady-state level of mitochondrial-encoded proteins in single cells can be labeled by immunofluorescence staining. Moreover, fluorescent labels are available to determine the copy number of mtDNA and various mt-mRNA transcripts. The combination of these assays with the established mitochondrial-FUNCAT approach allows the heterogeneity of mitochondrial populations to be investigated. In this context, the importance of local mitochondrial protein synthesis in the synaptic regions of neurons also needs to be deciphered. Several fluorescence-based assays exist to measure activity in individual synaptic boutons (Bilz et al., 2020; Riemann et al., 2018). Combining these assays with mitochondrial-FUNCAT in different functional states of neurons, such as basal activity, stimulated, or inhibited, may help to understand whether local mitochondrial protein synthesis is important for synaptic function.

In the second part, we introduced several candidates from the cellular kinases which are potentially associated with mitochondrial gene expression. We started exploring the mitochondrial translation phenotype in a few selected candidates by evaluating the mitochondrial OXPHOS function, steady state level of mitoribosomal components, and checking the synthesis of individual mitochondrial-encoded proteins. Overall, we observed diverse effects resulting from silencing the individual kinases. To determine what step of gene expression is affected, measuring the mtDNA content and individual mt-mRNA transcripts are of the highest importance for the future. Defining the subcellular localization, the phosphorylation targets, and the interacting partners of each candidate will allow speculating the functions more precisely. Accordingly, more individual experiments can be designed to decipher the molecular function of the kinases.

In conclusion, gene expression in mitochondria, as a unique system with a high association to numerous diseases, has been extensively studied in the cellular context. Thanks to novel methodologies such as mass spectrometry, next generation sequencing and cryo-EM analysis, several transcriptional and translational factors have been identified, many factors involved in RNA stability, modification, and turnover have been described, 3D structures of the mitochondrial transcription and translation machineries have been determined, and models have been proposed for the assembly of different components into the OXPHOS complexes. Simultaneously, more unanswered questions have been raised particularly in the regulatory processes of mitochondrial gene expression. For example, little is known about the coordination of the mitochondrial and cytosolic translation and how mitochondria modulate their protein synthesis in response to cellular stress. Additionally, the difference in the modulation of gene expression in mitochondria of different tissues is completely neglected. With recent gene editing technologies that have been developed for manipulating mtDNA and mRNA transcripts (Cruz-Zaragoza et al., 2021; J. C. Miller et al., 2011; Mok et al., 2020) and with combining these methods with the novel labeling approaches, new possibilities are open in deciphering the regulatory aspects of mitochondrial gene expression.

Chapter 5: Appendices

Bibliography

Acin-Perez, R., Salazar, E., Kamenetsky, M., Buck, J., Levin, L. R., & Manfredi, G. (2009). Cyclic AMP Produced inside Mitochondria Regulates Oxidative Phosphorylation. *Cell Metabolism*, *9*(3), 265–276. doi: 10.1016/j.cmet.2009.01.012

Ahola, S., Isohanni, P., Euro, L., Brilhante, V., Palotie, A., Pihko, H., Lönnqvist, T., Lehtonen, T., Laine, J., Tyynismaa, H., & Suomalainen, A. (2014). Mitochondrial EFTs defects in juvenile-onset Leigh disease, ataxia, neuropathy, and optic atrophy. *Neurology*, *83*(8), 743–751. doi: 10.1212/WNL.0000000000000716

Aldridge, J. E., Horibe, T., & Hoogenraad, N. J. (2007). Discovery of Genes Activated by the Mitochondrial Unfolded Protein Response (mtUPR) and Cognate Promoter Elements. *PLoS ONE*, *2*(9), e874. doi: 10.1371/journal.pone.0000874

Amiri, M., & Hollenbeck, P. J. (2008). Mitochondrial biogenesis in the axons of vertebrate peripheral neurons. *Developmental Neurobiology*, *68*(11), 1348–1361. doi: 10.1002/dneu.20668

Amunts, A., Brown, A., Toots, J., Scheres, S. H. W., & Ramakrishnan, V. (2015). Ribosome. The structure of the human mitochondrial ribosome. *Science (New York, N.Y.)*, *348*(6230), 95–98. doi: 10.1126/SCIENCE.AAA1193

Anderson, S., Bankier, A. T., Barrell, B. G., de Bruijn, M. H. L., Coulson, A. R., Drouin, J., Eperon, I. C., Nierlich, D. P., Roe, B. A., Sanger, F., Schreier, P. H., Smith, A. J. H., Staden, R., & Young, I. G. (1981). Sequence and organization of the human mitochondrial genome. *Nature*, *290*(5806), 457–465. doi: 10.1038/290457a0

Antonicka, H., & Shoubridge, E. A. (2015). Mitochondrial RNA Granules Are Centers for Posttranscriptional RNA Processing and Ribosome Biogenesis. *Cell Reports*, *10*(6), 920–932. doi: 10.1016/J.CELREP.2015.01.030

Apostolopoulos, A., & Iwasaki, S. (2022). Into the matrix: current methods for mitochondrial translation studies. *The Journal of Biochemistry*, *00*(00), 1. doi: 10.1093/JB/MVAC005

Area-Gomez, E., Guardia-Laguarta, C., Schon, E. A., & Przedborski, S. (2019). Mitochondria, OxPhos, and neurodegeneration: cells are not just running out of gas. *The Journal of Clinical Investigation*, *129*(1). doi: 10.1172/JCI120848

Aschrafi, A., Schwechter, A. D., Mameza, M. G., Natera-Naranjo, O., Gioio, A. E., & Kaplan, B. B. (2008). MicroRNA-338 Regulates Local Cytochrome c Oxidase IV mRNA Levels and

Oxidative Phosphorylation in the Axons of Sympathetic Neurons. *Journal of Neuroscience*, *28*(47), 12581–12590. doi: 10.1523/JNEUROSCI.3338-08.2008

Aschrafi, Armaz, Kar, A. N., Gale, J. R., Elkahloun, A. G., Vargas, J. N. S., Sales, N., Wilson, G., Tompkins, M., Gioio, A. E., & Kaplan, B. B. (2016). A heterogeneous population of nuclear-encoded mitochondrial mRNAs is present in the axons of primary sympathetic neurons. *Mitochondrion*, *30*, 18–23. doi: 10.1016/j.mito.2016.06.002

Aviner, R. (2020). The science of puromycin: From studies of ribosome function to applications in biotechnology. *Computational and Structural Biotechnology Journal*, *18*, 1074. doi: 10.1016/J.CSBJ.2020.04.014

Bagert, J. D., Xie, Y. J., Sweredoski, M. J., Qi, Y., Hess, S., Schuman, E. M., & Tirrell, D. A. (2014). Quantitative, Time-Resolved Proteomic Analysis by Combining Bioorthogonal Noncanonical Amino Acid Tagging and Pulsed Stable Isotope Labeling by Amino Acids in Cell Culture. *Molecular & Cellular Proteomics : MCP*, *13*(5), 1352. doi: 10.1074/MCP.M113.031914

Bai, Y., Shakeley, R. M., & Attardi, G. (2000). Tight control of respiration by NADH dehydrogenase ND5 subunit gene expression in mouse mitochondria. *Molecular and Cellular Biology*, *20*(3), 805–815. doi: 10.1128/MCB.20.3.805-815.2000

Baranov, S. v., Khattar, N. K., Yablonska, S., Baranova, O. v., Kretz, E. S., Larkin, T. M., Carlisle, D. L., & Friedlander, R. M. (2018). *Isolation of Highly Purified and Functionally Active Synaptic Mitochondria* (pp. 153–163). doi: 10.1007/978-1-4939-8739-9_9

Beynon, R. J., & Pratt, J. M. (2005). Metabolic Labeling of Proteins for Proteomics. *Molecular & Cellular Proteomics*, *4*(7), 857–872. doi: 10.1074/MCP.R400010-MCP200

Bhatta, A., Dienemann, C., Cramer, P., & Hillen, H. S. (2021). Structural basis of RNA processing by human mitochondrial RNase P. *Nature Structural & Molecular Biology 2021 28:9*, *28*(9), 713–723. doi: 10.1038/s41594-021-00637-y

Biesemann, C., Grønborg, M., Luquet, E., Wichert, S. P., Bernard, V., Bungers, S. R., Cooper, B., Varoqueaux, F., Li, L., Byrne, J. A., Urlaub, H., Jahn, O., Brose, N., & Herzog, E. (2014). Proteomic screening of glutamatergic mouse brain synaptosomes isolated by fluorescence activated sorting. *The EMBO Journal*, *33*(2), 157–170. doi: 10.1002/embj.201386120

Bilz, F., Geurten, B. R. H., Hancock, C. E., Widmann, A., & Fiala, A. (2020). Visualization of a Distributed Synaptic Memory Code in the Drosophila Brain. *Neuron*, *106*, 963-976.e4. doi: 10.1016/j.neuron.2020.03.010

Boehm, E., Zaganelli, S., Maundrell, K., Jourdain, A. A., Thore, S., & Martinou, J.-C. (2017). FASTKD1 and FASTKD4 have opposite effects on expression of specific mitochondrial RNAs, depending upon their endonuclease-like RAP domain. *Nucleic Acids Research*, *45*(10), 6135–6146. doi: 10.1093/nar/gkx164

Bogenhagen, D. F. (2012). Mitochondrial DNA nucleoid structure. *Biochimica et Biophysica Acta (BBA) - Gene Regulatory Mechanisms*, *1819*(9–10), 914–920. doi: 10.1016/j.bbagrm.2011.11.005

Bogenhagen, D. F., & Haley, J. D. (2020). Pulse-chase SILAC- based analyses reveal selective oversynthesis and rapid turnover of mitochondrial protein components of respiratory complexes. *Journal of Biological Chemistry*, *295*(9), 2544–2554. doi: 10.1074/JBC.RA119.011791/ATTACHMENT/A73218D0-98F9-40F3-B732-7C3DFEDB3E4F/MMC1.ZIP

Bohnsack, M. T., & Sloan, K. E. (2017). The mitochondrial epitranscriptome: the roles of RNA modifications in mitochondrial translation and human disease. *Cellular and Molecular Life Sciences 2017 75:2*, *75*(2), 241–260. doi: 10.1007/S00018-017-2598-6

Boutorine, A., Novopashina, D., Krasheninina, O., Nozeret, K., & Venyaminova, A. (2013). Fluorescent Probes for Nucleic Acid Visualization in Fixed and Live Cells. *Molecules*, *18*(12), 15357–15397. doi: 10.3390/molecules181215357

Bros, H., Hauser, A., Paul, F., Niesner, R., & Infante-Duarte, C. (2015). Assessing Mitochondrial Movement Within Neurons: Manual Versus Automated Tracking Methods. *Traffic*, *16*(8), 906–917. doi: 10.1111/TRA.12291

Brown, M. R., Sullivan, P. G., & Geddes, J. W. (2006). Synaptic Mitochondria Are More Susceptible to Ca2+Overload than Nonsynaptic Mitochondria. *Journal of Biological Chemistry*, *281*(17), 11658–11668. doi: 10.1074/JBC.M510303200

Brüser, C., Keller-Findeisen, J., & Jakobs, S. (2021). The TFAM-to-mtDNA ratio defines inner-cellular nucleoid populations with distinct activity levels. *Cell Reports*, *37*(8), 110000. doi: 10.1016/j.celrep.2021.110000

Cammarota, M., Paratcha, G., Bevilaqua, L. R. M., de Stein, M. L., Lopez, M., de Iraldi, A. P., Izquierdo, I., & Medina, J. H. (2002). Cyclic AMP-Responsive Element Binding Protein in

Brain Mitochondria. *Journal of Neurochemistry*, *72*(6), 2272–2277. doi: 10.1046/j.1471-4159.1999.0722272.x

Cardanho-Ramos, C., & Morais, V. A. (2021). Mitochondrial Biogenesis in Neurons: How and Where. *International Journal of Molecular Sciences*, *22*(23), 13059. doi: 10.3390/ijms222313059

Carlile, T. M., Rojas-Duran, M. F., Zinshteyn, B., Shin, H., Bartoli, K. M., & Gilbert, W. v. (2014). Pseudouridine profiling reveals regulated mRNA pseudouridylation in yeast and human cells. *Nature 2014 515:7525*, *515*(7525), 143–146. doi: 10.1038/nature13802

Chance, B., & Williams, G. R. (1956). RESPIRATORY ENZYMES IN OXIDATIVE PHOSPHORYLATION. *Journal of Biological Chemistry*, *221*(1), 477–489. doi: 10.1016/S0021-9258(18)65266-4

Chen, R., Aldred, M. A., Xu, W., Zein, J., Bazeley, P., Comhair, S. A. A., Meyers, D. A., Bleecker, E. R., Liu, C., Erzurum, S. C., & Hu, B. (2021). Comparison of whole genome sequencing and targeted sequencing for mitochondrial DNA. *Mitochondrion*, *58*, 303–310. doi: 10.1016/j.mito.2021.01.006

Cho, J. H., Lee, Y. K., & Chae, C. B. (2001). The modulation of the biological activities of mitochondrial histone Abf2p by yeast PKA and its possible role in the regulation of mitochondrial DNA content during glucose repression. *Biochimica et Biophysica Acta (BBA) - Gene Structure and Expression*, *1522*(3), 175–186. doi: 10.1016/S0167-4781(01)00333-5

Chomyn, A. (1996). [18] In vivo labeling and analysis of human mitochondrial translation products. *Methods in Enzymology*, *264*, 197–211. doi: 10.1016/S0076-6879(96)64020-8

Christian, B. E., & Spremulli, L. L. (2010). Preferential selection of the 5′-terminal start codon on leaderless mRNAs by mammalian mitochondrial ribosomes. *Journal of Biological Chemistry*, *285*(36), 28379–28386. doi: 10.1074/JBC.M110.149054/ATTACHMENT/747A016D-D8D0-472F-8C39-6D1B271DC1C4/MMC1.PDF

Cioni, J.-M., Koppers, M., & Holt, C. E. (2018). Molecular control of local translation in axon development and maintenance. *Current Opinion in Neurobiology*, *51*, 86–94. doi: 10.1016/j.conb.2018.02.025

Cioni, J.-M., Lin, J. Q., Holtermann, A. v., Koppers, M., Jakobs, M. A. H., Azizi, A., Turner-Bridger, B., Shigeoka, T., Franze, K., Harris, W. A., & Holt, C. E. (2019). Late Endosomes

Act as mRNA Translation Platforms and Sustain Mitochondria in Axons. *Cell*, *176*(1–2), 56-72.e15. doi: 10.1016/j.cell.2018.11.030

Clark, J. B., & Nicklas, W. J. (1970). The Metabolism of Rat Brain Mitochondria. *Journal of Biological Chemistry*, *245*(18), 4724–4731. doi: 10.1016/S0021-9258(18)62854-6

Cribbs, J. T., & Strack, S. (2007). Reversible phosphorylation of Drp1 by cyclic AMP-dependent protein kinase and calcineurin regulates mitochondrial fission and cell death. *EMBO Reports*, *8*(10), 939–944. doi: 10.1038/sj.embor.7401062

Crimi, M., O'Hearn, S. F., Wallace, D. C., & Comi, G. P. (2005). Molecular research technologies in mitochondrial diseases: the microarray approach. *IUBMB Life*, *57*(12), 811–818. doi: 10.1080/15216540500460269

Criscuolo, D., Avolio, R., Matassa, D. S., & Esposito, F. (2021). Targeting Mitochondrial Protein Expression as a Future Approach for Cancer Therapy. *Frontiers in Oncology*, *11*, 4925. doi: 10.3389/FONC.2021.797265/BIBTEX

Cruz-Zaragoza, L. D., Dennerlein, S., Linden, A., Yousefi, R., Lavdovskaia, E., Aich, A., Falk, R. R., Gomkale, R., Schöndorf, T., Bohnsack, M. T., Richter-Dennerlein, R., Urlaub, H., & Rehling, P. (2021). An in vitro system to silence mitochondrial gene expression. *Cell*, *184*(23), 5824-5837.e15. doi: 10.1016/j.cell.2021.09.033

Cui, H., Li, F., Chen, D., Wang, G., Truong, C. K., Enns, G. M., Graham, B., Milone, M., Landsverk, M. L., Wang, J., Zhang, W., & Wong, L. J. C. (2013). Comprehensive next-generation sequence analyses of the entire mitochondrial genome reveal new insights into the molecular diagnosis of mitochondrial DNA disorders. *Genetics in Medicine*, *15*(5), 388–394. doi: 10.1038/gim.2012.144

Cui, L., Jeong, H., Borovecki, F., Parkhurst, C. N., Tanese, N., & Krainc, D. (2006). Transcriptional Repression of PGC-1α by Mutant Huntingtin Leads to Mitochondrial Dysfunction and Neurodegeneration. *Cell*, *127*(1), 59–69. doi: 10.1016/j.cell.2006.09.015

das Neves, R. P., Jones, N. S., Andreu, L., Gupta, R., Enver, T., & Iborra, F. J. (2010). Connecting Variability in Global Transcription Rate to Mitochondrial Variability. *PLoS Biology*, *8*(12), e1000560. doi: 10.1371/journal.pbio.1000560

de la Cruz López, K. G., Toledo Guzmán, M. E., Sánchez, E. O., & García Carrancá, A. (2019). mTORC1 as a Regulator of Mitochondrial Functions and a Therapeutic Target in Cancer. *Frontiers in Oncology*, *9*, 1373. doi: 10.3389/FONC.2019.01373/BIBTEX

de Rasmo, D., Signorile, A., Papa, F., Roca, E., & Papa, S. (2010). cAMP/Ca2+ response element-binding protein plays a central role in the biogenesis of respiratory chain proteins in mammalian cells. *IUBMB Life*, n/a-n/a. doi: 10.1002/iub.342

de Rasmo, D., Signorile, A., Roca, E., & Papa, S. (2009). cAMP response element-binding protein (CREB) is imported into mitochondria and promotes protein synthesis. *FEBS Journal*, *276*(16), 4325–4333. doi: 10.1111/j.1742-4658.2009.07133.x

Dennerlein, S., Wang, C., & Rehling, P. (2017). Plasticity of Mitochondrial Translation. *Trends in Cell Biology*, *27*(10), 712–721. doi: 10.1016/J.TCB.2017.05.004

Dieck, S. T., M̈Uller, A., Nehring, A., Hinz, F. I., Bartnik, I., Schuman, E. M., & Dieterich, D. C. (2012). Metabolic Labeling with Noncanonical Amino Acids and Visualization by Chemoselective Fluorescent Tagging. *Current Protocols in Cell Biology / Editorial Board, Juan S. Bonifacino ... [et Al.]*, *0 7*(SUPPL.56), Unit7.11. doi: 10.1002/0471143030.CB0711S56

Diekmann, Y., & Pereira-Leal, J. B. (2013). Evolution of intracellular compartmentalization. *Biochemical Journal*, *449*(2), 319–331. doi: 10.1042/BJ20120957

Dieterich, D. C., Hodas, J. J. L., Gouzer, G., Shadrin, I. Y., Ngo, J. T., Triller, A., Tirrell, D. A., & Schuman, E. M. (2010). In situ visualization and dynamics of newly synthesized proteins in rat hippocampal neurons. *Nature Neuroscience*, *13*(7), 897. doi: 10.1038/NN.2580

Dieterich, D. C., Link, A. J., Graumann, J., Tirrell, D. A., & Schuman, E. M. (2006). Selective identification of newly synthesized proteins in mammalian cells using bioorthogonal noncanonical amino acid tagging (BONCAT). *Proceedings of the National Academy of Sciences*, *103*(25), 9482–9487. doi: 10.1073/pnas.0601637103

Dimauro, S. (2019). A Brief History of Mitochondrial Pathologies. *International Journal of Molecular Sciences 2019, Vol. 20, Page 5643*, *20*(22), 5643. doi: 10.3390/IJMS20225643

D'Souza, A. R., & Minczuk, M. (2018). Mitochondrial transcription and translation: overview. *Essays in Biochemistry*, *62*(3), 309. doi: 10.1042/EBC20170102

Elliott, H. R., Samuels, D. C., Eden, J. A., Relton, C. L., & Chinnery, P. F. (2008). Pathogenic Mitochondrial DNA Mutations Are Common in the General Population. *The American Journal of Human Genetics*, *83*(2), 254–260. doi: 10.1016/J.AJHG.2008.07.004

Elson, J. L., Smith, P. M., Greaves, L. C., Lightowlers, R. N., Chrzanowska-Lightowlers, Z. M. A., Taylor, R. W., & Vila-Sanjurjo, A. (2015). The presence of highly disruptive 16S rRNA

mutations in clinical samples indicates a wider role for mutations of the mitochondrial ribosome in human disease. *Mitochondrion*, *25*, 17. doi: 10.1016/J.MITO.2015.08.004

Emperador, S., Bayona-Bafaluy, M. P., Fernández-Marmiesse, A., Pineda, M., Felgueroso, B., López-Gallardo, E., Artuch, R., Roca, I., Ruiz-Pesini, E., Couce, M. L., & Montoya, J. (2016). Molecular-genetic characterization and rescue of a TSFM mutation causing childhood-onset ataxia and nonobstructive cardiomyopathy. *European Journal of Human Genetics 2017 25:1*, *25*(1), 153–156. doi: 10.1038/ejhg.2016.124

Faits, M. C., Zhang, C., Soto, F., & Kerschensteiner, D. (2016). Dendritic mitochondria reach stable positions during circuit development. *ELife*, *5*. doi: 10.7554/eLife.11583

Falkenberg, M. (2018). Mitochondrial DNA replication in mammalian cells: overview of the pathway. *Essays in Biochemistry*, *62*(3), 287–296. doi: 10.1042/EBC20170100

Falkenberg, M., Gaspari, M., Rantanen, A., Trifunovic, A., Larsson, N. G., & Gustafsson, C. M. (2002). Mitochondrial transcription factors B1 and B2 activate transcription of human mtDNA. *Nature Genetics*, *31*(3), 289–294. doi: 10.1038/NG909

Fierro-Monti, I., Racle, J., Hernandez, C., Waridel, P., Hatzimanikatis, V., & Quadroni, M. (2013). A Novel Pulse-Chase SILAC Strategy Measures Changes in Protein Decay and Synthesis Rates Induced by Perturbation of Proteostasis with an Hsp90 Inhibitor. *PLOS ONE*, *8*(11), e80423. doi: 10.1371/JOURNAL.PONE.0080423

Filograna, R., Mennuni, M., Alsina, D., & Larsson, N. (2021). Mitochondrial DNA copy number in human disease: the more the better? *FEBS Letters*, *595*(8), 976–1002. doi: 10.1002/1873-3468.14021

Gao, F., Wesolowska, M., Agami, R., Rooijers, K., Loayza-Puch, F., Lawless, C., Lightowlers, R. N., & Chrzanowska-Lightowlers, Z. M. A. (2018). Using mitoribosomal profiling to investigate human mitochondrial translation. *Wellcome Open Research 2018 2:116*, *2*, 116. doi: 10.12688/wellcomeopenres.13119.2

Gaur, R., Grasso, D., Datta, P. P., Krishna, P. D. V., Das, G., Spencer, A., Agrawal, R. K., Spremulli, L., & Varshney, U. (2008). A Single Mammalian Mitochondrial Translation Initiation Factor Functionally Replaces Two Bacterial Factors. *Molecular Cell*, *29*(2), 180–190. doi: 10.1016/J.MOLCEL.2007.11.021

Gazit, N., Vertkin, I., Shapira, I., Helm, M., Slomowitz, E., Sheiba, M., Mor, Y., Rizzoli, S., & Slutsky, I. (2016). IGF-1 Receptor Differentially Regulates Spontaneous and Evoked

Transmission via Mitochondria at Hippocampal Synapses. *Neuron*, *89*(3), 583. doi: 10.1016/J.NEURON.2015.12.034

Giacomello, M., Pyakurel, A., Glytsou, C., & Scorrano, L. (2020). The cell biology of mitochondrial membrane dynamics. *Nature Reviews Molecular Cell Biology*, *21*(4), 204–224. doi: 10.1038/s41580-020-0210-7

Gioio, A. E., Eyman, M., Zhang, H., Lavina, Z. S., Giuditta, A., & Kaplan, B. B. (2001). Local synthesis of nuclear-encoded mitochondrial proteins in the presynaptic nerve terminal. *Journal of Neuroscience Research*, *64*(5), 447–453. doi: 10.1002/JNR.1096

Giorgianni, F., Koirala, D., Weber, K., & Beranova-Giorgianni, S. (2014). Proteome Analysis of Subsarcolemmal Cardiomyocyte Mitochondria: A Comparison of Different Analytical Platforms. *International Journal of Molecular Sciences*, *15*(6), 9285–9301. doi: 10.3390/ijms15069285

Gleichmann, M., & Mattson, M. P. (2011). Neuronal Calcium Homeostasis and Dysregulation. *Antioxidants & Redox Signaling*, *14*(7), 1261–1273. doi: 10.1089/ars.2010.3386

Gopalakrishna, S., Pearce, S. F., Dinan, A. M., Schober, F. A., Cipullo, M., Spåhr, H., Khawaja, A., Maffezzini, C., Freyer, C., Wredenberg, A., Atanassov, I., Firth, A. E., & Rorbach, J. (2019). C6orf203 is an RNA-binding protein involved in mitochondrial protein synthesis. *Nucleic Acids Research*, *47*(17), 9386–9399. doi: 10.1093/nar/gkz684

Gorman, G. S., Chinnery, P. F., DiMauro, S., Hirano, M., Koga, Y., McFarland, R., Suomalainen, A., Thorburn, D. R., Zeviani, M., & Turnbull, D. M. (2016). Mitochondrial diseases. *Nature Reviews Disease Primers 2016 2:1*, *2*(1), 1–22. doi: 10.1038/nrdp.2016.80

Gorman, G. S., Schaefer, A. M., Ng, Y., Gomez, N., Blakely, E. L., Alston, C. L., Feeney, C., Horvath, R., Yu-Wai-Man, P., Chinnery, P. F., Taylor, R. W., Turnbull, D. M., & McFarland, R. (2015). Prevalence of nuclear and mitochondrial DNA mutations related to adult mitochondrial disease. *Annals of Neurology*, *77*(5), 753. doi: 10.1002/ANA.24362

Greber, B. J., Bieri, P., Leibundgut, M., Leitner, A., Aebersold, R., Boehringer, D., & Ban, N. (2015). Ribosome. The complete structure of the 55S mammalian mitochondrial ribosome. *Science (New York, N.Y.)*, *348*(6232), 303–308. doi: 10.1126/SCIENCE.AAA3872

Greber, B. J., Boehringer, D., Leibundgut, M., Bieri, P., Leitner, A., Schmitz, N., Aebersold, R., & Ban, N. (2014). The complete structure of the large subunit of the mammalian mitochondrial ribosome. *Nature*, *515*(7526), 283–286. doi: 10.1038/NATURE13895

Grevel, A., Pfanner, N., & Becker, T. (2019). Coupling of import and assembly pathways in mitochondrial protein biogenesis. *Biological Chemistry*, *401*(1). doi: 10.1515/HSZ-2019-0310

Haag, S., Sloan, K. E., Ranjan, N., Warda, A. S., Kretschmer, J., Blessing, C., Hübner, B., Seikowski, J., Dennerlein, S., Rehling, P., Rodnina, M. v, Höbartner, C., & Bohnsack, M. T. (2016). NSUN3 and ABH1 modify the wobble position of mt-tRNAMet to expand codon recognition in mitochondrial translation. *The EMBO Journal*, *35*(19), 2104–2119. doi: 10.15252/EMBJ.201694885

Haan, C., Walbrecq, G., Kozar, I., Behrmann, I., & Zimmer, A. D. (2016). Phosphorylation of the PDH complex precedes HIF-1-mediated effects and PDK1 upregulation during the first hours of hypoxic treatment in HCC cells. *Hypoxia*, *Volume 4*, 135–145. doi: 10.2147/HP.S99044

Hafner, A.-S., Donlin-Asp, P. G., Leitch, B., Herzog, E., & Schuman, E. M. (2019). Local protein synthesis is a ubiquitous feature of neuronal pre- and postsynaptic compartments. *Science*, *364*(6441). doi: 10.1126/science.aau3644

Hall, C. N., Klein-Flugge, M. C., Howarth, C., & Attwell, D. (2012). Oxidative Phosphorylation, Not Glycolysis, Powers Presynaptic and Postsynaptic Mechanisms Underlying Brain Information Processing. *Journal of Neuroscience*, *32*(26), 8940–8951. doi: 10.1523/JNEUROSCI.0026-12.2012

Handschin, C., Rhee, J., Lin, J., Tarr, P. T., & Spiegelman, B. M. (2003). An autoregulatory loop controls peroxisome proliferator-activated receptor γ coactivator 1α expression in muscle. *Proceedings of the National Academy of Sciences*, *100*(12), 7111–7116. doi: 10.1073/pnas.1232352100

Hansen, F. M., Kremer, L. S., Karayel, O., Kühl, I., Bludau, I., Larsson, N.-G., & Mann, M. (2022). Mitochondrial phosphoproteomes are functionally specialized across tissues. *BioRxiv*.

Hansen, K. G., & Herrmann, J. M. (2019). Transport of Proteins into Mitochondria. *The Protein Journal*, *38*(3). doi: 10.1007/S10930-019-09819-6

He, L. (2002). Detection and quantification of mitochondrial DNA deletions in individual cells by real-time PCR. *Nucleic Acids Research*, *30*(14), 68e–668. doi: 10.1093/nar/gnf067

Heddi, A., Lestienne, P., Wallace, D. C., & Stepien, G. (1993). Mitochondrial DNA expression in mitochondrial myopathies and coordinated expression of nuclear genes involved in ATP production. *Journal of Biological Chemistry*, *268*(16), 12156–12163. doi: 10.1016/s0021-9258(19)50321-0

Heerma Van Voss, M. R., Vesuna, F., Bol, G. M., Afzal, J., Tantravedi, S., Bergman, Y., Kammers, K., Lehar, M., Malek, R., Ballew, M., ter Hoeve, N., Abou, D., Thorek, D., Berlinicke, C., Yazdankhah, M., Sinha, D., Le, A., Abrahams, R., Tran, P. T., … Raman, V. (2018). Targeting mitochondrial translation by inhibiting DDX3: A novel radiosensitization strategy for cancer treatment. *Oncogene*, *37*(1), 63–74. doi: 10.1038/ONC.2017.308

Herrmann, J. M., Woellhaf, M. W., & Bonnefoy, N. (2013). Control of protein synthesis in yeast mitochondria: the concept of translational activators. *Biochimica et Biophysica Acta*, *1833*(2), 286–294. doi: 10.1016/J.BBAMCR.2012.03.007

Herzig, S., Long, F., Jhala, U. S., Hedrick, S., Quinn, R., Bauer, A., Rudolph, D., Schutz, G., Yoon, C., Puigserver, P., Spiegelman, B., & Montminy, M. (2001). CREB regulates hepatic gluconeogenesis through the coactivator PGC-1. *Nature*, *413*(6852), 179–183. doi: 10.1038/35093131

Hill, R. L., Kulbe, J. R., Singh, I. N., Wang, J. A., & Hall, E. D. (2018). Synaptic Mitochondria are More Susceptible to Traumatic Brain Injury-induced Oxidative Damage and Respiratory Dysfunction than Non-synaptic Mitochondria. *Neuroscience*, *386*, 265–283. doi: 10.1016/J.NEUROSCIENCE.2018.06.028

Hollander, J. M., Thapa, D., & Shepherd, D. L. (2014). Mitochondria in Cardiovascular Physiology and Disease: Physiological and structural differences in spatially distinct subpopulations of cardiac mitochondria: influence of cardiac pathologies. *American Journal of Physiology - Heart and Circulatory Physiology*, *307*(1), H1. doi: 10.1152/AJPHEART.00747.2013

Howden, A. J. M., Geoghegan, V., Katsch, K., Efstathiou, G., Bhushan, B., Boutureira, O., Thomas, B., Trudgian, D. C., Kessler, B. M., Dieterich, D. C., Davis, B. G., & Acuto, O. (2013). QuaNCAT: quantitating proteome dynamics in primary cells. *Nature Methods*, *10*(4), 343–346. doi: 10.1038/nmeth.2401

Hu, B., & Guo, Y. (2019). Inhibition of mitochondrial translation as a therapeutic strategy for human ovarian cancer to overcome chemoresistance. *Biochemical and Biophysical Research Communications*, *509*(2), 373–378. doi: 10.1016/J.BBRC.2018.12.127

Hubbard, W. B., Harwood, C. L., Prajapati, P., Springer, J. E., Saatman, K. E., & Sullivan, P. G. (2019). Fractionated mitochondrial magnetic separation for isolation of synaptic mitochondria from brain tissue. *Scientific Reports 2019 9:1*, *9*(1), 1–13. doi: 10.1038/s41598-019-45568-3

Imami, K., Selbach, M., & Ishihama, Y. (2021). Monitoring mitochondrial translation by pulse SILAC. *BioRxiv*.

Ingolia, N. T., Brar, G. A., Rouskin, S., McGeachy, A. M., & Weissman, J. S. (2012). The ribosome profiling strategy for monitoring translation in vivo by deep sequencing of ribosome-protected mRNA fragments. *Nature Protocols 2012 7:8*, *7*(8), 1534–1550. doi: 10.1038/nprot.2012.086

Ingolia, N. T., Ghaemmaghami, S., Newman, J. R. S., & Weissman, J. S. (2009). Genome-Wide Analysis in Vivo of Translation with Nucleotide Resolution Using Ribosome Profiling. *Science*, *324*(5924), 218–223. doi: 10.1126/science.1168978

Itoh, Y., Andréll, J., Choi, A., Richter, U., Maiti, P., Best, R. B., Barrientos, A., Battersby, B. J., & Amunts, A. (2021). Mechanism of membrane-tethered mitochondrial protein synthesis. *Science (New York, N.Y.)*, *371*(6531), 846. doi: 10.1126/SCIENCE.ABE0763

Jahn, R., & Fasshauer, D. (2012). Molecular machines governing exocytosis of synaptic vesicles. *Nature*, *490*(7419), 201–207. doi: 10.1038/nature11320

Jedynak-Slyvka, M., Jabczynska, A., & Szczesny, R. J. (2021). Human mitochondrial rna processing and modifications: Overview. *International Journal of Molecular Sciences*, *22*(15). doi: 10.3390/IJMS22157999

Johnston, I. G., Gaal, B., Neves, R. P. das, Enver, T., Iborra, F. J., & Jones, N. S. (2012). Mitochondrial Variability as a Source of Extrinsic Cellular Noise. *PLoS Computational Biology*, *8*(3), e1002416. doi: 10.1371/journal.pcbi.1002416

Jornayvaz, F. R., & Shulman, G. I. (2010). Regulation of mitochondrial biogenesis. *Essays in Biochemistry*, *47*, 69–84. doi: 10.1042/bse0470069

Jourdain, A. A., Popow, J., de la Fuente, M. A., Martinou, J.-C., Anderson, P., & Simarro, M. (2017). The FASTK family of proteins: emerging regulators of mitochondrial RNA biology. *Nucleic Acids Research*, *45*(19), 10941–10947. doi: 10.1093/nar/gkx772

Kang, J. S., Tian, J. H., Pan, P. Y., Zald, P., Li, C., Deng, C., & Sheng, Z. H. (2008). Docking of Axonal Mitochondria by Syntaphilin Controls Their Mobility and Affects Short-Term Facilitation. *Cell*, *132*(1), 137–148. doi: 10.1016/J.CELL.2007.11.024

Kashatus, J. A., Nascimento, A., Myers, L. J., Sher, A., Byrne, F. L., Hoehn, K. L., Counter, C. M., & Kashatus, D. F. (2015). Erk2 Phosphorylation of Drp1 Promotes Mitochondrial Fission and MAPK-Driven Tumor Growth. *Molecular Cell*, *57*(3), 537–551. doi: 10.1016/j.molcel.2015.01.002

Kasumov, T., Dabkowski, E. R., Shekar, K. C., Li, L., Ribeiro, R. F., Walsh, K., Previs, S. F., Sadygov, R. G., Willard, B., & Stanley, W. C. (2013). Assessment of cardiac proteome dynamics with heavy water: slower protein synthesis rates in interfibrillar than subsarcolemmal mitochondria. *American Journal of Physiology-Heart and Circulatory Physiology*, *304*(9), H1201–H1214. doi: 10.1152/ajpheart.00933.2012

KATZ, B., & MILEDI, R. (1967). Ionic Requirements of Synaptic Transmitter Release. *Nature*, *215*(5101), 651–651. doi: 10.1038/215651a0

Kaushal, P. S., Sharma, M. R., Booth, T. M., Haque, E. M., Tung, C. S., Sanbonmatsu, K. Y., Spremulli, L. L., & Agrawal, R. K. (2014). Cryo-EM structure of the small subunit of the mammalian mitochondrial ribosome. *Proceedings of the National Academy of Sciences of the United States of America*, *111*(20), 7284–7289. doi: 10.1073/PNAS.1401657111/-/DCSUPPLEMENTAL/PNAS.201401657SI.PDF

Koc, E. C., & Koc, H. (2012). Regulation of mammalian mitochondrial translation by post-translational modifications. *Biochimica et Biophysica Acta (BBA) - Gene Regulatory Mechanisms*, *1819*(9–10), 1055–1066. doi: 10.1016/j.bbagrm.2012.03.003

Kos, A., Wanke, K. A., Gioio, A., Martens, G. J., Kaplan, B. B., & Aschrafi, A. (2016). Monitoring mRNA Translation in Neuronal Processes Using Fluorescent Non-Canonical Amino Acid Tagging. *Journal of Histochemistry and Cytochemistry*, *64*(5), 323–333. doi: 10.1369/0022155416641604

Kotrasová, V., Keresztesová, B., Ondrovičová, G., Bauer, J. A., Havalová, H., Pevala, V., Kutejová, E., & Kunová, N. (2021). Mitochondrial Kinases and the Role of Mitochondrial Protein Phosphorylation in Health and Disease. *Life*, *11*(2), 82. doi: 10.3390/life11020082

Kotrys, A. v, Cysewski, D., Czarnomska, S. D., Pietras, Z., Borowski, L. S., Dziembowski, A., & Szczesny, R. J. (2019). Quantitative proteomics revealed C6orf203/MTRES1 as a factor

preventing stress-induced transcription deficiency in human mitochondria. *Nucleic Acids Research*, *47*(14), 7502–7517. doi: 10.1093/nar/gkz542

Kruse, R., & Højlund, K. (2017). Mitochondrial phosphoproteomics of mammalian tissues. *Mitochondrion*, *33*, 45–57. doi: 10.1016/j.mito.2016.08.004

Kummer, E., & Ban, N. (2021). Mechanisms and regulation of protein synthesis in mitochondria. In Nature Reviews Molecular Cell Biology (Vol. 22, Issue 5, pp. 307–325). Nature Research. doi: 10.1038/s41580-021-00332-2

Kuzniewska, B., Cysewski, D., Wasilewski, M., Sakowska, P., Milek, J., Kulinski, T. M., Winiarski, M., Kozielewicz, P., Knapska, E., Dadlez, M., Chacinska, A., Dziembowski, A., & Dziembowska, M. (2020). Mitochondrial protein biogenesis in the synapse is supported by local translation. *EMBO Reports*, *21*(8). doi: 10.15252/embr.201948882

Kwon, S.-K., Sando, R., Lewis, T. L., Hirabayashi, Y., Maximov, A., & Polleux, F. (2016). LKB1 Regulates Mitochondria-Dependent Presynaptic Calcium Clearance and Neurotransmitter Release Properties at Excitatory Synapses along Cortical Axons. *PLOS Biology*, *14*(7), e1002516. doi: 10.1371/journal.pbio.1002516

Lai, J. C. K., & Clark, J. B. (1976). Preparation and properties of mitochondria derived from synaptosomes. *Biochemical Journal*, *154*(2), 423–432. doi: 10.1042/bj1540423

Lai, J. C. K., Walsh, J. M., Dennis, S. C., & Clark, J. B. (1977). SYNAPTIC AND NON-SYNAPTIC MITOCHONDRIA FROM RAT BRAIN: ISOLATION AND CHARACTERIZATION. *Journal of Neurochemistry*, *28*(3), 625–631. doi: 10.1111/J.1471-4159.1977.TB10434.X

Lee, J., Kim, C.-H., Simon, D. K., Aminova, L. R., Andreyev, A. Y., Kushnareva, Y. E., Murphy, A. N., Lonze, B. E., Kim, K.-S., Ginty, D. D., Ferrante, R. J., Ryu, H., & Ratan, R. R. (2005). Mitochondrial Cyclic AMP Response Element-binding Protein (CREB) Mediates Mitochondrial Gene Expression and Neuronal Survival. *Journal of Biological Chemistry*, *280*(49), 40398–40401. doi: 10.1074/jbc.C500140200

Lee, K.-S., Huh, S., Lee, S., Wu, Z., Kim, A.-K., Kang, H.-Y., & Lu, B. (2018). Altered ER–mitochondria contact impacts mitochondria calcium homeostasis and contributes to neurodegeneration in vivo in disease models. *Proceedings of the National Academy of Sciences*, *115*(38). doi: 10.1073/pnas.1721136115

Lee, R. G., Gao, J., Siira, S. J., Shearwood, A. M., Ermer, J. A., Hofferek, V., Mathews, J. C., Zheng, M., Reid, G. E., Rackham, O., & Filipovska, A. (2020). Cardiolipin is required for

membrane docking of mitochondrial ribosomes and protein synthesis. *Journal of Cell Science*, *133*(14). doi: 10.1242/JCS.240374

Lewis, T. L., Turi, G. F., Kwon, S. K., Losonczy, A., & Polleux, F. (2016). Progressive Decrease of Mitochondrial Motility during Maturation of Cortical Axons In Vitro and In Vivo. *Current Biology : CB*, *26*(19), 2602–2608. doi: 10.1016/J.CUB.2016.07.064

Linn, T. C., Pettit, F. H., & Reed, L. J. (1969). α-KETO ACID DEHYDROGENASE COMPLEXES, X. REGULATION OF THE ACTIVITY OF THE PYRUVATE DEHYDROGENASE COMPLEX FROM BEEF KIDNEY MITOCHONDRIA BY PHOSPHORYLATION AND DEPHOSPHORYLATION. *Proceedings of the National Academy of Sciences*, *62*(1), 234–241. doi: 10.1073/pnas.62.1.234

Liu, Z., Song, Y., Li, D., He, X., Li, S., Wu, B., Wang, W., Gu, S., Zhu, X., Wang, X., Zhou, Q., Dai, Y., & Yan, Q. (2014). The novel mitochondrial 16S rRNA 2336T>C mutation is associated with hypertrophic cardiomyopathy. *Journal of Medical Genetics*, *51*(3), 176–184. doi: 10.1136/JMEDGENET-2013-101818

Lott, M. T., Leipzig, J. N., Derbeneva, O., Xie, H. M., Chalkia, D., Sarmady, M., Procaccio, V., & Wallace, D. C. (2013). mtDNA Variation and Analysis Using Mitomap and Mitomaster. *Current Protocols in Bioinformatics*, *44*, 1.23.1-26. doi: 10.1002/0471250953.bi0123s44

Lu, B., Lee, J., Nie, X., Li, M., Morozov, Y. I., Venkatesh, S., Bogenhagen, D. F., Temiakov, D., & Suzuki, C. K. (2013). Phosphorylation of Human TFAM in Mitochondria Impairs DNA Binding and Promotes Degradation by the AAA+ Lon Protease. *Molecular Cell*, *49*(1), 121–132. doi: 10.1016/j.molcel.2012.10.023

Lucero, M., Suarez, A. E., & Chambers, J. W. (2019). Phosphoregulation on mitochondria: Integration of cell and organelle responses. *CNS Neuroscience & Therapeutics*, cns.13141. doi: 10.1111/cns.13141

Lukyanenko, V., Chikando, A., & Lederer, W. J. (2009). Mitochondria in cardiomyocyte Ca2+ signaling. *The International Journal of Biochemistry & Cell Biology*, *41*(10), 1957–1971. doi: 10.1016/J.BIOCEL.2009.03.011

Lushchak, O. v., Piroddi, M., Galli, F., & Lushchak, V. I. (2014). Aconitase post-translational modification as a key in linkage between Krebs cycle, iron homeostasis, redox signaling, and metabolism of reactive oxygen species. *Redox Report*, *19*(1), 8–15. doi: 10.1179/1351000213Y.0000000073

Ly, C. v., & Verstreken, P. (2006). Mitochondria at the synapse. *Neuroscientist*, *12*(4), 291–299. doi: 10.1177/1073858406287661

MacAskill, A. F., & Kittler, J. T. (2010). Control of mitochondrial transport and localization in neurons. *Trends in Cell Biology*, *20*(2), 102–112. doi: 10.1016/J.TCB.2009.11.002

Mai, N., Chrzanowska-Lightowlers, Z. M. A., & Lightowlers, R. N. (2017). The process of mammalian mitochondrial protein synthesis. In Cell and Tissue Research (Vol. 367, Issue 1, pp. 5–20). Springer Verlag. doi: 10.1007/s00441-016-2456-0

Marinov, G. K., Wang, Y. E., Chan, D., & Wold, B. J. (2014). Evidence for Site-Specific Occupancy of the Mitochondrial Genome by Nuclear Transcription Factors. *PLoS ONE*, *9*(1), e84713. doi: 10.1371/journal.pone.0084713

Martinus, R. D., Garth, G. P., Webster, T. L., Cartwright, P., Naylor, D. J., Høj, P. B., & Hoogenraad, N. J. (1996). Selective Induction of Mitochondrial Chaperones in Response to Loss of the Mitochondrial Genome. *European Journal of Biochemistry*, *240*(1), 98–103. doi: 10.1111/j.1432-1033.1996.0098h.x

McBride, H. M., Neuspiel, M., & Wasiak, S. (2006). Mitochondria: More Than Just a Powerhouse. *Current Biology*, *16*(14), R551–R560. doi: 10.1016/j.cub.2006.06.054

Mercer, T. R., Neph, S., Dinger, M. E., Crawford, J., Smith, M. A., Shearwood, A.-M. J., Haugen, E., Bracken, C. P., Rackham, O., Stamatoyannopoulos, J. A., Filipovska, A., & Mattick, J. S. (2011). The Human Mitochondrial Transcriptome. *Cell*, *146*(4), 645–658. doi: 10.1016/j.cell.2011.06.051

Miller, J. C., Tan, S., Qiao, G., Barlow, K. A., Wang, J., Xia, D. F., Meng, X., Paschon, D. E., Leung, E., Hinkley, S. J., Dulay, G. P., Hua, K. L., Ankoudinova, I., Cost, G. J., Urnov, F. D., Zhang, H. S., Holmes, M. C., Zhang, L., Gregory, P. D., & Rebar, E. J. (2011). A TALE nuclease architecture for efficient genome editing. *Nature Biotechnology*, *29*(2), 143–148. doi: 10.1038/nbt.1755

Miller, J. L., Cimen, H., Koc, H., & Koc, E. C. (2009). Phosphorylated Proteins of the Mammalian Mitochondrial Ribosome: Implications in Protein Synthesis. *Journal of Proteome Research*, *8*(10), 4789–4798. doi: 10.1021/pr9004844

Minczuk, M., He, J., Duch, A. M., Ettema, T. J., Chlebowski, A., Dzionek, K., Nijtmans, L. G. J., Huynen, M. A., & Holt, I. J. (2011). TEFM (c17orf42) is necessary for transcription of human mtDNA. *Nucleic Acids Research*, *39*(10), 4284–4299. doi: 10.1093/NAR/GKQ1224

Misgeld, T., Kerschensteiner, M., Bareyre, F. M., Burgess, R. W., & Lichtman, J. W. (2007). Imaging axonal transport of mitochondria in vivo. *Nature Methods 2007 4:7*, *4*(7), 559–561. doi: 10.1038/nmeth1055

Misgeld, T., & Schwarz, T. L. (2017). Mitostasis in Neurons: Maintaining Mitochondria in an Extended Cellular Architecture. *Neuron*, *96*(3), 651–666. doi: 10.1016/j.neuron.2017.09.055

Mok, B. Y., de Moraes, M. H., Zeng, J., Bosch, D. E., Kotrys, A. v., Raguram, A., Hsu, F., Radey, M. C., Peterson, S. B., Mootha, V. K., Mougous, J. D., & Liu, D. R. (2020). A bacterial cytidine deaminase toxin enables CRISPR-free mitochondrial base editing. *Nature*, *583*(7817), 631–637. doi: 10.1038/s41586-020-2477-4

Montoya, J., Ojala, D., & Attardi, G. (1981). Distinctive features of the 5′-terminal sequences of the human mitochondrial mRNAs. *Nature*, *290*(5806), 465–470. doi: 10.1038/290465a0

Moraes, C. T., Atencio, D. P., Oca-Cossio, J., & Diaz, F. (2003). Techniques and Pitfalls in the Detection of Pathogenic Mitochondrial DNA Mutations. *The Journal of Molecular Diagnostics*, *5*(4), 197–208. doi: 10.1016/S1525-1578(10)60474-6

Morgenstern, M., Peikert, C. D., Lübbert, P., Suppanz, I., Klemm, C., Alka, O., Steiert, C., Naumenko, N., Schendzielorz, A., Melchionda, L., Mühlhäuser, W. W. D., Knapp, B., Busch, J. D., Stiller, S. B., Dannenmaier, S., Lindau, C., Licheva, M., Eickhorst, C., Galbusera, R., … Warscheid, B. (2021). Quantitative high-confidence human mitochondrial proteome and its dynamics in cellular context. *Cell Metabolism*, *33*(12), 2464. doi: 10.1016/J.CMET.2021.11.001

Morgenstern, M., Stiller, S. B., Lübbert, P., Peikert, C. D., Dannenmaier, S., Drepper, F., Weill, U., Höß, P., Feuerstein, R., Gebert, M., Bohnert, M., van der Laan, M., Schuldiner, M., Schütze, C., Oeljeklaus, S., Pfanner, N., Wiedemann, N., & Warscheid, B. (2017). Definition of a High-Confidence Mitochondrial Proteome at Quantitative Scale. *Cell Reports*, *19*(13), 2836–2852. doi: 10.1016/J.CELREP.2017.06.014

Münch, C., & Harper, J. W. (2016). Mitochondrial unfolded protein response controls matrix pre-RNA processing and translation. *Nature 2016 534:7609*, *534*(7609), 710–713. doi: 10.1038/nature18302

Natera-Naranjo, O., Kar, A. N., Aschrafi, A., Gervasi, N. M., Macgibeny, M. A., Gioio, A. E., & Kaplan, B. B. (2012). Local translation of ATP synthase subunit 9 mRNA alters ATP levels

and the production of ROS in the axon. *Molecular and Cellular Neuroscience*, *49*(3), 263–270. doi: 10.1016/j.mcn.2011.12.006

Nicklas, J. A., Brooks, E. M., Hunter, T. C., Single, R., & Branda, R. F. (2004). Development of a quantitative PCR (TaqMan) assay for relative mitochondrial DNA copy number and the common mitochondrial DNA deletion in the rat. *Environmental and Molecular Mutagenesis*, *44*(4), 313–320. doi: 10.1002/em.20050

Ohkubo, A., van Haute, L., Rudler, D. L., Stentenbach, M., Steiner, F. A., Rackham, O., Minczuk, M., Filipovska, A., & Martinou, J.-C. (2021). The FASTK family proteins fine-tune mitochondrial RNA processing. *PLOS Genetics*, *17*(11), e1009873. doi: 10.1371/journal.pgen.1009873

Ojala, D., Montoya, J., & Attardi, G. (1981). tRNA punctuation model of RNA processing in human mitochondria. *Nature*, *290*(5806), 470–474. doi: 10.1038/290470a0

Ojuka, E. O., Jones, T. E., Han, D., Chen, M., & Holloszy, J. O. (2003). Raising Ca^{2+} in L6 myotubes mimics effects of exercise on mitochondrial biogenesis in muscle. *The FASEB Journal*, *17*(6), 675–681. doi: 10.1096/fj.02-0951com

Palmer, J. W., Tandler, B., & Hoppel, C. L. (1986). Heterogeneous response of subsarcolemmal heart mitochondria to calcium. *Https://Doi.Org/10.1152/Ajpheart.1986.250.5.H741*, *250*(5 (19/5)). doi: 10.1152/AJPHEART.1986.250.5.H741

Parisi, M. A., Xu, B., & Clayton, D. A. (1993). A human mitochondrial transcriptional activator can functionally replace a yeast mitochondrial HMG-box protein both in vivo and in vitro. *Molecular and Cellular Biology*, *13*(3), 1951–1961. doi: 10.1128/mcb.13.3.1951-1961.1993

Pathak, D., Shields, L. Y., Mendelsohn, B. A., Haddad, D., Lin, W., Gerencser, A. A., Kim, H., Brand, M. D., Edwards, R. H., & Nakamura, K. (2015). The Role of Mitochondrially Derived ATP in Synaptic Vesicle Recycling. *Journal of Biological Chemistry*, *290*(37), 22325–22336. doi: 10.1074/jbc.M115.656405

Pearce, S. F., Rebelo-Guiomar, P., D'Souza, A. R., Powell, C. A., van Haute, L., & Minczuk, M. (2017). Regulation of Mammalian Mitochondrial Gene Expression: Recent Advances. *Trends in Biochemical Sciences*, *42*(8), 625–639. doi: 10.1016/j.tibs.2017.02.003

Popov, L. (2020). Mitochondrial biogenesis: An update. *Journal of Cellular and Molecular Medicine*, *24*(9), 4892–4899. doi: 10.1111/jcmm.15194

Prezant, T. R., Agapian, J. v., Bohlman, M. C., Bu, X., Öztas, S., Qiu, W. Q., Arnos, K. S., Cortopassi, G. A., Jaber, L., Rotter, J. I., Shohat, M., & Fischel-Ghodsian, N. (1993). Mitochondrial ribosomal RNA mutation associated with both antibiotic–induced and non–syndromic deafness. *Nature Genetics 1993 4:3*, *4*(3), 289–294. doi: 10.1038/ng0793-289

Prole, D. L., Chinnery, P. F., & Jones, N. S. (2020). Visualizing, quantifying, and manipulating mitochondrial DNA in vivo. *Journal of Biological Chemistry*, *295*(51), 17588–17601. doi: 10.1074/jbc.REV120.015101

Puigserver, P., Wu, Z., Park, C. W., Graves, R., Wright, M., & Spiegelman, B. M. (1998). A Cold-Inducible Coactivator of Nuclear Receptors Linked to Adaptive Thermogenesis. *Cell*, *92*(6), 829–839. doi: 10.1016/S0092-8674(00)81410-5

Quirós, P. M., Mottis, A., & Auwerx, J. (2016). Mitonuclear communication in homeostasis and stress. *Nature Reviews Molecular Cell Biology 2016 17:4*, *17*(4), 213–226. doi: 10.1038/nrm.2016.23

Rainbolt, T. K., Atanassova, N., Genereux, J. C., & Wiseman, R. L. (2013). Stress-Regulated Translational Attenuation Adapts Mitochondrial Protein Import through Tim17A Degradation. *Cell Metabolism*, *18*(6), 908–919. doi: 10.1016/j.cmet.2013.11.006

Rangaraju, V., Calloway, N., & Ryan, T. A. (2014). Activity-Driven Local ATP Synthesis Is Required for Synaptic Function. *Cell*, *156*(4), 825–835. doi: 10.1016/j.cell.2013.12.042

Rangaraju, V., Lauterbach, M., & Schuman, E. M. (2019). Spatially Stable Mitochondrial Compartments Fuel Local Translation during Plasticity. *Cell*, *176*(1–2), 73-84.e15. doi: 10.1016/J.CELL.2018.12.013

Rardin, M. J., Wiley, S. E., Naviaux, R. K., Murphy, A. N., & Dixon, J. E. (2009). Monitoring phosphorylation of the pyruvate dehydrogenase complex. *Analytical Biochemistry*, *389*(2), 157–164. doi: 10.1016/j.ab.2009.03.040

Richter-Dennerlein, R., Dennerlein, S., & Rehling, P. (2015). Integrating mitochondrial translation into the cellular context. *Nature Reviews. Molecular Cell Biology*, *16*(10), 586–592. doi: 10.1038/NRM4051

Richter-Dennerlein, R., Oeljeklaus, S., Lorenzi, I., Ronsör, C., Bareth, B., Schendzielorz, A. B., Wang, C., Warscheid, B., Rehling, P., & Dennerlein, S. (2016). Mitochondrial Protein Synthesis Adapts to Influx of Nuclear-Encoded Protein. *Cell*, *167*(2), 471. doi: 10.1016/J.CELL.2016.09.003

Riemann, D., Petkova, A., Dresbach, T., & Wallrafen, R. (2018). An Optical Assay for Synaptic Vesicle Recycling in Cultured Neurons Overexpressing Presynaptic Proteins. *Journal of Visualized Experiments : JoVE*, *2018*(136). doi: 10.3791/58043

Riva, A., Tandler, B., Loffredo, F., Vazquez, E., & Hoppel, C. (2005). Structural differences in two biochemically defined populations of cardiac mitochondria. *American Journal of Physiology - Heart and Circulatory Physiology*, *289*(2 58-2), 868–872. doi: 10.1152/AJPHEART.00866.2004/ASSET/IMAGES/LARGE/ZH40080541410004.JPEG

Rooijers, K., Loayza-Puch, F., Nijtmans, L. G., & Agami, R. (2013). Ribosome profiling reveals features of normal and disease-associated mitochondrial translation. *Nature Communications 2013 4:1*, *4*(1), 1–8. doi: 10.1038/ncomms3886

Rosenberg, T., Gal-Ben-Ari, S., Dieterich, D. C., Kreutz, M. R., Ziv, N. E., Gundelfinger, E. D., & Rosenblum, K. (2014). The roles of protein expression in synaptic plasticity and memory consolidation. *Frontiers in Molecular Neuroscience*, *7*(November), 86. doi: 10.3389/FNMOL.2014.00086/BIBTEX

ROSSIGNOL, R., FAUSTIN, B., ROCHER, C., MALGAT, M., MAZAT, J.-P., & LETELLIER, T. (2003). Mitochondrial threshold effects. *Biochemical Journal*, *370*(3), 751–762. doi: 10.1042/bj20021594

Rubio-Cosials, A., Sydow, J. F., Jiménez-Menéndez, N., Fernández-Millán, P., Montoya, J., Jacobs, H. T., Coll, M., Bernadó, P., & Solà, M. (2011). Human mitochondrial transcription factor A induces a U-turn structure in the light strand promoter. *Nature Structural & Molecular Biology*, *18*(11), 1281–1289. doi: 10.1038/nsmb.2160

Russell, O., & Turnbull, D. (2014). Mitochondrial DNA disease—molecular insights and potential routes to a cure. *Experimental Cell Research*, *325*(1), 38. doi: 10.1016/J.YEXCR.2014.03.012

Ruzzenente, B., Metodiev, M. D., Wredenberg, A., Bratic, A., Park, C. B., Cámara, Y., Milenkovic, D., Zickermann, V., Wibom, R., Hultenby, K., Erdjument-Bromage, H., Tempst, P., Brandt, U., Stewart, J. B., Gustafsson, C. M., & Larsson, N. G. (2012). LRPPRC is necessary for polyadenylation and coordination of translation of mitochondrial mRNAs. *The EMBO Journal*, *31*(2), 443–456. doi: 10.1038/EMBOJ.2011.392

Ryu, H., Lee, J., Impey, S., Ratan, R. R., & Ferrante, R. J. (2005). Antioxidants modulate mitochondrial PKA and increase CREB binding to D-loop DNA of the mitochondrial

genome in neurons. *Proceedings of the National Academy of Sciences*, *102*(39), 13915–13920. doi: 10.1073/pnas.0502878102

Saccone, C., Gissi, C., Lanave, C., Larizza, A., Pesole, G., & Reyes, A. (2000). Evolution of the mitochondrial genetic system: an overview. *Gene*, *261*(1), 153–159. doi: 10.1016/S0378-1119(00)00484-4

Saladi, S., Boos, F., Poglitsch, M., Meyer, H., Sommer, F., Mühlhaus, T., Schroda, M., Schuldiner, M., Madeo, F., & Herrmann, J. M. (2020). The NADH Dehydrogenase Nde1 Executes Cell Death after Integrating Signals from Metabolism and Proteostasis on the Mitochondrial Surface. *Molecular Cell*, *77*(1), 189-202.e6. doi: 10.1016/j.molcel.2019.09.027

Sasarman, F., Brunel-Guitton, C., Antonicka, H., Wai, T., Shoubridge, E. A., Allen, B., Burelle, Y., Charron, G., Coderre, L., DesRosiers, C., Laprise, C., Morin, C., & Rioux, J. (2010). LRPPRC and SLIRP interact in a ribonucleoprotein complex that regulates posttranscriptional gene expression in mitochondria. *Molecular Biology of the Cell*, *21*(8), 1315–1323. doi: 10.1091/MBC.E10-01-0047

Schmidt, E. K., Clavarino, G., Ceppi, M., & Pierre, P. (2009). SUnSET, a nonradioactive method to monitor protein synthesis. *Nature Methods*, *6*(4), 275–277. doi: 10.1038/NMETH.1314

Schmidt, O., Harbauer, A. B., Rao, S., Eyrich, B., Zahedi, R. P., Stojanovski, D., Schönfisch, B., Guiard, B., Sickmann, A., Pfanner, N., & Meisinger, C. (2011). Regulation of Mitochondrial Protein Import by Cytosolic Kinases. *Cell*, *144*(2), 227–239. doi: 10.1016/j.cell.2010.12.015

Sebastián, D., & Zorzano, A. (2018). Mitochondrial dynamics and metabolic homeostasis. *Current Opinion in Physiology*, *3*, 34–40. doi: 10.1016/J.COPHYS.2018.02.006

Sheng, Z.-H. (2014). Mitochondrial trafficking and anchoring in neurons: New insight and implications. *Journal of Cell Biology*, *204*(7), 1087–1098. doi: 10.1083/jcb.201312123

Sheng, Z.-H., & Cai, Q. (2012). Mitochondrial transport in neurons: impact on synaptic homeostasis and neurodegeneration. *Nature Reviews Neuroscience*, *13*(2), 77–93. doi: 10.1038/nrn3156

Shepherd, G. M. G., & Harris, K. M. (1998). Three-Dimensional Structure and Composition of CA3→CA1 Axons in Rat Hippocampal Slices: Implications for Presynaptic Connectivity

and Compartmentalization. *Journal of Neuroscience*, *18*(20), 8300–8310. doi: 10.1523/JNEUROSCI.18-20-08300.1998

Shin, J.-H., Ko, H. S., Kang, H., Lee, Y., Lee, Y.-I., Pletinkova, O., Troconso, J. C., Dawson, V. L., & Dawson, T. M. (2011). PARIS (ZNF746) Repression of PGC-1α Contributes to Neurodegeneration in Parkinson's Disease. *Cell*, *144*(5), 689–702. doi: 10.1016/j.cell.2011.02.010

Sickmann, A., Reinders, J., Wagner, Y., Joppich, C., Zahedi, R., Meyer, H. E., Schönfisch, B., Perschil, I., Chacinska, A., Guiard, B., Rehling, P., Pfanner, N., & Meisinger, C. (2003). The proteome of Saccharomyces cerevisiae mitochondria. *Proceedings of the National Academy of Sciences of the United States of America*, *100*(23), 13207–13212. doi: 10.1073/PNAS.2135385100

Smeitink, J. A. M., Elpeleg, O., Antonicka, H., Diepstra, H., Saada, A., Smits, P., Sasarman, F., Vriend, G., Jacob-Hirsch, J., Shaag, A., Rechavi, G., Welling, B., Horst, J., Rodenburg, R. J., van den Heuvel, B., & Shoubridge, E. A. (2006). Distinct Clinical Phenotypes Associated with a Mutation in the Mitochondrial Translation Elongation Factor EFTs. *The American Journal of Human Genetics*, *79*(5), 869–877. doi: 10.1086/508434

Smith, P. M., Elson, J. L., Greaves, L. C., Wortmann, S. B., Rodenburg, R. J. T., Lightowlers, R. N., Chrzanowska-Lightowlers, Z. M. A., Taylor, R. W., & Vila-Sanjurjo, A. (2014). The role of the mitochondrial ribosome in human disease: searching for mutations in 12S mitochondrial rRNA with high disruptive potential. *Human Molecular Genetics*, *23*(4), 949. doi: 10.1093/HMG/DDT490

Smit-Rigter, L., Rajendran, R., Silva, C. A. P., Spierenburg, L., Groeneweg, F., Ruimschotel, E. M., van Versendaal, D., van der Togt, C., Eysel, U. T., Heimel, J. A., Lohmann, C., & Levelt, C. N. (2016). Mitochondrial Dynamics in Visual Cortex Are Limited In Vivo and Not Affected by Axonal Structural Plasticity. *Current Biology*, *26*(19), 2609–2616. doi: 10.1016/J.CUB.2016.07.033

Sondheimer, N., Fang, J. K., Polyak, E., Falk, M. J., & Avadhani, N. G. (2010). Leucine-rich pentatricopeptide-repeat containing protein regulates mitochondrial transcription. *Biochemistry*, *49*(35), 7467–7473. doi: 10.1021/BI1008479

Stauch, K. L., Purnell, P. R., & Fox, H. S. (2014). Quantitative Proteomics of Synaptic and Nonsynaptic Mitochondria: Insights for Synaptic Mitochondrial Vulnerability. *Journal of Proteome Research*, *13*(5), 2620–2636. doi: 10.1021/pr500295n

Stiburek, L., Fornuskova, D., Wenchich, L., Pejznochova, M., Hansikova, H., & Zeman, J. (2007). Knockdown of human Oxa1l impairs the biogenesis of F1Fo-ATP synthase and NADH:ubiquinone oxidoreductase. *Journal of Molecular Biology*, *374*(2), 506–516. doi: 10.1016/J.JMB.2007.09.044

Sudhof, T. C. (2012). Calcium Control of Neurotransmitter Release. *Cold Spring Harbor Perspectives in Biology*, *4*(1), a011353–a011353. doi: 10.1101/cshperspect.a011353

Suzuki, T., Yashiro, Y., Kikuchi, I., Ishigami, Y., Saito, H., Matsuzawa, I., Okada, S., Mito, M., Iwasaki, S., Ma, D., Zhao, X., Asano, K., Lin, H., Kirino, Y., Sakaguchi, Y., & Suzuki, T. (2020). Complete chemical structures of human mitochondrial tRNAs. *Nature Communications 2020 11:1*, *11*(1), 1–15. doi: 10.1038/s41467-020-18068-6

Szabadkai, G., Mishmar, D., Jones, N. S., Aryaman, J., & Johnston, I. G. (2019). *Mitochondrial Heterogeneity*. doi: 10.3389/fgene.2018.00718

Szklarczyk, R., Wanschers, B. F. J., Cuypers, T. D., Esseling, J. J., Riemersma, M., van den Brand, M. A. M., Gloerich, J., Lasonder, E., van den Heuvel, L. P., Nijtmans, L. G., & Huynen, M. A. (2012). Iterative orthology prediction uncovers new mitochondrial proteins and identifies C12orf62 as the human ortholog of COX14, a protein involved in the assembly of cytochrome c oxidase. *Genome Biology*, *13*(2). doi: 10.1186/GB-2012-13-2-R12

Taanman, J. W. (1999). The mitochondrial genome: structure, transcription, translation and replication. *Biochimica et Biophysica Acta*, *1410*(2), 103–123. doi: 10.1016/S0005-2728(98)00161-3

Thompson, K., Mai, N., Oláhová, M., Scialó, F., Formosa, L. E., Stroud, D. A., Garrett, M., Lax, N. Z., Robertson, F. M., Jou, C., Nascimento, A., Ortez, C., Jimenez-Mallebrera, C., Hardy, S. A., He, L., Brown, G. K., Marttinen, P., McFarland, R., Sanz, A., … Taylor, R. W. (2018). OXA1L mutations cause mitochondrial encephalopathy and a combined oxidative phosphorylation defect. *EMBO Molecular Medicine*, *10*(11). doi: 10.15252/EMMM.201809060

Tian, Q., Taupin, J. L., Elledge, S., Kobertson, M., & Anderson, P. (1995). Fas-activated serine/threonine kinase (FAST) phosphorylates TIA-1 during Fas-mediated apoptosis. *The Journal of Experimental Medicine*, *182*(3), 865. doi: 10.1084/JEM.182.3.865

Toyama, E. Q., Herzig, S., Courchet, J., Lewis, T. L., Losón, O. C., Hellberg, K., Young, N. P., Chen, H., Polleux, F., Chan, D. C., & Shaw, R. J. (2016). AMP-activated protein kinase

mediates mitochondrial fission in response to energy stress. *Science*, *351*(6270), 275–281. doi: 10.1126/science.aab4138

Truckenbrodt, S., Viplav, A., Jähne, S., Vogts, A., Denker, A., Wildhagen, H., Fornasiero, E. F., & Rizzoli, S. O. (2018). Newly produced synaptic vesicle proteins are preferentially used in synaptic transmission. *The EMBO Journal*, *37*(15), e98044. doi: 10.15252/EMBJ.201798044

Uittenbogaard, M., & Chiaramello, A. (2014). Mitochondrial Biogenesis: A Therapeutic Target for Neurodevelopmental Disorders and Neurodegenerative Diseases. *Current Pharmaceutical Design*, *20*(35), 5574–5593. doi: 10.2174/1381612820666140305224906

Vakifahmetoglu-Norberg, H., Ouchida, A. T., & Norberg, E. (2017). The role of mitochondria in metabolism and cell death. *Biochemical and Biophysical Research Communications*, *482*(3), 426–431. doi: 10.1016/J.BBRC.2016.11.088

van Laar, V. S., Arnold, B., Howlett, E. H., Calderon, M. J., st. Croix, C. M., Greenamyre, J. T., Sanders, L. H., & Berman, S. B. (2018). Evidence for Compartmentalized Axonal Mitochondrial Biogenesis: Mitochondrial DNA Replication Increases in Distal Axons As an Early Response to Parkinson's Disease-Relevant Stress. *The Journal of Neuroscience*, *38*(34), 7505–7515. doi: 10.1523/JNEUROSCI.0541-18.2018

Van Haute, L., Powell, C. A., & Minczuk, M. (2017). Dealing with an Unconventional Genetic Code in Mitochondria: The Biogenesis and Pat hogenic Defects of the 5-Formylcytosine Modification in Mitochondrial tRNAMet. *Biomolecules*, *7*(4), 24. doi: 10.3390/biom7010024

Verstreken, P., Ly, C. v., Venken, K. J. T., Koh, T. W., Zhou, Y., & Bellen, H. J. (2005). Synaptic mitochondria are critical for mobilization of reserve pool vesicles at Drosophila neuromuscular junctions. *Neuron*, *47*(3), 365–378. doi: 10.1016/J.NEURON.2005.06.018

Virbasius, J. v, & Scarpulla, R. C. (1994). Activation of the human mitochondrial transcriptionfactor A gene by nuclear respiratory factors: a potential regulatory linkbetween nuclear and mitochondrial gene expression in organellebiogenesis. *Proceedings of the National Academy of Sciences*, *91*(4), 1309–1313. doi: 10.1073/pnas.91.4.1309

Vogel, F., Bornhövd, C., Neupert, W., & Reichert, A. S. (2006). Dynamic subcompartmentalization of the mitochondrial inner membrane. *Journal of Cell Biology*, *175*(2), 237–247. doi: 10.1083/jcb.200605138

Walter, C., Marada, A., Suhm, T., Ernsberger, R., Muders, V., Kücükköse, C., Sánchez-Martín, P., Hu, Z., Aich, A., Loroch, S., Solari, F. A., Poveda-Huertes, D., Schwierzok, A., Pommerening, H., Matic, S., Brix, J., Sickmann, A., Kraft, C., Dengjel, J., … Meisinger, C. (2021). Global kinome profiling reveals DYRK1A as critical activator of the human mitochondrial import machinery. *Nature Communications*, *12*(1). doi: 10.1038/S41467-021-24426-9

Wang, J., Venegas, V., Li, F., & Wong, L. (2011). Analysis of Mitochondrial DNA Point Mutation Heteroplasmy by ARMS Quantitative PCR. *Current Protocols in Human Genetics*, *68*(1). doi: 10.1002/0471142905.hg1906s68

Weraarpachai, W., Antonicka, H., Sasarman, F., Seeger, J., Schrank, B., Kolesar, J. E., Lochmüller, H., Chevrette, M., Kaufman, B. A., Horvath, R., & Shoubridge, E. A. (2009). Mutation in TACO1, encoding a translational activator of COX I, results in cytochrome c oxidase deficiency and late-onset Leigh syndrome. *Nature Genetics 2009 41:7*, *41*(7), 833–837. doi: 10.1038/ng.390

Weraarpachai, W., Sasarman, F., Nishimura, T., Antonicka, H., Auré, K., Rötig, A., Lombs, A., & Shoubridge, E. A. (2012). Mutations in C12orf62, a factor that couples COX I synthesis with cytochrome c oxidase assembly, cause fatal neonatal lactic acidosis. *American Journal of Human Genetics*, *90*(1), 142–151. doi: 10.1016/J.AJHG.2011.11.027

Wheeler, J. H., Young, C. K. J., & Young, M. J. (2019). Analysis of Human Mitochondrial DNA Content by Southern Blotting and Nonradioactive Probe Hybridization. *Current Protocols in Toxicology*, *80*(1). doi: 10.1002/cptx.75

Wiedemann, N., & Pfanner, N. (2017). *Mitochondrial Machineries for Protein Import and Assembly*. doi: 10.1146/annurev

Wright, D. C., Geiger, P. C., Han, D.-H., Jones, T. E., & Holloszy, J. O. (2007). Calcium Induces Increases in Peroxisome Proliferator-activated Receptor γ Coactivator-1α and Mitochondrial Biogenesis by a Pathway Leading to p38 Mitogen-activated Protein Kinase Activation. *Journal of Biological Chemistry*, *282*(26), 18793–18799. doi: 10.1074/jbc.M611252200

Wu, Z., Puigserver, P., Andersson, U., Zhang, C., Adelmant, G., Mootha, V., Troy, A., Cinti, S., Lowell, B., Scarpulla, R. C., & Spiegelman, B. M. (1999). Mechanisms Controlling Mitochondrial Biogenesis and Respiration through the Thermogenic Coactivator PGC-1. *Cell*, *98*(1), 115–124. doi: 10.1016/S0092-8674(00)80611-X

Yarham, J. W., Elson, J. L., Blakely, E. L., Mcfarland, R., & Taylor, R. W. (2010). Mitochondrial tRNA mutations and disease. *Wiley Interdisciplinary Reviews. RNA*, *1*(2), 304–324. doi: 10.1002/WRNA.27

Zhang, W., Cui, H., & Wong, L.-J. C. (2012). Comprehensive One-Step Molecular Analyses of Mitochondrial Genome by Massively Parallel Sequencing. *Clinical Chemistry*, *58*(9), 1322–1331. doi: 10.1373/clinchem.2011.181438

Zorkau, M., Albus, C. A., Berlinguer-Palmini, R., Chrzanowska-Lightowlers, Z. M. A., & Lightowlers, R. N. (2021). High-resolution imaging reveals compartmentalization of mitochondrial protein synthesis in cultured human cells. *Proceedings of the National Academy of Sciences*, *118*(6). doi: 10.1073/pnas.2008778118

List of Figures

INTRODUCTION

Figure 1. Mitochondria structure, function, and protein biogenesis. 4

Figure 2. Mitochondrial biogenesis in neurons. 8

Figure 4. Methods to analyze gene expression at translation level in mitochondria. ……18

MANUSCRIPT 1

Figure 1. Visualizing mitochondrial translation in the cellular context. ……...…..28

Figure 2. Different levels of gene expression in mitochondria of a single cell....……..30

Figure 3. Utilizing HPG labeling in a disease context and mapping mitochondrial translation with super resolution microscopy. ……...31

Figure 4. Mitochondrial translation in neurons. ……...….32

Figure EV1. ……38

Figure EV2. ……39

Figure EV3. ……40

MANUSCRIPT 2

Figure 1. Depletion of cellular kinases affects mitochondrial translation. 47

Figure 2. Ablation of kinases affects mitochondrial function and ATP levels. 50

Figure 3. Downregulation of selected kinases changes the cellular energetic state and mitoribosome integrity. 52

Figure 4. Effect of downregulation of selected kinases on individual mitochondrial proteins......54

Figure S1. 69

Figure S2. 70

Figure S3. 71

List of Abbreviations

°C	degree Celsius
×*g*	relative centrifugal force
3D	three dimentional
A-site	amino acid site
ADCK2	aarF domain containing kinase 2
ADP	adenosine 5′-diphosphate
AF488	alexafluor 488
AF647	alexafluor 647
AMP	adenosine 5′-monophosphate
ANK-G	Ankyrin G
ARAF	Serine/threonine-protein kinase A-Raf
ATP	adenosine 5′-triphosphate
ATP5B	ATP synthase subunit beta
ATP6	ATP synthase membrane subunit 6
ATP8	ATP synthase membrane subunit 8
AURKAIP1	aurora kinase A-interacting protein 1
BONCAT	Bio-Orthogonal Non-canonical Amino acid Tagging
BSA	bovine serum albumin
CALM1	Calmodulin-1
CAMK2D	Calcium/calmodulin-dependent protein kinase type II subunit delta
cAMP	cyclic adenosine 5′-monophosphate
CAP	chloramphenicol
CCCP	carbonyl cyanide-m-chlorophenylhydrazone
Chl	chloramphenicol
Chx	Cycloheximide
CI	complex I
CII	complex II

CIII	complex III
CIV	complex IV
CKMT2	mitochondrial creatine kinase 2
cm^2	Square Centimeter
CO2	carbon dioxide
COA6	cytochrome c oxidase assembly factor 6
CoQ	coenzyme Q
COX1	Cytochrome c oxidase subunit 1
COX2	Cytochrome c oxidase subunit 2
COX3	Cytochrome c oxidase subunit 3
CREB	cAMP-response element binding protein
CRISPR	clustered regularly interspaced short palindromic repeats
cryo-EM	Cryogenic electron microscopy (
CT	cycle threshold
CuAAC	Cu(I)-catalysed azide-alkyne cycloaddition
CV	complex V
CYTB	Cytochrome b
DHX30	DExH-box helicase 30
DiO	3,3’-dioctadecyloxacarbocyanine perchlorate
DMEM	Dulbecco's modified Eagle's medium
DMF	dimethylformamide
DNA	deoxyribonucleic acid
DTT	Dithiothreitol
DYRK4	Dual Specificity Tyrosine Phosphorylation Regulated Kinase 4
ECAR	Extracellular acidification rate
ER	endoplasmic reticulum
f-Met	N-formyl methionine
$FADH_2$	1,5-dihydro-flavin adenine dinucleotide

FASTK	Fas-activated Serine/Threonine kinases
FCCP	Carbonyl cyanide-p-trifluoromethoxyphenylhydrazone
FN3K	Fructosamine 3 Kinase
FRAP1	FKBP12-rapamycin-associated protein 1
FUNCAT	Fluorescent Non-canonical Amino acid Tagging
GCK	glucokinase
h	hour
H-strand	heavy strand
Harr	Harringtonine
HBSS	Hank's Balanced Salt Solution
HEK	embryonic human kidney
HEPES	N-2-Hydroxyethylpiperazine-N'-2-Ethanesulfonic Acid
HK1	hexokinase 1
HOMER1	Homer protein homolog 1
HPA	Human Protein Atlas
HPG	homopropargylglycine
HSP	heavy strand promoter
IF1	initiation factor 1
IMM	inner mitochondrial membrane
IMS	intermembrane space
iPSCs	induced pluripotent stem cells
ISR	integrated stress response
kbp	kilo base pair
KCl	potasium chloride
KD	knockdown
kD	kilo Dalton
KH_2PO_4	Monopotassium phosphate
L-strand	light strand

LE	late endosomes
LRPPRC	leucine-rich PPR-motif-containing protein
LSP	light strand promoter
MAPK	mitogen-activated protein kinase
MAPK11	mitogen-activated protein kinase 11
mEF-Tu	mitochondrial elongation factor Tu
MeOH	methanol
Met	methionine
MET	tyrosine-protein *kinase Met*
min	minute(s)
ml	milliliter
mM	millimolar
MOK	MOK Protein Kinase
MRG	mitochondrial RNA granule
mRNA	messenger RNA
MRPL1	39S ribosomal protein L1, mitochondrial
MRPL53	39S ribosomal protein L53, mitochondrial
MRPS12	28S ribosomal protein S12, mitochondrial, gene
MRPS16	28S ribosomal protein S16, mitochondrial, gene
MS	mass spectrometry
mt-SSU	mitochondrial small subunit
MTCO1	mitochondrially encoded cytochrome C oxidase 1
mtDNA	mitochondrial DNA
mTERF1	mitochondrial termination factor 1
mtIF2	mitochondrial translation initiation factor 2
MTND3	mitochondrially encoded NADH-ubiquinone oxidoreductase core subunit 3
mtPAP	mitochondrial poly(A) polymerase

MTRES1	mitochondrial transcription rescue factor 1
mtUPR	mitochondrial unfolded protein response
Na_2HPO_4	Disodium phosphate
NaCl	sodium chloride
NADH	Nicotinamide adenine dinucleotide
ND2	NADH-ubiquinone oxidoreductase chain 2
ND4	NADH-ubiquinone oxidoreductase core subunit 4
ND4-L	NADH-ubiquinone oxidoreductase core subunit 4L
ND6	NADH-ubiquinone oxidoreductase core subunit 6
nDNA	nuclear DANN
nm	nanometer
OCR	oxygen consumption rate
OMM	outer mitochondrial membrane
OXA1L	Oxidase assembly 1-like protein
OXPHOS	oxidative phosphorylation
PBS	Phosphate-buffered saline
PCC	pearson correlation coefficient
PCR	polymerase chain reaction
PDC	pyruvate dehydrogenase
PDGFRB	Platelet-derived growth factor receptor beta
PFA	paraformaldehyde
PGC-1α	peroxisome proliferator-activated receptor-gamma-coactivator-1 alpha
PI3K-AKT	Phosphoinositide 3-kinase-Protein kinase B
PIK3C3	Phosphatidylinositol 3-kinase catalytic subunit type 3
PLK1	Polo like kinase 1
PLL	poly L-lysine
PMSF	phenylmethylsulfonyl fluoride

POLRMT	mitochondrial RNA polymerase
pSILAC	pulsed Stable Isotope Labeling of Amino acid in Cell culture
PTM	post-transcriptional modifications
PVDF	Polyvinylidenfluorid
qRT-PCR	quantitative real-time polymerase chain reaction
RNA	ribonucleic acid
RNase P	ribonuclease P
RNaseZ	ribonuclease Z
RPL28	60S ribosomal protein L28 gene
rRNA	ribosomal RNA
RT-PCR	real time-polymerase chain reaction
s	second
SDHA	Succinate dehydrogenase [ubiquinone] flavoprotein subunit, mitochondrial
SDS-PAGE	Sodium dodecyl-sulfate polyacrylamide gel electrophoresis
SEM	standrard error of mean
siNT	non-targeting siRNA
siRNA	Small interfering RNA
SLIRP	stem-loop interacting RNA-binding protein
SRA	steroid receptor RNA activator
STED	stimulated emission depletion
TACO1	translational activator of mitochondrially encoded cytochrome C oxidase 1
TBK1	TANK Binding Kinase 1
TEFM	transcription elongation factor, mitochondria
TFAM	transcription factor A, mitochondrial
TFB2M	Transcription Factor B2, Mitochondrial
TOM20	translocase of outer mitochondrial membrane 20
TOM70	Mitochondrial import receptor subunit TOM70

tRNA	transfer RNA
UCK2	Uridine-Cytidine Kinase 2
UTR	untranslated regions
V/V	volume per volume
VGLUT1	Vesicular glutamate transporter 1
WT	wildtype
µCi	microcurie
µg	microgram
µm	micrometer
µM	micromolar

Acknowledgment

In the fascinating journey of my PhD, I am indebted to all the guidance, support, and help that I received from many amazing people to whom I would like to express my sincere gratitude.

I would like to start with expressing my deep appreciation to my supervisor, Prof. Peter Rehling, who welcomed me in his group, trusted me with this challenging, yet very interesting project, and supported me through all the steps. I am very thankful for his ideas, immense knowledge, enthusiasm, and fruitful discussions which led the project forward every time that an obstacle hit. I will never forget how supportive and motivating Peter was when we got a rejection from one of the journals and then we had to extensively reshape the paper in a very short time to be accepted at the end. I learnt so much from him, personally and scientifically, that will definitely help me achieve my longstanding goals.

Next, I would like to express my sincere appreciation to Dr. David Pacheu Grau for being an amazing supervisor and a wonderful friend. Beginning my work in the lab under David's supervision was the best start anyone can ask for. David did not only introduce me to the secrets and tricks of the protocols, but he also made sure that I was welcomed and integrated in the group. I am extremely thankful to David for always being there for me and making me feel comfortable to discuss everything with him. Not only has he always come up with great ideas, but he has also been extremely open to my ideas and helped me develop them. David has been a great source of motivation to me during the whole time and his support never stopped even after he left the lab. My experience in the lab was much more fun and fruitful because of him and for that I will always be thankful.

Special thanks go to Prof. Silvio Rizzoli who has been an exceptional support from day one of my project and even before. He advised me on choosing this project and has never left my side since then. I am very grateful to him for being available every time that I would need help with designing the experiments, interpreting, and analyzing the data. I would like to thank Silvio for the time he has invested in my project, being the second reviewer of this thesis, and having many more small meetings to discuss the project. The advice that he provided on how to present my data and prepare the figures for the paper was absolutely outstanding and crucial to me. Seeing his hardworking and passion for science has been very influential to me and I hope to be as passionate as he is in what I will peruse in the future.

I would like to thank Prof. Stefan Jakobs for the time he invested in the project, his ideas and fruitful discussions during our meetings. As a member of my thesis advisory committee, he

always ensured that the project was going smoothly and that I was happy and comfortable working in the lab. This has been extremely heart-warming and for that I am very thankful. Additionally, I would like to thank Dr. Alexander Stein, Dr. Sarah Adio, and Dr. Sonja Lorenz for accepting to evaluate my thesis and attending my thesis defense as extended members of the thesis committee.

I am very thankful to all the collaborators who contributed to our published paper, especially Dr. Eugenio Fornasiero. I learnt a lot from Eugenio about microscopy techniques, designing experiments, and presenting my work during my Master's thesis and that helped me in many steps of my PhD project. I could always reach Eugenio and ask many questions by knocking on his door and he was always kind and patient in helping me. Similarly, amazing people in Fornasiero lab, Opazo lab, and Rizzoli lab always stepped in to help me whenever I had a question or needed help with microscopes. I was very lucky to spend my Master's project there and continue to collaborate with them during my PhD. I am very grateful to all of them.

I would like to extent my heartfelt gratitude to the International Max Planck Research School in Molecular Biology program, especially Dr. Steffen Burkhardt and Kerstin Grüniger. This program provided the best environment for us to pursue our scientific interests, meet many excellent people and make wonderful friends. I am forever thankful for all the support that I received from Steffen and Kerstin, which started already before I arrived in Germany. There is no single thing that the MolBio office has not helped us with, whether it is finding an apartment or finding our future careers! I wish them a continuous success and everlasting happiness in the future.

I am very grateful to Dr. David Pacheu Grau, Dr. Luis Daniel Zaragoza, Dr. Ana Patricia Kutschat, and Anusha Valpadashi for critically reviewing this thesis and providing many valuable suggestions. Additional thanks go to Anusha for illustrating the figures of the introduction and to Dr. Elaheh Vojgani for her kind advice on the statistics.

A special thank you to all the former and present colleagues in the cellular biochemistry department and Rehling lab, the secretary, all the technicians, PIs, PhD students and Post Docs for making a friendly, supportive, and fun environment to work in. Special thanks to the amazing people in the room 1.435. I was always very happy and proud that we had the cleanest and the most organized lab! So, Thank you Mirjam, Sabine, Frank, Sylvie, Markus, Abhijith, Luis, and Anusha. I learnt a lot from our casual yet deep discussions with Luis and Anusha, about science, entrepreneurship, and world cinema! It was a great pleasure for me to be part of this lab and work with people who would always be ready to help whenever I needed them.

My time in the lab as a PhD student would not be as fun without my friends. We had the most supportive PhD and Post Doc community with whom I could share my concerns, doubts, frustrations of failed experiments and excitements of having a positive result. Although pandemic separated us for a long time, I am very happy that we got the chance to sit together again at lunches and enjoy fun and fruitful discussions. So, I would like to thank them all: Metin, Angela, Naintara, Goksemin, Sabine, Bettina, Anusha, Ridhima, Arpita, Abhishek, and Luis.

With no doubt, the best part of my PhD journey was meeting many genuine people who have become my closest friends and family. I cannot imagine my life in the past few years without them. Ana, Gaurika, Anuruti, Ninadini, Jennifer, Liezel, and Ima, you are the most caring friends that anyone can ask for. You have always listened to me, cheered me up, got my back in the ups and downs, and kept me sane. We shared so many fun, beautiful, and delicious (!) moments and remembering them always warms my heart.

Moreover, I owe a big part of my fascinating time in Göttingen to my Iranian friends who selflessly offered me their help and support from the beginning, welcomed me in their homes, showed me their love in times of happiness and trouble, made Göttingen my second home, and truly became my second family. Saeedeh, Ali, Faranak, Mansour, Iraj, Azam, Firouzeh, Mehran, Arghavan, Mostafa, Samira, Soheil, Fatemeh, Moein, Salime, Mohsen, Elaheh, Salma and Samaneh, I am forever thankful to all of you.

I am truly indebted to people who raised me, nurtured me, believed in me and supported me to follow my dreams. My whole family are my endless source of love and inspiration. I deeply appreciate my in-laws for their continued support and kindness and for always packing our suitcases with lots of souvenirs from Iran so that we would never miss the taste of delicious food! I owe who I am today to my dad, Seifollah, who taught me the true values in life, to my mom, Tahereh, who showed me faith to follow my heart, and to my little sister, Rosha, who showed me the taste of unconditional love.

No words can express my appreciation to my husband, Peyman. He is my best friend, forever supporter and the love of my life. Peyman supported me in all and every step of the way, as he always does with patience, kindness, humor, and love. Thank you for believing in me more than I believe in myself. This thesis is yours as much as it is mine.

And above all, I would like to thank God, who has blessed me in all the ways I could imagine…

Resume

Roya Yousefi

roya.yousefi@med.uni-goettingen.com
www.linkedin.com/in/roya-yousefi

Education

2018-present	University of Göttingen; PhD candidate in Molecular Biology
2016-2018	University of Göttingen; Masters in Molecular Biology
2015-2017	University of Tehran; Masters in Medical Biotechnology
2011-2015	University of Tehran; Bachelor in Biotechnology
2010-2011	Young Scholars' Club, Tehran, Iran; gold medalist of the National Biology Olympiad

Research Experience

2018-present	**Department of Cellular Biochemistry, University Medical Center, Goettingen, Germany** Project: Monitoring mitochondrial translation with spatial resolution and in high throughput
2017-2018	**Department of Neuro- and Sensory Physiology, University Medical Center, Goettingen, Germany** Project: Evaluation of Protein Turnover in Different Subcellular Locations and Functional States Using SNAP-tag Fusion Constructs
2015-2016	**Department of Biotechnology, University of Tehran, Tehran, Iran** Project: Evaluation of Hsf1 silencing on sensitivity of prostate cancer cell line (PC-3) to anti-cancer drugs in 2D cultures

Scientific Experience

2018-present	**Teaching assistant** Teaching assistant in Biochemistry and Biology for master students of Max-Plank research school of Molecular Biology
2017-2019	**Organizer of 15th and 16th Horizons in Molecular Biology Conference**
2011-2016	**Biology Olympiad Instructor** Conducting preparatory courses for high-schoolers, participants of national and international Biology Olympiad.

Awards and Certificates

2016-present	International Max Planck Research School Stipend
2011-2016	Full scholarship from Iran's National Elites Foundation
2011-2016	MSRT Fellowship for Exceptional Talents from Iranian Ministry of Science, Research and Technology
2011-2016	Member of National Organization for Development of Exceptional Talents
2010	Gold medalist in National Biology Olympiad

Languages

English	Fluent
German	Intermediate
Farsi	Mother tongue